Influence of Na$^+$, K$^+$-ATPase and Na$^+$/Ca^{2+} exchanger on developmental ion signaling and MBP synthesis in murine oligodendrocyte precursor cells

Dissertation

Zur Erlangung des Grades

Doktor der Naturwissenschaften

Am Fachbereich Biologie

Der Johannes Gutenberg-Universität Mainz

Jens Hammann

geb. am 06.11.1982 in Bernkastel-Kues

Mainz, Mai 2018

Dekan:

1. Berichterstatter:

2. Berichterstatter:

Tag der mündlichen Prüfung: 27.06.2018

Inhaltsverzeichnis

List of Figures

List of Tables

Abbreviations

$[Ca^{2+}]_i$	intracellular calcium concentration
$[Ca^{2+}]_t$	calcium transients
$[K^+]_e$	extracellular potassium concentration
$[Na^+]_i$	intracellular sodium concentration
AEP	anterior entopeduncular eminence
AMPA	aminomethylphosphonic acid
ATP	adenosine triphosphate
BMP	bone morphogenetic protein
CaM	Calmodulin
CaMK	calmodulin kinase
CBD	calcium binding domain
CNP	2', 3'-cyclic nucleotide 3'- phosphodiesterase
CNS	central nervous system
CNTF	cytokine ciliaryneurotrophic factor
Cosc	cortical organotypic slice culture
DIV	day in vitro
ER	endoplasmatic reticulum
FGF	fibroblast growth factor
golli	gene of oligodendrocyte lineage
GPR	G protein-coupled receptor
hnRNP	heterogeneous nuclear ribonucleoprotein
IGF	insuline-like growth factor
IP3	inositol (1,4,5)-trisphosphate
IPL	intraperiod line
K_D	dissociation constant
kDa	kilo Dalton
LGE/CGE	lateral/caudal ganglionic eminence
MAG	myeliin-associated glycoprotein
MBP	myelin basic protein
MDL	major dense lines
MGE	medial ganglionic eminence
MOBP	myelin-associated oligodendrocyte basic protein
NCKX	$Na^+/Ca^{2+}-K^+$ exchanger
NCX	sodium/calcium exchanger
NF	neurofilament

NG2	neural/glial antigen 2
NKA	sodium, potassium ATPase
NMDA	N-methyl-D-aspartate receptor
NT-3	neurotrophin
OGB1	Oregon Green Bapta-1
Olig2	oligodendrocyte transcription factor
OPC	oligodendrocyte precurser cell
P3	postnatal day 3
PAX6	paired box protein 6
PDGFR-α	platelet-derived growth factor receptor alpha
PIP2	phosphatidylinositol (4,5)-bisphosphate
PLC	phospholipase C
PLP	proteins proteolipid protein
PMCA	plasma membrane Ca^{2+} ATPases
PNS	peripheral nervous system
PTP	protein-tyrosine phosphatase
ROI	region of interest
RTKs	receptor tyrosine kinases
SBFI	sodium benzofuran iosphtalate
SERCA	sarcoendoplasmic reticular Ca^{2+} ATPases
Shh	sonic hedgehog
siRNA	small interfering ribonucleic acid
sncRNA715	small non-coding RNA 715
T3	triiodothyronine
TOG	tumor overexpressed gene
UTR	untranslated region
VGCC	voltage-gated calcium channels
V$_{max}$	maximal velocity
VZ	ventricular zone
α2-NKA	alpha2 subunit of the sodium, potassium ATPase

Summary

In the central nervous system (CNS) neuronal axons are myelinated by oligodendrocytes. This leads to a facilitating rapid propagation of action potentials. Myelin basic protein (MBP) is an essential component of myelin and its absence results in severe hypomyelination. Myelination in the CNS is dependent on axon-oligodendocyte precursor cell (OPC) interaction. It was hypothesized that the expression of MBP, an "executive molecule of myelin", could be altered by local $[Na^+]_i$ and $[Ca^{2+}]_i$ transients occurring in murine OPCs. In OPC monocultures MBP synthesis starts at around DIV4. Therefore, experiments in OPC monocultures at day in vitro (DIV) 2-6 were performed. Interestingly, also transient elevations of resting $[Ca^{2+}]_i$ and $[Na^+]_i$ in OPCs were observed at DIV4-5. A similar but slower increase of resting $[Ca^{2+}]_i$ and $[Na^+]_i$ was also observed in acute callosal brain slices. A chronic treatment of OPCs for 24 hours with culture medium containing elevated $[K^+]$ (+5 mM) decreased resting $[Na^+]_i$ and enhanced MBP synthesis. At the same time, blocking the reverse mode of the Na^+, Ca^{2+} exchanger (NCX) for 12 hours with KB-R7943 (1 µM) elevated resting $[Na^+]_i$ and decreased MBP synthesis. OPC depolarization after 12 hours of chronic application of ouabain (500 nM), a Na+, K+-ATPase (NKA) blocker, stimulated MBP synthesis as well. At single cell level NCX blockade, the elevation of extracellular $[K^+]$ and partial NKA inhibition led to $[Na^+]_i$ transients OPCs. The latter two, $[K^+]_e$ elevations and NKA blockade, resulted in $[Ca^{2+}]_i$ oscillations. Those $[Ca^{2+}]_i$ oscillations were blocked by application of KB-R7943 (1 µM) but not with Cd^{2+} (100 µM), indicating an involvement of the NCX reverse mode. Already small concentrations of ouabain (10 nM) successfully induced $[Ca^{2+}]_i$ oscillations as well. Moreover, it was demonstrated that cultured OPCs express the alpha2 isoform of NKA (α2-NKA) which has a high affinity for ouabain. Therefore it was hypothesized that the $[Ca^{2+}]_i$ oscillations are mediated by α2-NKA. Similar to its blocking, knocking down the α2-NKA with small interfering (si)RNA (α2-siRNA) significantly potentiated MBP synthesis at DIV4 and 5. This potentiation was completely abolished by a chronic application of KB-R7943 (1 µM) for 24 hours. Additional to the MBP potentiation, α2-NKA knockdown also increased the frequency of NCX-mediated spontaneous Ca^{2+} transients ($[Ca^{2+}]_t$) at DIV4, while in control cultures comparable frequency of $[Ca^{2+}]_t$

was observed at DIV5. The $[Ca^{2+}]_t$ were only observed in a narrow time window (DIV4-5) and disappeared nearly completely at DIV6, in control as well as in α2 siRNA-treated cultures. However, knockdown of MBP did not show any influence on the α2-NKA expression, but the $[Ca^{2+}]_t$ remained even at DIV6. A homogeneous distribution of α2-NKA was detected via immunocytochemical analyses and showed co-localization with MBP in proximal processes of immature OPCs. Later in cell development, the co-localization was only weakly present in MBP-enriched membrane sheets. In cortical organotypic slice cultures the knockdown of α2-NKA did not alter the levels of MBP but reduced co-localization of neurofilament- and MBP-positive compartments.

Summarizing the results, it is suggested that α2-NKA keeps the local membrane potential of the OPCs close to the reversal potential of NCX. A depolarization, caused by a neuronal activity dependent elevation of $[K^+]_e$ in the vicinity, leads to a flip of the NCX into reverse mode, intruding Ca^{2+} into the cell. This Ca^{2+} influx initiates $[Ca^{2+}]_t$ in OPCs which seems to positively influence the local MBP expression.

immature oligodendrocyte
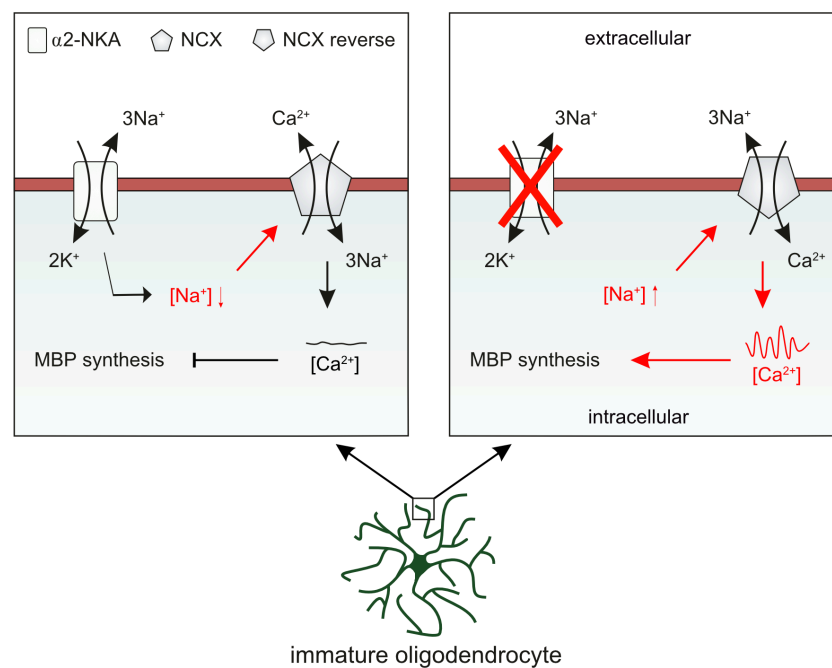
1   Introduction

1.1   The central nervous system

The nervous system of vertebrates is a complex system of excitatory, inhibitory and glial cells, which control and coordinate body functions and enable the communication with the environment. It is divided into the peripheral nervous system (PNS) and the central nervous system (CNS) (Figure 1-1).
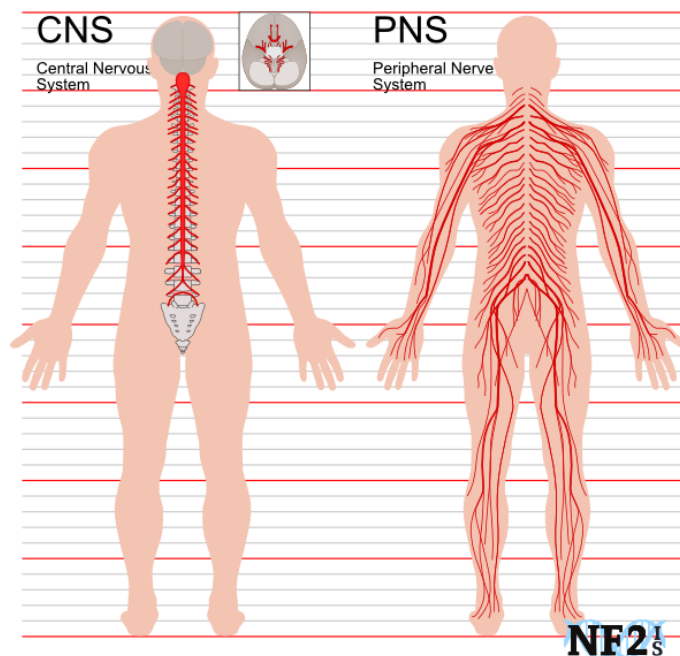
Figure 1-1: The nervous system

The nervous system of vertebrates is subdevided into the central nervous system (left) and the peripheral nervous system (right). The central nervous system consits of brain and spinal cord, while all the remaining nerves and ganglia belong to the peripheral nervous system (derived from http://sites.middlebury.edu/geog0240als/biology/).

The PNS consists of all the nerves and ganglia that do not belong to the brain or spinal cord. According to its functions the peripheral nervous system can be subdivided into the somatic nervous system and the autonomic nervous system. In the somatic nervous system sensory nerves (afferent nerves) propagate signals from environmental influences to

the CNS and motor nerves (efferent nerves) receive commands from the CNS, which they then send out to the muscles to stimulate their contraction. The autonomic nervous system influences the function of the inner organs. While the functions of the somatic nervous system can be influenced and controlled, the ones of the autonomic nervous system cannot. The autonomic nervous system is also subdivided into three subtypes: sympathetic, parasympathetic and enteric nervous system.

The CNS is divided into two major regions: the brain and the spinal chord. It coordinates the function of the internal organs and the skeletal muscles and is divided into grey and white matter. The grey matter contains all of the cell bodies, the white matter is composed of all the neuronal processes (Silbernagl and Despopoulos 2012; Trepel 2017).

1.1.1   Cells of the central nervous system

The CNS is basically composed of two major cell groups: neurons and glial cells.
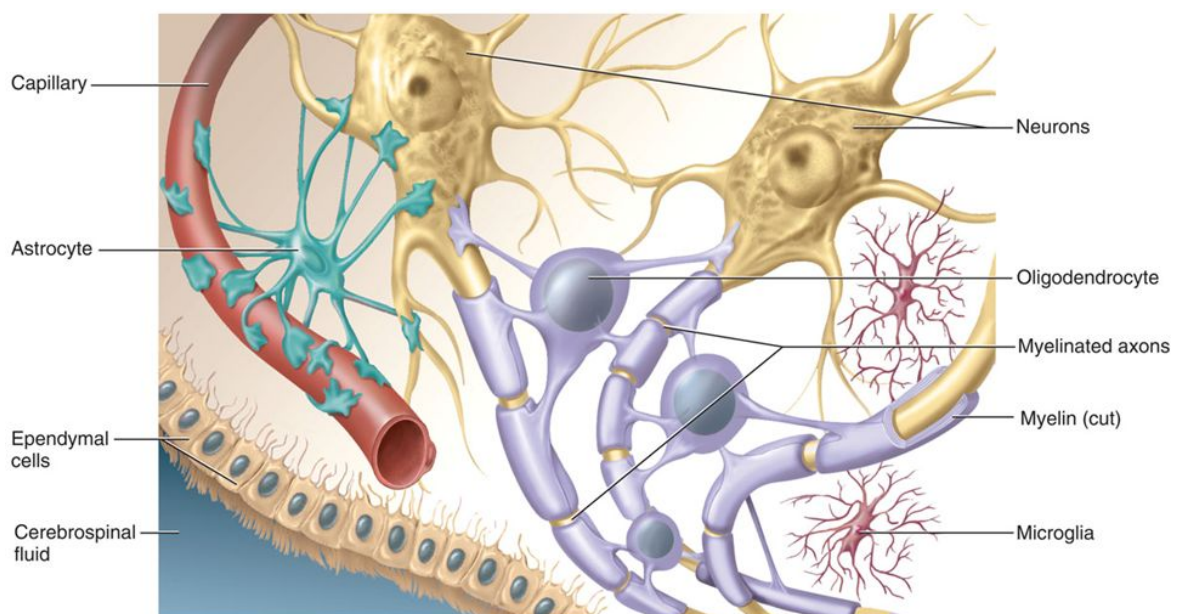
Figure 1-2: Cells of the central nervous system

The central nervous system is composed of neurons and glial cells. Neurons (yellow) form the electrically excitable network and are capable of processing and propagating informations. Glial cells like astrocytes (green), microglia (red) and oligodendrocytes (purple) interact with neurons and play a supportive role in maintaining and protecting the network (modified from https://www.78stepshealth.us/human-physiology/supporting-cells.html).

1.1.1.1 Neurons

Neurons (Figure 1-2, yellow cells) are electrically excitable cells, which can transmit information over very long distances along a directed membrane potential. Many different subtypes of neurons are known, but their structure is mostly the same. Incoming information is received by highly branched processes: the dendrites. The dendrites propagate the signal over the cell body to the axon. The axon, a potentially very long and thin process, leads the signal to the target cell. The velocity of the signal propagation is dependent on the diameter of the axon; the bigger the diameter, the faster the signal is transmitted (Rushton 1951; Waxman 1997; Hartline and Colman 2007). Neurons are organized in networks and share the ability to communicate with each other via neuron-neuron contact sites, which are called synapses. Electrical stimuli, so called action potentials, are propagated along the axon and lead to a release of neurotransmitter containing vesicles at the end of the axon, the presynaptic terminal. The released neurotransmitters bind to specific postsynaptic receptors (chemical synapses). This depolarizes the neighboring cell, which causes again an action potential and the signal is propagated further (excitatory synapses). Besides the excitatory synapses also inhibitory synapses exist. Here, the binding of neurotransmitter to their receptors leads to a hyperpolarization of the neighboring neuron. The ratio of incoming excitatory and inhibitory finally decides, if an action potential in the postsynaptic neuron is evoked or not (Alberts et al. 2004).

Another form of cell-cell interaction is mediated by electrical synapses or gap junctions. In this case integral membrane proteins – the connexins – build gates that enable the exchange of ions and small molecules between cytoplasm of adjacent cells (Nielsen et al. 2012).

1.1.1.2 Glial cells

The second main cell types are glial cells. Glial cells were initially thought to be supporter cells, which merely glue neurons together (glia = greek for glue). Nowadays it is known that certain types of glial cells enwrap axons to speed up the signal propagation or they remove cell debris. Another feature of this cell type is providing nutrients and maintainingthe ionic composition inside and outside the neuron and thereby influencing their ac-

tivity. While dealing with all these tasks glial cells are a crucial component in maintaining the homeostasis inside the brain (Trepel 2017).

1.1.2 Types of glial cells in the CNS

Depending on their size, glial cells are subdivided into two different groups: micro- and macroglia. The different types will be further explained in the following paragraphs.

1.1.2.1 Microglia

Since the brain is almost isolated from the immune system of the body by the blood brain barrier, microglia (Figure 1-2, red cells) function as the immune cells of the brain. By producing and releasing proinflammatory factors they control the removal and recycling of cell debris in the CNS. It is also hypothesized that microglia can remove and thereby adjust incorrect synaptic connections by phagocytosis. Since this thesis mainly focuses on macroglia – especially oligodendrocytes – this section about microglia will not be discussed in further detail (Trepel 2017; Fahlke et al. 2015; Silbernagl and Despopoulos 2012).

1.1.2.2 Macroglia

The second category of glial cells in the CNS, the macroglia, is again subdivided into ependymal cells, astrocytes, NG2-positive cells and oligodendrocytes.

Ependymal cells

Ependymal cells (Figure 1-2, light brown cells) are multiciliated epithelial cells that line the ventricles in the brain and the central canal in the spinal cord. With their motile cilia they are responsible for moving the cerebrospinal fluid inthe ventricles (Liu et al. 2014).

Astrocytes

Astrocytes (Figure 1-2, turquoise cells) are named for their star-shaped morphology. Since they are the cells that connect blood vessels and neurons, it has long been known that astrocytes provide structural and nutritional support for neurons. They control the extracellular concentrations of neurotransmitters in the synaptic cleft and thereby play an im-

portant role in the precise coding of synaptic signals (tripartite synapse) (Panatier, Arizono and Nagerl 2014).

NG2+ cells

Within the last years of neurobiological research another type of glial cells was discovered in the CNS. They were named NG2+ cells, since they express the proteoglycan NG2. The cells were initially thought to be oligodendrocyte precursor cells but it could be shown that they also play an important role in the maintenance of synaptic contacts. Therefore their integration into the neuronal network can be assumed (Nishiyama et al. 2009; Sakry, Karram and Trotter 2011).

Oligodendrocytes

Oligodendrocytes (Figure 1-2, purple cells) are the myelinating cells of the vertebrates CNS. Myelination is the process of enwrapping a nearby axon with membrane sheaths provided by the oligodendrocytes. This leads to an axonal isolation and thereby faster signal propagation to the receiving cell. For a sufficient isolation it is essential that the oligodendrocytes provide a massive amount of proteins and lipids. One single oligodendrocyte can myelinate up to 50 different axonal segments (Friedrich 1993).

Since this thesis is related to oligodendrocyte myelination, the development, the structure of the myelin membrane and its protein- and lipid composition will be described in detail in the following chapters.

1.2   Origin and development of myelination in the CNS

1.2.1   Origin of oligodendrocytes

Two hypotheses were postulated in the beginning of origin of oligodendrocytes research: (1) Since mature oligodendrocytes were found in all regions of the adult brain in the same density, it was thought that they were generated in all parts of the embryonic ventricular zone (VZ) homogeneously. (2) A specialized domain is the source of oligodendrocytes and is located in the ventral VZ of the embryonic spinal cord. Meanwhile it has been shown that oligodendrocytes arise from multipotent neural stem cells which differentiate into oligodendrocyte precursor cells (OPCs) and then further develop to mature, myelin form-

ing cells. The origin of the multipotent neural stem cells is induced in the motor neuron progenitor domain of the dorsal and ventral neuroepithelium (Cai et al. 2005). Generation of OPCs in the developing rodent forebrain ventricular zone is established in three consecutive waves (Figure 1-3). At around 12.5 days after fertilization or embryonic day 13 (E13) "first OPCs originate in the medial ganglionic eminence (MGE) and anterior entopeduncular area (AEP) in the ventral forebrain...a second wave of OLPs from the lateral and/or caudal ganglionic eminences (LGE and CGE). Finally, a third wave arises within the postnatal cortex." (Fogarty, Richardson and Kessaris 2005). These early arising oligodendrocyte precursor cells have a higher motility, a faster proliferation rate and a better survival compared to the oligodendrocytes generated later in life (Tang, Tokumoto and Raff 2000; Ruffini et al. 2004).

Generation, migration and differentiation of OPCs need a very tightly controlled regulation and depend on extra- and intracellular factors. The main factors that drive the development of neural stem cells to OPCs are the morphogenes sonic hedgehog (Shh) and the fibroblast growth factor (FGF). The notochords excretes ventral Shh which binds to notch1 receptors on the surface of nearby precursor cells, that induces the expression of the transcription factors Nkx6 and Olig2 and subsequently leads to the initiation of the first wave of oligodendrocyte generation (Pringle et al. 1996; Orentas et al. 1999). The bone morphogenic protein (BMP) and Wnt/bCantenin inhibit this effect on the dorsal side. The dorso-ventral gradient of BMP/Wnt leads to an activation of different transcription factors like PAX6, Olig2, Nkx2.2, Nkx6.1 and Nkx6.2 which are responsible for the definition of the different domains (Vallstedt, Klos and Ericson 2005). The transcription factor with a helix-loop-helix motif Olig2 is activated by Shh and plays an important role in the generation of oligodendrocytes in the early embryonic phase, whereas FGF substitutes Olig2 in later developmental stages of the embryo (Chandran et al. 2003; Kessaris et al. 2004).

Even though OPCs derive from different areas, it was assumed that they do not show functional differences. Knock down experiments or diphtheria toxin mediated ablation of any one of these developmental oligodendrocyte waves showed that the following waves compensated the loss of OPC numbers and the individuals didn't show any neurological

differences (Kessaris et al. 2004; Kessaris et al. 2006; Richardson, Kessaris and Pringle 2006). Also whole-cell patch clamping experiments couldn't show any alteration in respect to their membrane properties between dorsally and ventrally derived OPCs (Tripathi et al. 2011; Clarke et al. 2012). However, recent research has shown that there are differences in OPCs deriving from dorsal and ventral areas. After demyelination experiments in mature CNS dorsally derived OPCs proliferated, migrated and differentiated faster then than OPCs with ventral origin (Zhu et al. 2011; Crawford et al. 2016).
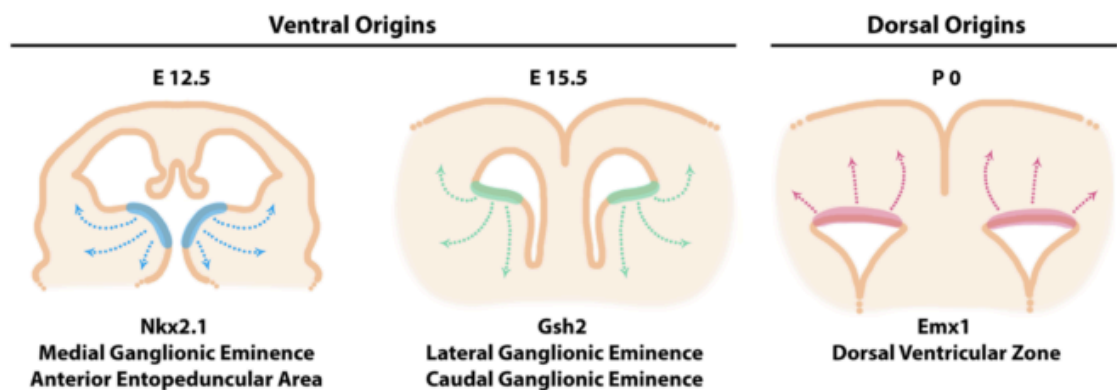
Figure 1-3: Generation of OPCs in the developing rodent forebrain

Within three consecutive waves OPCs are generated in the ventricular zone (from left to right). The first wave starts at around 12.5 days post fertilisation (E12.5) in the medial ganglionic eminence (MGE) and anterior entopeduncular area (AEP) in the ventral forebrain. The second wave originates in the the lateral and/or caudal ganglionic eminences (LGE and CGE) at around E15.5. The third wave starts in the dorsal ventricular zone at postnatal day 0 (P0) (modified from Newville et al. 2017).

After reaching OPC state, the cells start expressing the antigen A2B5, the proteoglycan NG2 and the platelet-derived growth factor receptor alpha which are commonly used as marker for this specific cell type. The OPCs either remain in this NG2+ stage in which they can still proliferate (Nishiyama et al. 2009) or they can differentiate into oligodendrocytes (Figure 1-4). *In vitro* NG2+ cells can even differentiate into astrocytes and neurons, while these properties are still not proven in *in vivo* situation (Kondo and Raff 2000; Richardson et al. 2011). Again, extra- and intracellular signals determine the fate of the cells. The differentiation to mature oligodendrocytes via an immature or pre-oligodendrocyte stage is

initiated by the insulin-like growth factor (IGF), the cytokine ciliary neurotrophic factor (CNTF) and the thyroid hormone triiodothyronine T3. Also the upregulation of the transcription factors Olig1, Olig2, Nkx2.2, Nkx2.6 and Sox10 is essential for the development into immature oligodendrocytes, whereas the expression of BMPs and Sox5 and Sox6 inhibit the differentiation (Miron, Kuhlmann and Antel Jack P. 2011).
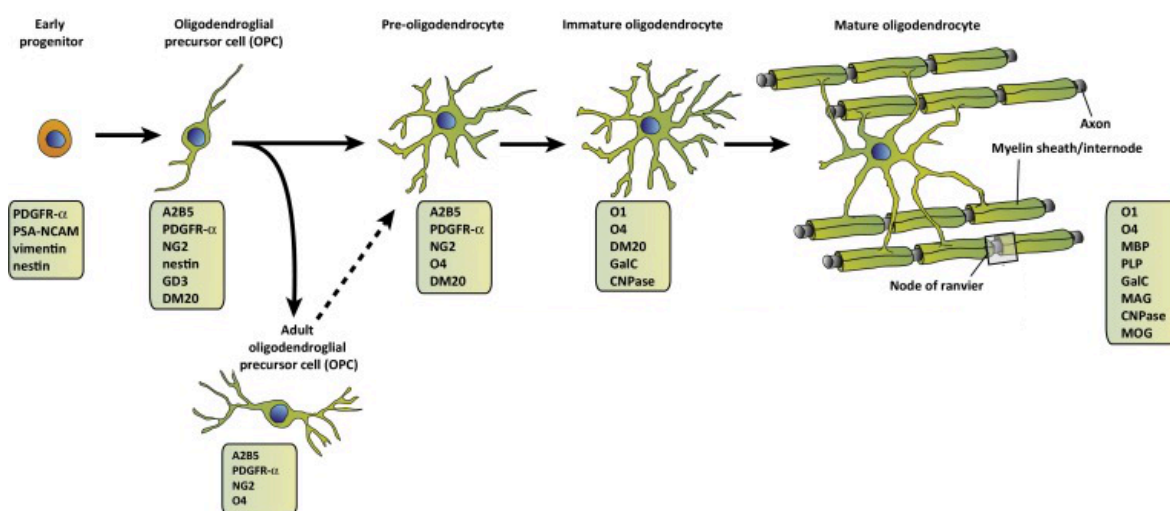
Figure 1-4: The different stages in oligodendroglial development

The development of an oligodendrocyte starts as a multi-potent neural stem cell over a oligodendroglial precursor cell (OPC) and immature oligodendrocyte to the mature myelinating oligodendrocyte. The different developmental steps are under control of many transcription factors and other intrinsic and external factors. These factors can be used as markers for specific developmental stages of the oligodendrocytes (modified from Kremer, 2016).

After migration to their final target, immature oligodendrocytes need to get into contact with a nearby nude axon to develop further into a mature oligodendrocyte. The maturation of the OPCs is characterized by an increased ramification of their processes, followed by an expansion of uncompacted myelin membrane (Michalski and Kothary 2015). Numerous growth and trophic factors like PDGF-A, FGF-2, IGF-1, NT-3 and CNTF, have been identified to regulate oligodendrocyte development (Barres, Lazar and Raff 1994; Miller 2002; Baron, Colognato and Ffrench-Constant 2005). The importance of the maintenance of the homeostasis of these factors was shown by experiments where an overexpression of PDGF-A led to increased numbers of OPCs and subsequently an ectopic production of

oligodendrocytes in the mouse spinal cord (Calver et al. 1998). This indicates that a large number of immature oligodendrocytes die so that only the needed amount of mature oligodendrocytes develop further. Also cell adhesion molecules like PSA-NCAM, contactin/F3, MAG and the notch1 receptor stimulate oligodendrocyte development. As soon as the axon-glial contact is established, multiple intracellular molecular mechanisms are initiated. A very important communication point in the development is the SRC-kinase Fyn which can be inhibited by the transmembrane protein LINGO-1 (leucine-rich repeat and immunoglobulin domain-containing-1). On the other side the interaction of the notch receptor and the axonal ligand F3/contactin can activate Fyn which then translates the extracellular signal into a intracellular signal and subsequently leads to expression of transcription factors like AscI/Mash1 und Olig2 that promote development (Parras et al. 2007; Yu et al. 2013).

1.2.2   The role of oligodendrocytes

The probably best-known feature of oligodendrocytes is the formation of myelin sheaths and thus the isolation of the axons. This function leads to faster signal propagation. In invertebrates that lack the ability to produce myelin, the velocity of the signal propagation is dependent on the diameter of an axon. The smaller the axon, the higher the resistance. In consequence this means a thicker axon can propagate a signal faster than a thinner one. To counteract this waste of space, myelin evolved in vertebrates (Kaplan et al. 1997; Kaplan et al. 2001). With this isolation of the main parts of the axon (internodes) the signal can only jump towards and thereby along the unmyelinated parts (saltatory conduction), called the nodes of Ranvier. The myelination also leads to a clustering of sodium channels to provide the saltatory nerve conduction (Kaplan et al. 1997; Kaplan et al. 2001). Since the ion current is restricted to the nodes of Ranvier myelinated axons also reduce the energy costs for maintaining the membrane potential via Na+/K+-ATPases (NKAs) to a minimum. Even though myelination is an elegant way to keep the axon diameter small, oligodendrocytes only select axons above 0.2 μm (Simons and Trajkovic 2006). But the molecular reason for this is still unknown.

Besides the isolating properties oligodendrocytes are also responsible for the trophic support. The support of the neurons via oligodendrocytes was shown by specific knock

out mouse models. Mice lacking the myelin proteins proteolipid protein (PLP) or 2', 3'-cyclic nucleotide 3'- phosphodiesterase (CNP) just showed very little morphological differences within the myelin sheath but a severe degeneration of the enwrapped axons was found. This leads to the assumption that oligodendrocytes also play a neuro-protective role in the central nervous system (Griffiths et al. 1998; Lappe-Siefke et al. 2003). Further experiments showed that axons with modified myelin sheaths alter in axonal transport rates or amount of microtubules or stability, assuming that oligodendrocytes interfere with even normal axonal transport processes (Edgar et al. 2004; Kirkpatrick et al. 2001; Frühbeis et al. 2013).

Additionally it was shown that oligodendrocytes are able to deliver exosomes to axons (Frühbeis et al. 2013). Exosomes are micro-vesicles which cells can exchange proteins, RNAs and miRNAs with. This cell-cell communication is already described in a variety of different cell types (Denzer et al. 2000). Oligodendrogial exosomes can protect axons from oxidative stress and thereby facilitate the survivalof neurons (Frühbeis et al. 2013). In cortical oligodendrocyte-neuron co-cultures oligodendroglial exosomes influence neuronal activity and might be able to modulate the neuronal network (Frohlich et al. 2014).

1.2.3   Organization of the myelin membrane

Appraisals lead to the conclusion that one single oligodendrocyte can grow a membrane surface area of approximately 20×10^5 µm, which makes it the most powerful membrane producer in the body (Friedrich 1993). Modern live-imaging analysis of myelination in zebrafish has also shown that oligodendrocytes are able to produce a new myelin sheath within only five hours (Czopka, Ffrench-Constant and Lyons 2013).
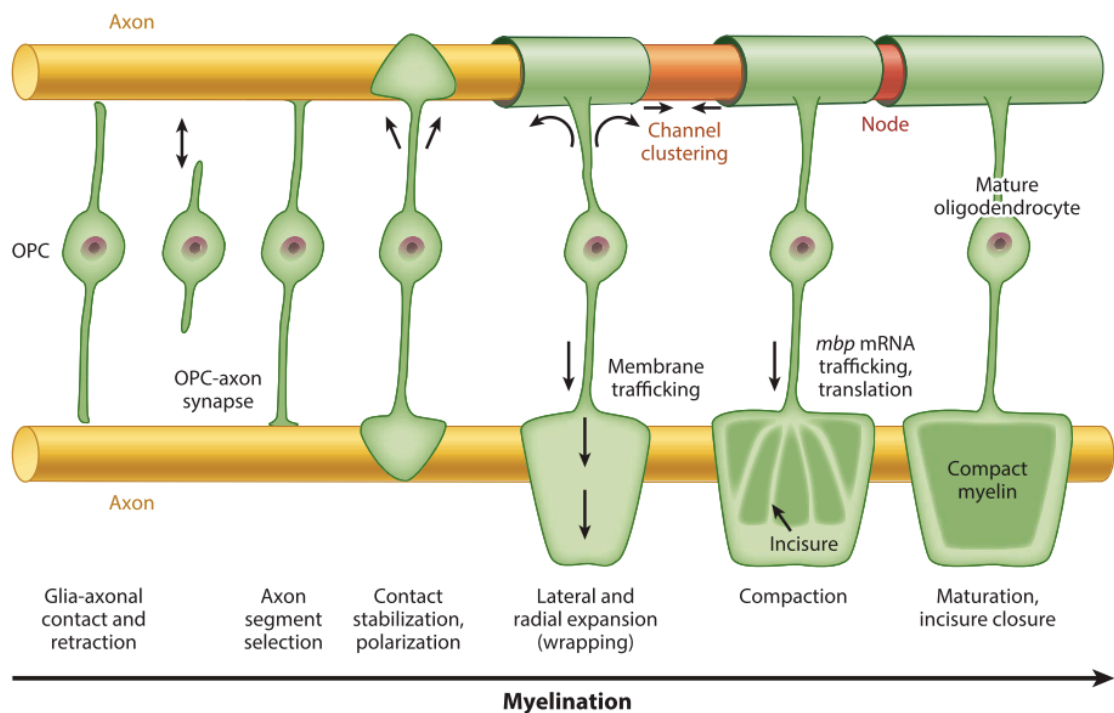
Figure 1-5: The myelination process of oligodendrocytes

Detection of an axonal segment by the OPC leads to an expansion of its process.The membrane is extended laterally and radially and the newly synthesized layer is pushed below the already existing layers. Retraction of the cytoplasm leads to compaction of the myelin and ends the wrapping process (modified from Nave & Werner 2014).

Figure 1-5 shows that immature oligodendrocytes are able to extend and retract their processes and thereby look for nude axons to be myelinated (Nave and Werner 2014). As soon as an axon is detected, the oligodendrocyte starts wrapping its process around it. While the membrane is extended laterally and radially, the newly synthesized layer is pushed below the already existing layers (Snaidero et al. 2014). After the enwrapping is accomplished, the cytoplasm is retracted out of the process. This effect leads to the compaction of the myelin. The inner sides of the membrane are then fused together. These fused areas have a higher density compared to the unfused parts. Because of this higher density these areas can be detected with the electronic microscope as dark lines and are called major dense lines (MDL). The lighter line between the MDLs is called intraperiod line (IPL) and represents the stacks of extracellular membranes, which have a lower density than the MDLs (Figure 1-6, left). The myelin layers that are located closely to the axon are termed adaxonal myelin, the outer layers are abaxonal myelin. Images from electronic

microscopes also show radially running channels filled with cytoplasm, named radial components (Figure 1-6, right). It is assumed that they play an important role in the maintenance and stability of the myelin sheaths (Nave and Werner 2014).
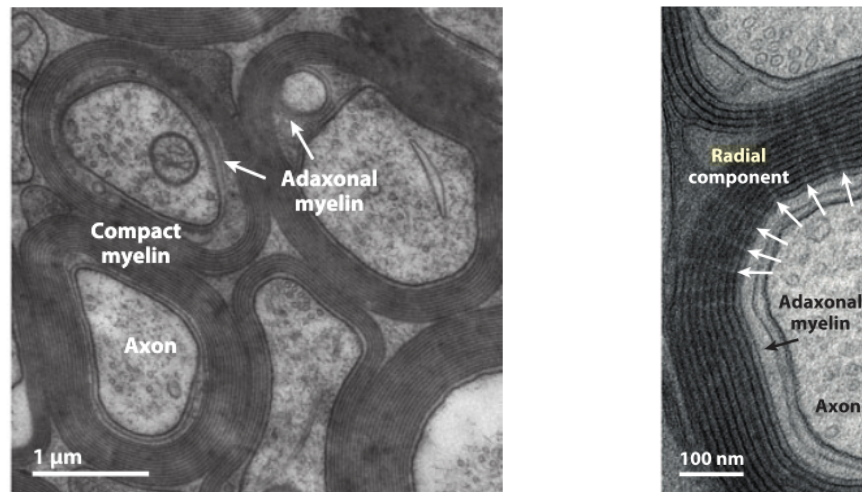
Figure 1-6: Structure of compact myelin

Electron-microscopic image of a cross-section through an optical nerve. The dark areas depict the layers of compact myelin around the lighter appearing axon. On the higher magnification image (right) the major dense lines (MDLs), the intraperiod lines (IPLs) and the radial component (white arrows) are visible (modified from Nave & Werner 2014).

1.2.4   Myelin lipids and proteins

The myelin membrane has a very characteristic composition. Unlike other bio membranes it contains a high amount of lipids, which is necessary to establish the isolating feature of the oligodendrocytes. The dry weight of myelin is composed of approximately 70-75% of lipids. Highly myelinated areas in the CNS appear to be white and are therefore named white matter. The main myelin lipids are glycosphingolipids, galactolipids, phospholipids and cholesterol (Norton 1984). Cholesterol is the key molecule to form lipid-rich micro-domains and plays an important role in activation of signaling pathways via axon-glial contact leading to myelination of axons (White and Krämer-Albers 2014).

The most abundant myelin proteins are the proteolipid protein (PLP) and its smaller splice isoform DM20 (accounted for 30-45% of total myelin protein), myelin basic protein (MBP)

(22.35%), 2', 3'-cyclic nucleotide 3'-phosphodiesterase (CNP) (4-15%), myelin-associated oligodendrocyte basic protein (MOBP) and the myelin-associated glycoprotein (MAG) (Jahn, Tenzer and Werner 2009).

1.2.5   Myelin basic protein (MBP)

The gene coding for MBP was identified in mouse and human and was named gene of oligodendrocyte lineage (golli). It contains three starting sites and seven exons from which the golli proteins and the classical MBP proteins can be synthesized.

The golli proteins are not exclusively found in oligodendrocytes but are also expressed by neurons and cells of the immune system (Fulton, Paez and Campagnoni 2010). They are preferentially localized in the nucleus and the soma of differentiating oligodendrocytes. It is assumed that they play a role in homeostasis since they enhance the influx of calcium ions during the early phase of oligodendroglial differentiation (Paez et al. 2007).

Myelin basic protein (MBP) is a peripheral membrane protein. It is a basic protein, which is positively charged at normal intracellular pH values. Via electrostatic bonds MBP can interact with the negatively charged phospholipids on the intracellular myelin membranes and fuses them together, leading to the compacting of myelin (Wood, Vella and Moscarello 1984). Alternative splicing results in four isoforms in human (17.2 kDa, 18.5 kDa, 20.2 kDa und 21.5 kDa) and in six isoforms in mice (14-21.5 kDa) (Harauz and Boggs 2013; Kamholz, Toffenetti and Lazzarini 1988). The importance of the MBP proteins becomes obvious in their absence. Mutations in the gene lead to a lack of MBP in Shiverer mice and Long-Evans shaker rats, resulting in a severe CNS hypomyelination (Kwiecien et al. 1998; Readhead and Hood 1990). Thus MBP has been denoted as the 'executive molecule of myelin' (Boggs 2006). Additionally to its compaction feature, MBP can also aggregate and thereby act as a molecular sieve: it prevents molecules with big cytoplasmic domains to diffuse into future myelin compartments and thus forming compact myelin (Aggarwal et al. 2013).

MBP synthesis is an exception compared to most other proteins. MBP mRNA is transported from the nucleus to the axon-glial contact side in a translationally inhibited state

(Müller et al. 2013). Neuron-oligodendrocyte communication now triggers the translation so that every process can synthesize independently the needed amount of protein. MBP mRNA is detectable already one day before the protein is synthesized, which means that there must be mechanisms controlling the repression of translation (Colello et al. 1995; Besse and Ephrussi 2008). This local translation has several benefits: it is very time and energy efficient and it prevents the MBP protein to falsely fuse other membranes on its way to the point of destination (Staugaitis, Smith and Colman 1990).

1.2.6   MBP mRNA transport

Figure 1-7 shows how the transport of MBP mRNA from the nucleus to the periphery is organized in large ribonucleoprotein complexes termed RNA granules (Ainger et al. 1997; Brophy, Boccaccio and Colman 1993). In all of the MBP isoforms a specific sequence of eleven nucleotides is conserved in the 3'-UTR of the MBP mRNA (Munro et al. 1999). The trans-acting trafficking factor, heterogeneous nuclear ribonucleoprotein (hnRNP) A2 binds to this cis-acting trafficking sequence, named hnRNP A2 response element (A2RE) in the nucleus and guides the mRNA into the cytoplasm. Here, further RNA-binding proteins like tumor overexpressed gene (TOG) and the hnRNPs F, E1, K and CBF-A bind to the RNA (Kosturko 2005; Kosturko et al. 2006; White et al. 2012; Laursen, Chan and Ffrench-Constant 2009; Raju et al. 2008). Also components of the translational complex like the elongation factor 1a, the aminoacyl tRNA synthetase and ribosomal RNA are incorporated into the granule. Additional molecular motors like the kinesin Kif1b finally transport the granules along the microtubules to the cell periphery where several extracellular signals can lead to the translation of the protein. For the local translation at the axon-glial contact siteMBP mRNA must be transported in a translational inhibited state. This inhibition is achieved by the binding of the small non-coding RNA 715 (sncRNA715) (Bauer et al. 2012) and might also be influenced by the hnRNP E1 (Kosturko et al. 2006). SncRNA 715 is a regulatory RNA of a length of 21 nucleotides and is highly expressed in oligodendrocyte precursor cells compared to the other cell types of the CNS (Bauer et al. 2012). Like hnRNP A2 sncRNA715 also binds to a specific region in the 3'-UTR of the MBP mRNA. Overexpression or knock-down experiments showed that the more sncRNA715 is expressed in an oligodendrocyte precursor cell, the lower the MBP protein levels was and

vice versa, meaning that sncRNA715 and MBP synthesisare negatively correlated. Also in lesions of human multiple sclerosis patients, where MBP is strongly reduced, an upregulation of sncRNA715 was observed (Bauer et al. 2012). At the axon-glial contact side the axonal L1 binds to the oligodendroglail F3/contactin complex and this subsequently leads to an activation of the src-kinase Fyn, which phosphorylates components of the RNA granule like A2 and F and thereby initiates the dissociation of the granule (Müller et al.
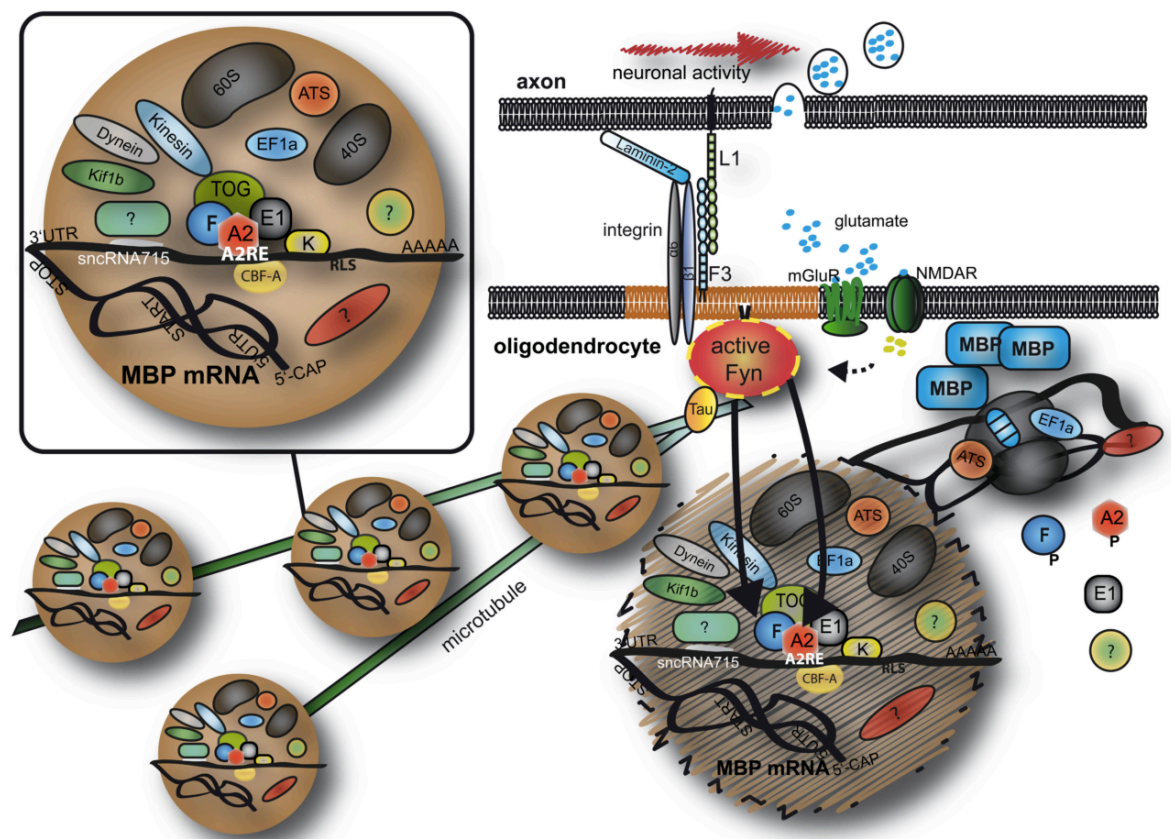
2015; Müller et al. 2013; White et al. 2008; White et al. 2012).

Figure 1-7: mRNA transport and local translation of MBP

Schematic representation of the transport of *MBP* mRNA in RNA granules along microtubules towards the axon-glial contact site. RNA granules further contain several different RNA-binding proteins ad motor proteins as well as parts of the translation machinery. Axonal signals lead to an activation of Fun kinase and subsequently the initiation of local translation (modified from Müller 2013).

1.3   Ion signaling

1.3.1   The membrane potential

All living cells are surrounded by membranes. They enable different conditions inside the cells compared to their environment. Cell membranes are composed of a phospholipid bilayer in which membrane proteins are imbedded. Those biomembranes are usually impermeable for big molecules and charged particels (ions). Incorporation of channels, transporters and pumps into the lipophilic membrane makes it permeable for certain molecules/ions. Transport proteins play an important role in the transport of specific molecules through the membrane. An imbalance of ions between extra- and intracellular space leads to a specific transmembrane potential, the resting potential.

One of the most important key players for maintaining the resting potential are K^+ ions (Figure 1-8). The high intracellular K^+ concentrations are achieved by the actionof the sodium potassium ATPase (NKA). It pumps three sodium ions out of the cell and two potassium ions into the cell at the same time by using ATP. This leads to an enrichment of Na^+ in the extracellular space and the important high concentration of K^+ inside the cell. At the same time NKA keeps the cell negatively charged compared to the extracellular space. Most of the cell membranes contain K^+ channels, which let the K^+ ions flow along their gradient out of the cell. Losing positively charged K^+ makes the cell subsequently more negative. This rising electrical gradient has an electromagnetic effect on the K^+ ions outside the cell and drags them back into the cell. If the electrical force of one specific ion is as big as its chemical force, there is no net ion flow anymore and the resulting potential is called equilibrium potential for this ion.
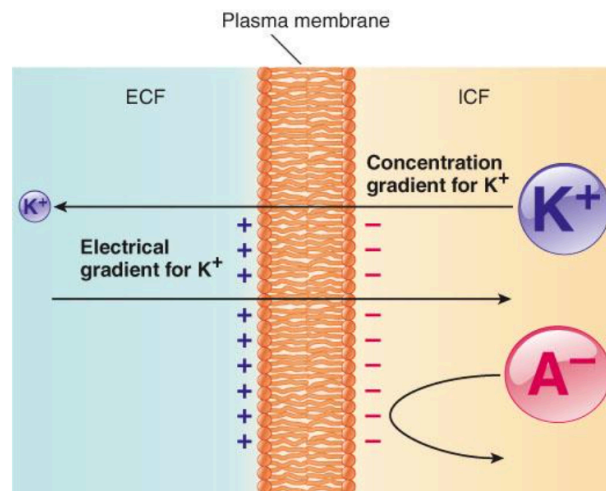
Figure 1-8: The K+ equilibrium potential

Schematic representation of the concentration gradient and the electrical gradient of K+. High intracellular K+ levels are achieved by NKA activity under ATP hydrolysis. K+ channels enable diffusion of the K+ over the membranes along the concentration gradient. The electromagnetic effect of the intracellular fluid pulls the K+ ions back into the cell. The equilibrium potential for K+ is adjusted when both forces have the same strength (modified from https://www.memorangapp.com/flashcards/78571/CCF+Physiology+L5+Resting+Membrane+Potential/).

Not only K^+ ions play a role in the maintenance of the resting membrane potential. On both sides of the membrane ions exist in different concentrations. The most important positively charged particles or cations are sodium (Na^+), potassium (K^+) and calcium (Ca^{2+}). Negatively charged anions are mainly chloride (Cl^-) and negatively charged proteins. Each of those ions has its own specific equilibrium potential (Figure 1-9). If added together, all of the equilibrium potentials of these important ions build up the final potential of the cell, the membrane potential. Ca^{2+} channels are an exception since they are mainly closed, meaning that Ca^{2+} does not considerably influence the resting membrane potential (Silbernagl and Despopoulos 2012; Fahlke et al. 2015).

Ion	Cytosolic	Extracellular	E_0 at 37°C
K^+	150 mM	6 mM	– 86 mV
Na^+	15 mM	150 mM	+ 62 mV
Ca^{2+}	100 nM	1.2 mM	+ 126 mV
Cl^-	9 mM	150 mM	– 70 mV

Figure 1-9: Equilibrium potentials of the main ions

List of cytosolic and extracellular ion concentrations under physiological conditions. the equilibrium potentials of these important ions build up the final potential of the cell, the membrane potential. Ca^{2+} channels are an exception since they are mainly closed, meaning that Ca^{2+} does not considerably influence the resting membrane potential (derived from https://basicmedicalkey.com/pharmacology-of-cell-excitation/).

1.3.2 Transmembrane proteins for ion permeability

The cell membrane is a barrier between the extracellular space and the cytosol or the cytosol and the lumen of intracellular compartments. Because of its hydrophobic bio-chemical composition it prevents big and/or hydrophilic molecules from passing. To make the cell membrane permeable for the important ions described in 1.3.1 and subsequently influence the membrane potential, it is necessary to have specific transmembrane proteins allowing the ions to pass the membrane; either in a passive or active manner. In the following chapter the most common classes of transmembrane proteins will be described (Silbernagl and Despopoulos 2012; Fahlke et al. 2015; Speckmann et al. 2013).

1.3.2.1 Channels

Channels are transmembrane proteins that create hydrophilic and highly selective pores, allowing just specific molecules to enter the cell/compartment. They can change between two different conformations: a closed and an open conformation. Three main different subtypes of channels are known, based on their ability to switch the conformation: (1) voltage-gated ion channels open after a change of membrane potential, (2) ligand-gated ion channels open after binding a ligand (extracellular or intracellular) and (3) mechanical-ly opened channels. Once the channel is open, it allows the fast diffusion through the membrane. Some channels are specific just for one ion but there are also not selective channels like AMPA which is permeable for Na^+ and K^+ or NMDA which is permeable for Na^+, K^+ and Ca^{2+} (Speckmann et al. 2013; Silbernagl and Despopoulos 2012).

1.3.2.2 Primary, secondary and tertiary active transporter

While in channels the electrochemical gradient is the only driving force for the transport through the membrane (passive transport), other transmembrane proteins make use of a secondary force that provides the energy to transport molecules against their electrochemical gradient into or outside the cell. They are distinguished into three main groups: the primary, secondary and tertiary active transporters.

The primary transporters or ion pumps use the hydrolysis of an energy provider – mainly ATP - to transfer ions against their electrochemical gradient through the membrane. By doing so, an ion pump is responsible for establishing and maintaining the membrane potential and providing a steep ion gradient which is needed for secondary transporters.

A secondary transporter has one or several binding sites for its ion. Binding of the ion(s) to the binding site leads to a conformation change, which brings the ion(s) onto the opposite side of the membrane. Some transporters carry just one type of ion from one side of the membrane to the other (uniporter). Other transporters couple the transfer of two different types of ions by using the electrochemical gradient of one of them to move the other one against its gradient. If the transfer of both is catalyzed in the same direction the transporter is termed symporter, while the protein transferring the ions in the opposite direction is called antiporter.

Tertiary transporters use gradients prior established by secondary transporters. This kind of transporter plays an important role in the re-absorption of dipeptides in the renal tubule.

The maximal velocity (V_{max}) reflects how fast the transporter can catalyze the reaction. Another important value for the interpretation of the kinetics of the transporter is the affinity of the protein to its ion (K_m or K_D). It describes the ion concentration at which half of the transporters binding sites are occupied. A high K_D means the transporter has a low affinity to the ions, with a low K_D the transporter has a high affinity. Like in enzymes transporter can also have competitive inhibitors, meaning inhibitors can bind to the ion binding site and block the transport (Speckmann et al. 2013; Fahlke et al. 2015).

1.3.3   Oligodendroglial transmembrane proteins

In previous chapters it was already discussed that maturation of oligodendrocytes is enhanced, if connections between immature oligodendrocytes and axons are established. Since axons are capable of vesicular glutamate (Ziskin et al. 2007; Kukley, Capetillo-Zarate and Dietrich 2007) and ATP release (Stevens et al. 2002), while OPCs express several receptors for glutamate and ATP (Ziskin et al. 2007; Káradóttir et al. 2005; Luyt, Varadi and Molnar 2003; Matute et al. 2007; Kirischuk et al. 1995), it was demonstrated that other axon-glial communications in addition to cell-cell contact promote myelination. However, neuronal fibers contain only a small number of vesicles and the axon-OPC cleft is relatively wide (Ziskin et al. 2007; Kukley, Capetillo-Zarate and Dietrich 2007). This suggests that in addition to neurotransmitters other pathways may exist to mediate neuron-OPC interactions.

In fact, the application of $[K^+]_e$ to 15mM reduces $[Na^+]_i$ in OPCs from 15mM to 4.7mM (Ballanyi and Kettenamann 1990), but it was also shown that $[K^+]_e$ elevation can induce responses of $[Ca^{2+}]_i$ via voltage-gated calcium channels (Paez et al. 2009; Kirischuk et al. 1995) and/or the switch of NCX into reverse mode (Belachew et al. 2000; Chen et al. 2007). Interestingly, it has been demonstrated that NCX in OPCs appears to be of crucial importance for myelination, since a knock-out of the NCX3 isoform in mice led to reduced MBP synthesis in cultured OPCs and a hypomyelination of the spinal cord of knock-out animals.

1.3.4 Na^+/Ca^{2+} exchanger (NCX)

Homeostasis of important cations between extracellular, cytosolic and subcellular compartments is crucial for maintaining membrane potential and ion signaling in all kind of cells. Calcium is the most important secondary messenger in the cell and plays a role in nearly all processes responsible for cell survival and function (e.g. cell contraction, hormone secretion, gene transcription and control of enzyme activity). Because of its chemical structure it can bind to several different molecules. Therefore it is important to keep the intracellular Ca^{2+} levels at a very low concentration (~100nM) (Giladi, Tal and Khananshvili 2016).

One of the most important antiporters controlling $[Ca^{2+}]_i$ levels is the NCX. NCX exchanges three Na^+ ions for one Ca^{2+} ion, while the normal direction is transporting Na^+ into the cell and Ca^{2+} out of the cell. Since it is an electrogenic antiporter, the direction of its function depends on Ca^{2+} and Na^+ transmembrane gradients and membrane potential, meaning that except its forward direction, where it extrudes Ca^{2+}, it can also shift into reverse mode and intrude Ca^{2+} (Khananshvili 2013; Khananshvili 2014). It has a low Ca^{2+} affinity and a high transport capacity, giving it the possibility to make rapid adjustments (Clapham 2007). Three different genes are known to belong to the NCX family: NCX1, NCX2 and NCX3 and are widely expressed in various mammalian species, but also in nonmammalian species like Drosophila or Xenopus (Blaustein and Lederer 1999). The gene consists of 12 exons, which can generate at least 17 splice variants by alternative splicing (Giladi et al. 2016). X-ray structure analysis of archeal NCX_Mj (Methanococcus jannaschii) revealed the architecture of the protein: it consists of 10 transmembrane helices (TM) which are arranged in 'pseudosymmetrical halves' (TM1-5 and TM6-10) and containing highly conserved regions (a-repeats). Four binding sites were detected, referred to as internal (S_{int}), external (S_{ext}), Ca^{2+}-binding (S_{Ca}) and middle (S_{mid}), all located in the center of the protein and occluded from the environment. TM1 and TM6 build the ion transport core and seem to form a cluster whose sliding is believed to be the main conformational change during the transport cycle. Mammalian NCX seems to consist of nine TMs with a large cytoplasmatic loop between TM5 and TM6 containig two Ca^{2+} binding domains (CBDs) (Figure 1-10). Binding of Ca^{2+} to its binding sites is the main factor for NCX regulation. Even though big steps in revealing the structure of NCX were made, its exact mechanism is still poorly understood (Giladi et al. 2016).
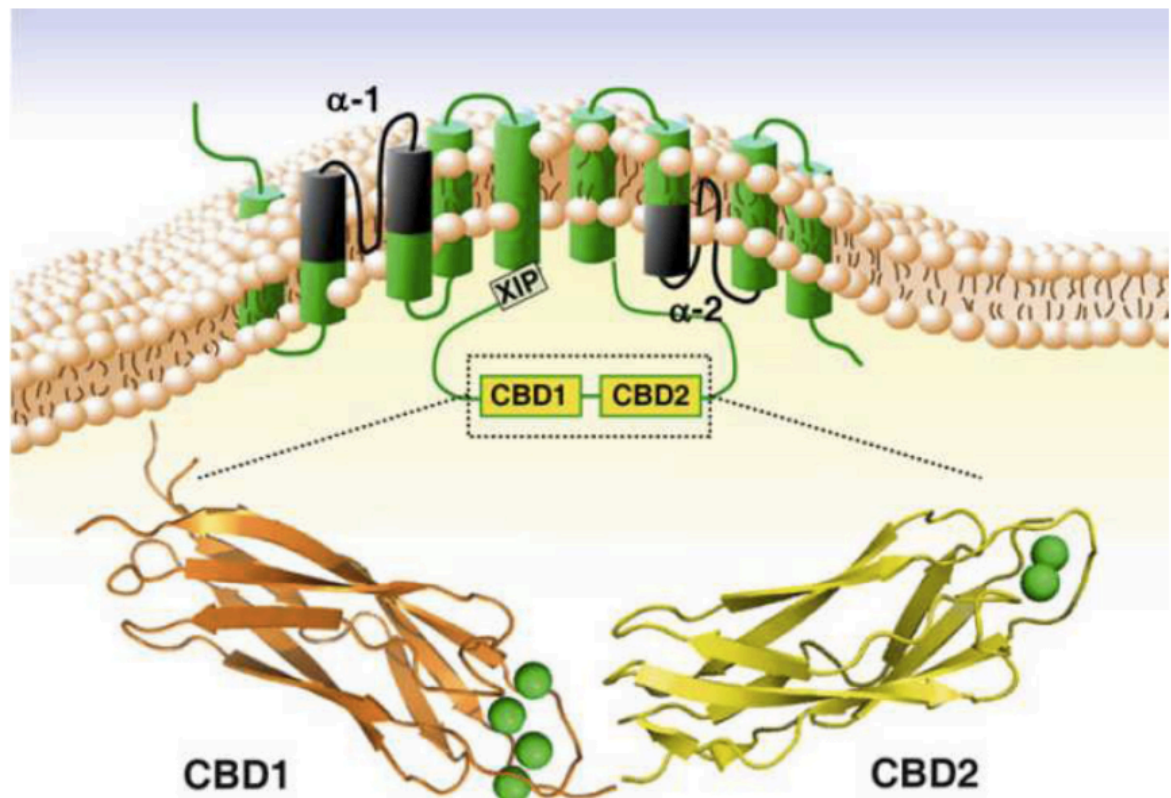
Figure 1-10: Na$^+$/Ca^{2+} exchanger

Schematic representation of the molecular structure of the NCX1. The extracellular space is on top, the cytosolic part of the cell at the bottom. The highly conserved pseudo symmetrical halves with the alpha regions critical for transport (α-1 and α-2) are marked in black. Both halves are linked by an intracellular loop, containing two Ca^{2+}-binding domains (CBD1/2) which are needed for exchange activity. The green balls in the magnification of the CBD1/2 domain represent bound Ca^{2+} (from Nicoll et al. 2013).

1.3.5   Na$^+$/K$^+$ ATPase (NKA)

In chapter 1.3.1 it the importance of NKA for maintaining a steep electrochemical gradient was already mentioned. In this chapter, this ion pump is introduced in a more detailed way.

NKA is expressed in all cells and its minimal functional composition consists of a catalytic (α) subunit with a molecular mass of about 100 kDa and a glycoprotein (β) subunit with a molecular mass of 55 kDa, required for the correct incorporation of the enzyme complex into the membrane (Blanco 2005; Crambert et al. 2000) (Figure 1-11). Investigations of the catalytic and functional properties of this enzyme revealed the existence of several

isoform of each subunit. Four different α subunits (Shull, Greeb and Lingrel 1986; Shamraj, Lingrelt and Hoffman 1994) and four β subunits were identified. Additionally some auxiliary proteins like FXYD polypeptides were reported (γ subunits) (Kuster et al. 2000). The different isoforms of the NKA are non-homogeneously expressed in the CNS. $\alpha 1$ is the most abundant isoform and is ubiquitously expressed by all cells. NKAs containing the $\alpha 1$ subunit show a high affinity for $[Na^+]_i$ and $[K^+]_e$, leading to the conclusion that they play a housekeeping role in all cells. The $\alpha 3$ subunit is expressed by neurons and is believed to be activated by increased $[Na^+]_i$ levels after bursts of action potentials. Glial cells (astrocytes and oligodendrocytes) mainly express the $\alpha 2$ isoform of the NKA ($\alpha 2$-NKA). The $\alpha 2$-NKA has a lower apparent affinity for $[Na^+]_i$ and $[K^+]_e$ and is voltage- and $[Ca^{2+}]_i$-sensitive (Blanco 2005; Crambert et al. 2000; Blanco and Mercer 1998). These $\alpha 2$-NKA properties suggest that it may function as a neuronal activity sensor. Intriguingly, the expression of $\alpha 2$-NKA has been demonstrated in neuron-OPC co-cultures and in the optic nerve during the myelination phase but the expression in OPC monocultures has not yet been shown. Furthermore $\alpha 2$-NKA of astrocytes shows the same distribution as the Na^+/K^+ exchanger, indicating a possible coupled contribution of these two transmembrane proteins in local ion homeostasis (Juhaszova and Blaustein 1997). Tissue specific expression of the different isoforms is shown best by the $\alpha 4$ subunit, which is only expressed in testis (Shamraj, Lingrelt and Hoffman 1994; Blanco et al. 1999), more precisely in spermatozoa, where its inhibition leads to an elimination of sperm motility (Woo, James and Lingrel 2000).
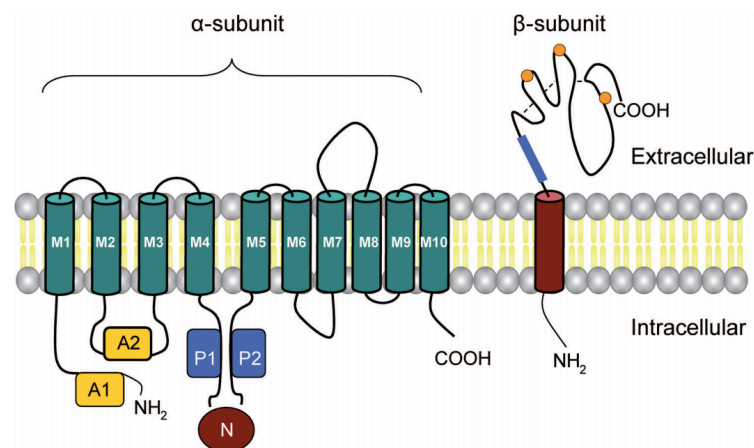
Figure 1-11: Na$^+$,K$^+$-ATPase (NKA)

Schematic representation of the molecular structure of the NKA. On the left side the catalytic α subunit with its ten transmembrane α-helices and the cytosolic N- (nucleotide binding), P- (phosphorylation), and A- (actuator) domains are depicted. The smaller β subunit on the right is anchoring the a subunit into the plasma membrane, but also influences the NKA functional activity (Benarroch, 2011).

A combination of heterologous expression and site-directed chemical labeling of cysteine mutants of the α subunit revealed five exposed extracellular loops, ten transmembrane segments since both termini are located intracellular and four intracellular loops (Figure 1-11). While the big external loop between transmembrane segment (M) 7 and 8 provides the contact region with the associated β subunit (Fambrough et al. 1994), three main intracellular structures were identified: one loop between M2 and M3 with a length of about 120 amino acids, a large central loop between M4 and M5 with a length of 420 amino acid residues and the N-terminal tail of 90 amino acid residues. Three important catalytic sites are formed by those structures: the nucleotide-binding domain (N) and the phosphorylation domain (P) are built by the M4M5 loop, the actuator domain (A) by the N-terminal tail (Toyoshima et al. 2000).

The β subunit is a protein with a size of about 370 amino acids from which around 300 amino acids reach into the extracellular space. It was first suggested that the β subunit was only necessary for the anchoring of the α subunit into the plasma membrane, but further experiments showed conformational changes of β when different ligands were

bound to the α subunit indicating its involvement in the NKA functional activity (Lutsenko and Kaplan 1994).

Figure 1-12 demonstrates a cycle of the active transport starting with the E_1 conformation of the enzyme. At the E_1 conformation $[Na^+]_i$ can bind to the protein leading to its phosphorylation by previously bound ATP. The phosphorylation of the enzyme leads to the conformation E_1P which occludes the bound Na^+ ions (Glynn and Karlish 1990). With another conformational change the Na^+ ions are released at the extracellular surface. At this state the protein is termed E_2P and it opens the K^+ binding site at the extracellular surface. The binding leads to a dephosphorylation introducing another conformational change occluding the K^+ ions (E_2K_2). Binding of ATP releases the K^+ ions at the inner surface and ends the catalytic cycle, changing the conformation of the enzyme from E_2K_2 to E_1 (Kaplan 2002).
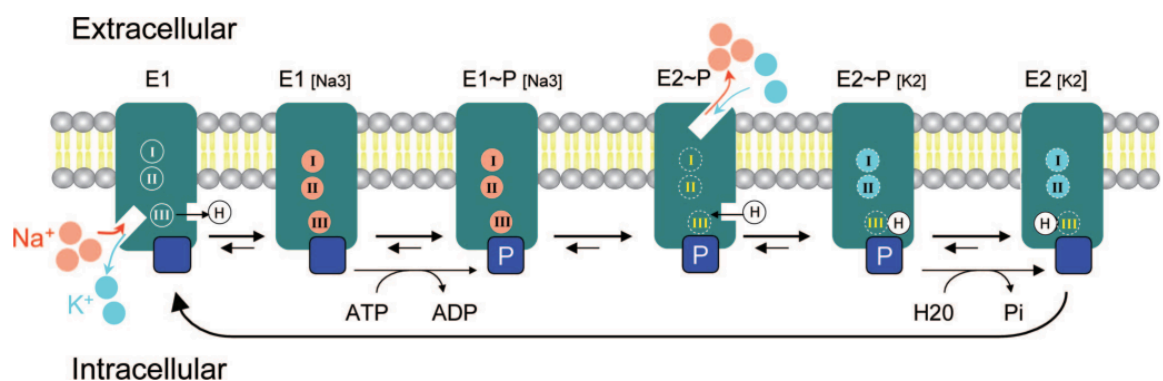
Figure 1-12: Mechanism of NKA's ion transport

Schematic representation of one enzyme cycle. Under the hydrolysis of ATP NKA transports 3 Na+ ions out of the cell and brings 2 K+ back into the cell (Benarroch, 2011). See text for details.

Besides its binding sites for Na^+, K^+, Mg^{2+}, NKA also has a binding site for glycosides like ouabain. This binding site is formed by the extracellular loops of M1/M2, M3/M4 and M5/M6 (Qiu et al. 2005). As a member of the cardiac glycosides ouabain belongs to a large pool of naturally derived compounds. It is a cardiotonic steroid that was initially discovered in plants and has later also been demonstrated to be an endogenous factor secreted by the adrenal glands of several mammals including humans (Schoner 2002). For

the biosynthesis of ouabain cholesterol and progesterone are processed which is under tight regulation by other hormones like renin-angiotensin, endothelin and adrenalin (Qazzaz et al. 2004). Ouabain is an NKA antagonist leading to its blockade. Blocking NKA subsequently increases the $[Na^+]_i$ which in turn can flip the nearby located NCX into reverse mode leading to a Ca^{2+} influx into the cell. This mechanism is best-studied in cardiac myocytes where the increase of $[Ca^{2+}]_i$ levels result in higher contractility of the cells and thereby helps to treat heart diseases. A high dose can completely block the NKA causing cell death. However it has also been shown that binding of nanomolar concentrations of ouabain to the NKA leads to a conformational change of the α subunit, which activates neighboring SRC proteins triggering a pathway that starts calcium oscillations (Zhang et al. 2006; Liang et al. 2006). This process is independent from its function as an ion pump (Segall et al. 2003).

1.3.6 Calcium signaling

The levels of Ca^{2+} concentrations between intra- and extracellular space differ with a magnitude of 10^5 units. The extracellular space has an average concentration of free Ca^{2+} of around several mM, whereas the cytosol shows a concentration of around 100 nM. Since Ca^{2+} is a highly reactive ion, it is believed that initially cells tried to reduce the cytosolic levels to avoid dangerous Ca^{2+}-protein interactions, but later in evolution invented mechanisms to use the binding energy for signal transduction. As Ca^{2+} is an ion and cannot be changed chemically to become inhibited, the cells had to find a way to chelate, compartmentalize or extrude it. In general, cells use a variety of channels, carriers, pumps and cytosolic buffers to control intracellular calcium levels. To achieve the very low intracellular Ca^{2+} concentrations, cells actively pump Ca^{2+} into intracellular calcium stores, such as the endoplasmatic reticulum (ER) via the sarcoendoplasmic reticular Ca^{2+} ATPases (SERCAs) or out of the cell via plasma membrane Ca^{2+} ATPases (PMCAs). Also carriers like NCX or the Na^+/Ca^{2+}-K^+ exchanger (NCKX) help extruding the Ca^{2+} ions out of the cell using the Na^+ transmembrane gradient (Silbernagl and Despopoulos 2012).

The initiation of calcium signaling usually happens through Ca^{2+} ion entry across plasma membrane via electrical or mechanical stimulation or through Ca^{2+} release from inner stores like the ER. While voltage-gated calcium channels (VGCC) are the fastest Ca^{2+} sig-

naling proteins, also the carrier NCX can flip its direction of ion transport depending on the membrane potential and/or the transmembrane ion gradients (see 1.3.4) and subsequently bring Ca^{2+} ions into the cell. Additional to VGCC and NCX, receptors like those for glutamate and ATP can lead to Ca^{2+} influx (Silbernagl and Despopoulos 2012).

In nonexcitable cells the Ca^{2+} release from the ER is achieved by hormone-receptor interaction. The most common way here is the IP3 pathway. Two receptor classes mediate this pathway: 1) G protein-coupled receptors (GPRs) and 2) receptor tyrosine kinases (RTKs). While GCRs activate the phospholipase Cβ (PLCβ), RTKs activate phospholipase Cγ (PLCγ). Both phospholipases cleave phosphatidylinositol (4,5)-bisphosphate (PIP2) into diacylglycerol and inositol (1,4,5)-trisphosphate (IP3) from which the latter acts as a second messenger and binds to IP3 receptors at the ER membrane. This binding subsequently leads to a Ca^{2+} release from ER stores (Clapham 1995).

Special protein domains like EF hand domains (from E and F regions of parvalbumin) evolved in hundreds of cells where Ca^{2+} is bound within a 12 amino acid loop and chelated via amine and carboxylate groups. Calmodulin (CaM) is an important Ca^{2+}-binding protein containing four EF hand domains and is expressed in all eukaryotic cells. Binding of four Ca^{2+} ions leads to a conformational change allowing the protein to interact with and activate numerous target proteins. For example, interaction of the Ca^{2+}/calmodulin complex counters the autoinhibition of the catalytic domain of the calmodulin kinase (CaMK) family enzymes, leading to an autophosphorylation and subsequently activation of the enzyme (Silbernagl and Despopoulos 2012; Speckmann, Hescheler and Köhling 2013).

In oligodendrocytes Ca^{2+} signaling has been shown to be involved in maturation and myelination (Simpson and Armstrong 1999; Waggener et al. 2013). In OPCs, where golli myelin basic proteins were over-expressed, slow Ca^{2+} oscillations were detected, followed by a stimulation of cell migration (Paez et al. 2009), though the treatment led to hypomyelination *in vitro* and *in vivo* (Jacobs et al. 2009). In the contrary, it was demonstrated that MBP expression inhibits Ca^{2+} influx after depolarization in mature oligodendrocytes (Smith et al. 2011). Additionally, it was shown that intracellular monovalent ions can influence MBP folding (Nowak and Berman 1991) and MBP-lipid interaction (Jo and Boggs

1995).

1.4   Aim of the study

One oligodendrocyte is able to myelinate several axonal segments at the same time. Recent studies suggest that the strength of myelination depends on the axonal diameter and its activity. Like in synapses, also axons are capable of vesicular glutamate and ATP release. In addition to this, it has been demonstrated that OPCs express different ionotropic and metabotropic receptors like NMDA, AMPA, metabotropic glutamate, P2X und P2Y receptors. However, electrophysiological and electron-microscopy data show that there are only small amounts of vesicles in axons and the axon-oligodendrocyte cleft is realtively wide. In addition it has also been shown that axonal vesicles are not always co-localized with oligodendrocyte processes, indicating that there might be more ways to provide a communication between axons and OPC processes.

Kirischuk et al. (Kirischuk et al. 1995) showed that small elevation of extracellular K^+ (10 or 20 mM) induces Ca^{2+} transients in the tips of OPC processes. It was also demonstrated that protein-tyrosine phosphatase alpha (PTPα) dephosphorylates Fyn and thereby activates it (Wang et al. 2009). This in turn leads to local translation of MBP mRNA (Krämer-Albers and White 2011). Since in neurons the Ca^{2+}-mediated activation of CaMKII is suggested to phosphorylate and activate PTPα, it could be assumed that this cascade ($Ca^{2+} \rightarrow$ CaMKII $\rightarrow$ PTP$\alpha \rightarrow$ Fyn) may be functional in oligodendrocytes processes.

The aims of this study were to answer the following questions:

1) Do intracellular Na^+ and Ca^{2+} concentrations in OPCs show developmental changes?

2) Do OPCs demonstrate spontaneous Ca^{2+} transients in any specific time-winow during development?

3) Can NCX and/or NKA partial blockade influence Ca^{2+} transients? If so, in which time-window does it occur?

4) Does Ca^{2+} activity affect MBP synthesis and in which time-window?

2   Material & Methods

2.1   Devices and Materials

Table 2-1 Devices and Materials

Designation	Name	Company
Cell dissociation	gentleMACS™ Octo Dissociator	Miltenyi Biotec
	quadro MACS	Miltenyi Biotec
	MACS Mix	Miltenyi Biotec
Centrifuges	Centrifuge 5415R	Eppendorf
	Centrifuge 5424R	Eppendorf
	MiniSpin plus	Eppendorf
	Labofuge 6000	Heraeus
	Micro centrifuge	Roth
	Megafuge 1.0R	Thermo Scientific
Gel running chambers	Mini-Protean Tetra System	Biorad
	Novex Mini Cell	Invitrogen
	Mini Gel II	VWR
Heating block	DRI-Block DB2D	Techne
Imaging station	Chemidoc XRS	Biorad
Incubators	Orbital incubator SI50	Stuart
	Hera Cell 240(i)	Heraeus
	Teco 20	Selutec

Magnetic stirrer	MR-Hei-Standard	Heidolph
Microscopes/Objectives	LEITZ DMRIB	Leica
	TCS SP5	Leica
	40x HCX PL APO CS 1.3 oil	Leica
	IX81	Olympus
	20x objective UPlanFLN (NA=0.50)	Olympus
	40x objective UPlanFLN (NA=0.75)	Olympus
	Flourescence CCD-Camera XM10	Olympus
	Axioscope FS	Zeiss
	20x water immersion objective	Zeiss
Monochromator	Polychrome II	Till Photonics
Microwave	DMW120	Durabrand
pH benchtop meter	FiveEasy Plus	Mettler Toledo
Pipettes	Research	Eppendorf
Pneumatic isolation mount	Type XL-G	Newport
Pump	Vacusip	Integra
Rocking shaker	Duomax 1030	Heidolph
Scales	EX2202	Ohaus
	EX224	Ohaus
Sterile working benches	Biowizard	Kojair
Temperaturcontroller	Temperaturcontroller III	Luigs & Neumann

Thermomixer	Thermomixer comfort	Eppendorf
Tissue chopper	McIlwain Tissue Chopper	Ted Pella, Inc
Vortexer	RS-VA10	Phoenix Instruments
Vibrating Microtome	5000mz	Campden Instruments

Materials

Glassware was purchased from Schott or Gibco. Cell culture plastics as well as Falcon tubes were purchased from Greiner, Nunc or Sigma-Aldrich.

2.2   Reagents, buffers and solutions

2.2.1   Reagents

Table 2-2: Reagents

Name	Ref. number	Company
Agarose NEEO Ultra-Qualität	2267.2	Roth
ANG2	91007.1	TEFLAB
Anti-AN2 Microbeads	130-097-170	Miltenyi Biotec
ATP magnesium salt	A9187	Sigma-Aldrich
Cadmiumchlorid	210B897411	Merck
DAPI	D9542	Sigma-Aldrich
DMEM	31966-021	Life Technologies
DMSO	D8418/A994.1	Sigma-Aldrich/Roth
EDTA	X986.1	Roth
Ethanol (70%/99%)	T913.3/5054.3	Roth

Fura-2, AM	F1201	Invitrogen
Glucose	X997.2	Roth
Glutamax	35050-038	Life Technologies
Glycin	3790.1	Roth
HBSS	14175-053	Life technologies
HCl, 37%	2607.1	Roth
Horse serum	26050-088	Life Technologies
Immobilon ™ Western Chemiluminescent HRP Substrate	WBKLS0500	Millipore
KCl	6781.3	Roth
KB-R7943	1244/10	Tocris
MACS NeuroBrew-21	130-093-566	Miltenyi Biotec
MEM	31095-029	Life technologies
Methanol	4627.1	Roth
MgCl	2189.2	Roth
Milk powder	T145.3	Roth
NaCl	HN00.2	Roth
Neural Tissue Dissociation Kit (P)	130-092-628	Miltenyi Biotec
NuPAGE® LDS Buffer (4x)	NP0007	Life technologies
NuPAGE® MOPS SDS Running Buffer (20x)	NP0001 NP0002	Life technologies
OGB-1-AM	06806	Invitrogen
Ouabain	ALX-803-050-C100	Enzo Life Science

PenStrep	15070-063	Life Technologies
Phosphatase inhibitor	04906837001	Roche Applied Science
Pluronic F-127	P3000MP	Invitrogen
Protease inhibitor	04693159001	Roche Applied Science
RNAiMax	P/N56531	Life technologies
Roti Histofix (PFA)	P087.5	Roth
SBFI-AM	S1263	Invitrogen
TRIS	AE15.2	Roth
Triton X-100	T-8787	Sigma-Aldrich
Tween20	P1379	Sigma-Aldrich

2.2.2   Buffers, media and solutions

Table 2-3: Buffers, media and solutions

Buffer/Medium/Solution	Composition
ACSF	125 mM NaCl; 2.5 mM KCl; 10 mM glucose; 1.25 mM NaH_2PO_4, 25 mM $NaHCO_3$, 2.5 mM $CaCl_2$ and 1 $MgCl_2$. pH was buffered to 7.3 by continuous bubbling with 5% CO_2/95% O_2 mixture
Agarose gel, 1.5%	1,5 g Agarose NEEO Ultra; 100 ml 1x TAE
Blocking solution	4% (w/V) milk powder in TBST
DMEM 1%/10% HS	DMEM + 1%/10% horse serum
GHG medium	100 ml MEM (1x) + GlutaMAX I + Earle`s Salts + 25 mM HEPES; 50 ml Horse Serum;

	45 ml HBSS; 1 ml Glutamax [200 mM]; 4 ml Glucose [300 mg/ml] diluted in HBSS; pH 7,2
Lysis buffer	50 mM Tris; 150 mM NaCl; 1 mM EDTA; 1% (v/v) Triton X-100; 1 PhosStop Phosphatase Inhibitor; 1 Complete EDTA-free Protease inhibitor
MACS Cultivation Medium	MACS Neuro Medium; 2 mM Glutamine; 1:50 NeuroBrew; 100 units Penicil-lin/Streptomycin
Mowiol	7,2 g Mowiol 4-88; 18 g glycerol; 18 ml H_2O; 36 ml 0,2 M Tris
SDS Running Buffer	10x Rotiphorese 1:10 or 20x MOPS 1:20 diluted in ddH_2O
PBS	150 mM NaCl; 8 mM Na_2HPO_4; 1,7 mM NaH_2PO_4; pH 7,2
Poly-L-lysine (PLL)	1 g Poly-L-lysine diluted in 1 l dH_2O
TAE (50x)	242 g Tris (2 M); 100 ml 0,5 M EDTA pH 8,0 (50 mM); 57,1 ml acetic acid; fill up with ddH_2O until 1 l
TBS	150 mM NaCl; 50 mM Tris; pH 7,2
TBST	TBS + 0,1% (v/v) Tween 20
Western Blot Stripping Buffer	1 M Glycin; pH 2,0
Western Blot Transfer Buffer	24 mM Tris; 192 mM Glycine; 20% (v/v) Ethanol abs.

2.3   Software

Table 2-4: Software

Software	Developer
MS Office 2013	Microsoft
Photoshop C55	Adobe
ImageJ	Open source, NIH
LAS AF Microscope Software	Leica
Mendeley Desktop	Mendeley Ltd.
Origin 7.5	OriginLab
GraphPad Prism 5	GraphPad Software Inc.
CorelDraw X7	Corel
Image Lab	Biorad

2.4   Antibodies

Table 2-5: Antibodies

Monoclonal primary antibodies				
Antigen	**Antibody Name**	**Host**	**Application**	**Company**
α-tubulin	T6199	mouse	1:5000 WB	Sigma-Aldrich
CNPase	C5922	mouse	1:50 ICC	Sigma-Aldrich
MBP	MCA409S	rat	1:500 WB/IHC; 1:50 ICC	AbDSerotec
SMI-312 (neurofilament)	ab24574	mouse	1:1000 IHC	Abcam

Polyclonal primary antibodies				
Antigen	Antibody Name	Host	Application	Company
ATP1A2 (α2-NKA)	55179-1-AP	rabbit	1:800 WB; 1:20 ICC	Proteintech
GAPDH	A300-641A	rabbit	1:5000 WB	Bethyl
Olig-2	AB9610	rabbit	1:1000 ICC	Milliopre

2.5   Cell culture

2.5.1   Preparation and culturing of primary oligodendrocytes

Primary OPC cultures were prepared from postnatal day (P) 8-10 C57BL/6J mouse brains using MACS Technology (MiltenyiBiotec). The brains were dissociated with the Neuronal Tissue Dissocation Kit (Papain) and the gentle MACSDissociator (MiltenyiBiotec) according to the manufacturer's protocol. Instead of Ca^{2+} and Mg^{2+}-containing Hanks' Balanced Salt Solution (HBSS), the cells were resuspended in DMEM + 1% horse serum (HS). Isolation of OPCs was achieved by using the anti-AN2 (NG2 orthologin mice) MicroBeads (MiltenyiBiotec). Isolated OPCs were subsequently plated on 0.01% poly-L-lysine-coated wells of 24-well plates (Greiner) in MACS Neuro Medium containing 2% (v/v) NeuroBrew-21 (MiltenyiBiotec), 2 mM L-glutamine and penicillin-streptomycin (100 U/ml). For imaging and immunocytochemistry experiments glass coverslips were placed in the wells before coating. Every second day half of the medium was replaced with new culture medium.

2.5.2   Preparation and culturing of cortical organotypic slice cultures (Cosc)

Cortical organotypic slice cultures were prepared from P3 C56BL/6 mice and cultured similar as described previously (Denter et al. 2010; Stoppini, Buchs and Muller 1991). Briefly, mice were killed by decapitation. Brains were quickly removed and transferred into ice-cold culture medium with the following composition: MEM (Gibco) supplemented with 25% horse serum and HBSS+/+, 1 mM Glutamax, 6 mg/mL of glucose, and pH adjusted to 7.2. Neocortical hemispheres were isolated from the hippocampus, thalamus, and striatum, and 350 µm thick coronal slices containing the parietal cortex were cut with a tissue

chopper (McIlwain, Mickle Laboratory Engineering, Surrey, UK). Cortical slices were transferred onto Millicell membranes (Sigma-Aldrich) placed into 35 mm Petri dishes as support for explants. Slices were kept at 37 °C in humidified 95% air and 5% CO_2. Culture medium was renewed every 3 days.

2.5.3   Preparation of acute callosal slices

All experiments were conducted with pigmented C57BL/6J mice pups of P10-35. Animals were decapitated under deep isoflurane anesthesia. The brain was removed quickly and transferred into ice-cold saline that contained (in mM): 125 NaCl, 2.5 KCl, 10 glucose, 1.25 NaH_2PO_4 , 25 $NaHCO_3$, 0.5 $CaCl_2$, and 2.5 $MgCl_2$ constantly bubbled with 5% CO_2 /95% O_2 mixture (pH = 7.3). Coronal slices (300 M) were cut on a vibratome (Campden Instruments Ltd., UK). After preparation, slices were stored for at least 30 min at room temperature in artificial cerebrospinal fluid (ACSF) that contained (in mM): 125 NaCl, 2.5 KCl, 10 glucose, 1.25 NaH_2PO_4 , 25 $NaHCO_3$, 2.5 $CaCl_2$, and 1 $MgCl_2$. pH was buffered to 7.3 by continuous bubbling with 5% CO_2 /95% O_2 mixture. ACSF with elevated $[K^+]$ was prepared by equimolar replacement of 5 mM NaCl with 5 mM KCl.

2.6   Molecular biology

2.6.1   siRNA-Transfections

NG2+ primary oligodendrocytes ($1.25x10^5$/24well; $2,5x10^5$/12well) for immunocytochemistry and for Western blot analysis were seeded into 24well plates with 500 μl or 12well plates with 1000 μl MACS cultivation medium and cultured for up to six days. Cortical organotypic slice cultures (Cosc) were cultured on Millicell membranes (Sigma-Aldrich) in 6well plates using 1 ml GHG medium. After DIV2 the primary oligodendrocytes and Cosc were transfected using Lipofectamine RNAiMax (Life Technologies). An amount of 20 or 40 pmol siRNA was used for the transfection of the cell culture (for 24well or 12well); for cortical slice cultures 80 pmol siRNA was used.

Table 2-6: Mastermix 1

Reagent	24well	12well	6well
	Volume (µl)		
MACS cultivation medium/GHG	25	50	100
Lipofectamin™ RNAiMax	0.5	1	2

First, mastermix 1 was prepared and incubated for 5 minutes at room temperature. In the meantime mastermix 2 was prepared.

Table 2-7: Mastermix 2

Reagent	24well	12well	6well
	Volume (µl)		
MACS cultivation medium/GHG	23	46	92
siRNA (20µM)	2	4	8

After incubation of mastermix 1 mastermix 2 was added, resuspended and incubated for 20 minutes at room temperature. Afterwards the mixture was added to the primary oligodendrocytes/cosc.

Table 2-8: siRNAs

Name	Item	Company
siGENOME Mouse Atp1a2 SMARTpool; 5nmol	M059276010005	GE Healthcare Dharmacon
ON-TARGETplus SMART-pool mouse MBP; 5nmol	Not available anymore	GE Healthcare Dharmacon
ON-TARGETplus Non-targeting pool	D-001810-10-05	GE Healthcare Dharmacon

ATP1A2-siRNA (siGENOMESMARTpool siRNA, GCACUCCUCUGCUUCUUAG, GAUCAUCU-CUUCCCACGGU, GGACUGGGAUGAUCGGACU, AUAUCUAGGUAUCGUGCUA)

MBP-siRNA (ON-TARGETplusSMARTpool, CCUCACAGCGAUCCAAGUA, CUCCCAAGGCACAGAGACA, GGGCAUCCUUGACUCCAUC, GGCCACAGCAAGUACCAUG)

negative control-siRNA (ON-TARGETplus Non-targeting pool, UGGUUUACAUGUCGACUAA, UGGUUUACAUGUUGUGUGA, UGGUUUACAUGUUUUCUGA, UGGUUUACAU-GUUUUCCUA).

2.6.2 Lysate preparation

2.6.2.1 Lysate from primary oligodendrocytes

Primary oligodendrocytes were washed with cold PBS and afterwards scraped off the culture dish in ice-cold lysis buffer (Table 2-3). The lysates were incubated on a rotating wheel for 45 min at 4°C and then cleared from nuclei and debris by centrifuging at 2000x g and 4°C for 5 min. The supernatants containing the proteins were transferred to new reaction tubes.

2.6.2.2 Lysate from acute callosal slices

The brain was removed quickly and coronal slices of 1 mm were cut on a vibratome (Campden Instruments Ltd., UK). Afterwards the tissue from the corpus callosum area was extracted with a biopsy puncher (1 mm diameter) and immediately transferred into a

reaction tube containing 100 µl lysis buffer. After resuspending the tissue-buffer mixture, the lysates were incubated on a rotating wheel for 3 hours at 4°C and then cleared from nuclei and debris by centrifuging at 2000x g and 4°C for 5 min. The supernatants containing the proteins were transferred to new reaction tubes.

2.6.3   SDS-PAGE and Western Blotting

Proteins and molecular mass markers (Bio-Rad or NEB, USA) were separated by SDS-PAGEusing a Mini PROTEAN system (Bio-Rad) with 14% sodium dodecyl sulfate polyacrylamide gels at 175 V for 60 min or a NovexNuPAGE SDS-PAGE Gel system (Life technologies or Thermo Fischer scientific, USA) at 200 V for 50 min (MOPS buffer) and transferred onto Roti-polyvinylidenefluoride membranes (0.45 µm, Roth). Membranes were blocked in Tris buffered saline containing 0.01% Tween 20 and 4% milk powder for 30 min, probed with antibodies for 1 hour at room temperature and detected with horseradish peroxidase (HRP)-coupled secondary antibodies (1:10000, Dianova) in an enhanced chemiluminescence reaction. Images were acquired with a ChemiDoc™ XRS+ System (Bio-Rad). Densitometric analysis was performed by using the Image lab software (Bio-Rad).

2.6.4   Immunocytochemistry

2.6.4.1 Immunostainings of primary oligodendrocytes

For protein immunostainings OPC cultured were fixed with 4% paraformaldehyde for 15 min and permeabilized with 0.1% Triton-X-100 in PBS. DMEM+10% HS was used as blocking buffer for 15 min and primary antibodies were diluted in blocking buffer. OPC cultures were incubated in this medium for 1 hour. For detection, Cy2, Cy3 and Cy5 coupled secondary antibodies (Dianova) were diluted in blocking medium and incubated for 30 min at room temperature. Nuclei were stained with DAPI (Sigma, 1:1000) and cells were mounted in Mowiol.

2.6.4.2 Acquisition and analysis of immunocytochemistry

Images were acquired by using a 40x/0.75 NA objective lens connected to a monochrome fluorescence CCD-camera (XM10) and using cell^F software (Olympus). Images were adjusted with Adobe Photoshop and ImageJ software. The co-localization of α2-NKA and

MBP in the resulting images was quantified using the JACoP plug-in for ImageJ software ((Abràmoff, Magalhães, and Ram 2004), NIH, Bethesda, USA), which allowed the calculation of Pearson´s coefficient. This measure reflects linear correlation between the signal intensities and can range from -1 (mutual exclusion) to 1 (perfect co-localization). Costes´ automatic thresholding algorithm was used to exclude from the calculation background pixels in an observer-independent way (Bolte and Cordelières 2006). Three to four regions of interest with fixed dimensions (100 μm^2) were manually selected in order to isolate specific cellular structures, namely proximal processes, distal processes and myelin sheets. This selection was carried out based on morphological criteria and distance from the soma. Processes were considered proximal if they were located within 25 μm from the soma, or distal if the distance was more than 50 μm.

2.6.5 Immunohistochemistry

2.6.5.1 Immunostainings of cortical organotypic slice cultures

Before staining the slices were washed three times with PBS and subsequently fixed with 4% paraformaldehyde for one hour. Next the slices were washed again three times, 10 min each time. The fixed slices were then blocked for one hour with blocking solution containing 3% horse serum, 2% fetal calf serum and 0.5% Triton X-100 diluted in PBS. Next, the slices were incubated for three days with primary antibodies, which were diluted in the blocking solution. After three more washing steps with PBS slices were incubated with secondary antibodies for 24 hours. At the following day the slices were stained with DAPI, also diluted in blocking solution, placed on microscope slides and mounted with Mowiol.

2.6.5.2 Acquisition and analysis of immunohistochemistry

Images were acquired with a TCS SP5 confocal microscope using 40x HCX PL APO CS 1.3 oil objective connected to a fast resonance scanner and the LAS AF software (Leica Microsystems CMS GmbH). The bidirectional acquisition was done at a speed of 400 Hz. Image size was set to 2048x2048 pixels. The distance between planes in a Z-stack was set to 0.17 μm. Artefacts caused by scattered light from the culture membrane may occur during acquisition of the stacks. To avoid their inclusion, the first 1.7 μm from the bottom

were omitted from the later analysis. In order to quantify myelination a custom macro for ImageJ was developed. All stacks were pre-processed in order to maximize the signal to noise ratio using a combination of background subtraction, median filters and unsharp masks. ´Moments´ algorithm was then used to automatically determine threshold values for converting the greyscale stacks to binary stacks. For each slice in the neurofilament channel stack, the function ´Analyze particles´ was used to identify non-circular segments with sufficiently large areas (>25 µm), which were then used as a mask for the corresponding slice on the MBP channel. Therefore it was possible to calculate the average area of the neurofilaments per slice and of the fraction of their area which had overlapping MBP signal (expressed as percentage). While this step was repeated for the whole stack, the generated masks were collected in a separate stack, in order to allow visual control over the operation. This cycle was then repeated inverting the channels, with the MBP channel undergoing the ´analyze particles´ function to create a mask used for the evaluation of neurofilaments. This step allowed the calculation of average MBP segments area per slice, as well as the percentage of non-overlap between the masks and the neurofilaments channel (100-percentage of overlap), defined as free myelin.

2.7 Digital imaging

Sodium-binding benzofuran isophthalate (SBFI) was used to measure $[Na^+]_i$ levels. Fura-2 or Oregon Green BAPTA 1 (OGB1) were used to record $[Ca^{2+}]_i$ signals. To load OPCs with a Na^+- or Ca^{2+}-sensitive probe, coverslips with OPCs were incubated in artificial cerebrospinal fluid (ACSF) supplemented with 0.02% Pluronic F-127 and 10 µM cell-permeable form of selected indicator (SBFI-AM, Fura-2-AM or OGB1-AM) for 20 min at 36 °C. ACSF contained (in mM): 125 NaCl, 2.5 KCl, 10 glucose, 1.25 NaH_2PO_4, 25 $NaHCO_3$, 2.5 $CaCl_2$, and 1 $MgCl_2$. pH was buffered to 7.3 by continuous bubbling with 5% CO_2/95% O_2 mixture. After loading, cells were washed twice with ACSF and transferred into recording chamber (~0.4 ml volume) on the microscope stage (Axioscope FS, Zeiss, Germany) equipped with phase contrast optics. Measurements started after at least 15 min storage in ACSF to ensure deesterification of the indicator. Cultures were submerged with a constant flow of oxygenated ACSF. Flow rate was set to 2 ml/min. A 20x water immersion objective (Zeiss, Germany) was used in all experiments. At the end of each experiment

ATP (100 μM) was applied to check cell viability (Kirischuk et al. 1995). Only cells in which ATP-induced Ca^{2+} response was observed were used for further analysis.

The excitation wavelength was controlled by a fast monochromator system, and a cooled CCD camera was used to record fluorescence signals (TILL Photonics, München, Germany). SBFI and Fura-2 were alternatively excited at 360 and 390 nm. OGB1 was excited at 490 nm. The excitation and emission light was separated using a 510 nm dichroic mirror (Zeiss). Emitted light was filtered using a 530 nm long-pass filter (Zeiss). Images were acquired and evaluated using Vision 4.0 software (TILL Photonics). All measurements were performed using 2x2 binning. Exposure time was between 200 and 400 ms. Acquisition rate was set to one image per second. Background fluorescence was calculated from a region in the immediate vicinity of the tested cell and subtracted. OGB1 fluorescence signals were expressed as relative changes from pre-stimulus levels ($\Delta F/F_0$). Recorded signals from ratiometric dyes (SBFI and Fura-2) were expressed as a ratio ($R = F_{360}/F_{390}$).

All imaging experiments were performed at 32-33 $^{\circ}$C. Substances were applied for 2 min followed by at least 4 min washout period. ACSF with elevated $[K^+]$ was prepared by equimolar replacement of 5 mM NaCl with 5 mM KCl. Eight min of continuous recordings were used to characterize spontaneous Ca^{2+} activity in OPCs. As spontaneous Ca^{2+} transients in OPCs differ in shape and duration, evaluation of spontaneous activity were performed visually. Only events with a fast rise phase (approximately 1% DF/F_0 change within 3 consecutive frames) or a visually detectable inflection point on the rise phase were counted. Amplitude analysis of events was not performed because of their relatively low frequency.

2.8   Statistics

All results are presented as mean ± S.E.M. The error bars in all figures indicate S.E.M. Differences between means were tested for significance using One-way ANOVA with Tukey post-hoc test, unless otherwise stated. * symbolizes $p < 0.05$, ** - $p < 0.01$, *** - $p < 0.001$, ns - not significant.

3   Results

3.1   Myelination onset and intracellular ion changes coincide

Since the initiation of myelination seems to be driven at least in part by an intrinsic molecular program in oligodendrocytes, it was first decided to determine the onset of myelination in oligodendrocyte monocultures. MBP expression has been selected as a readout of "myelination" in this reduced (without neurons) model.
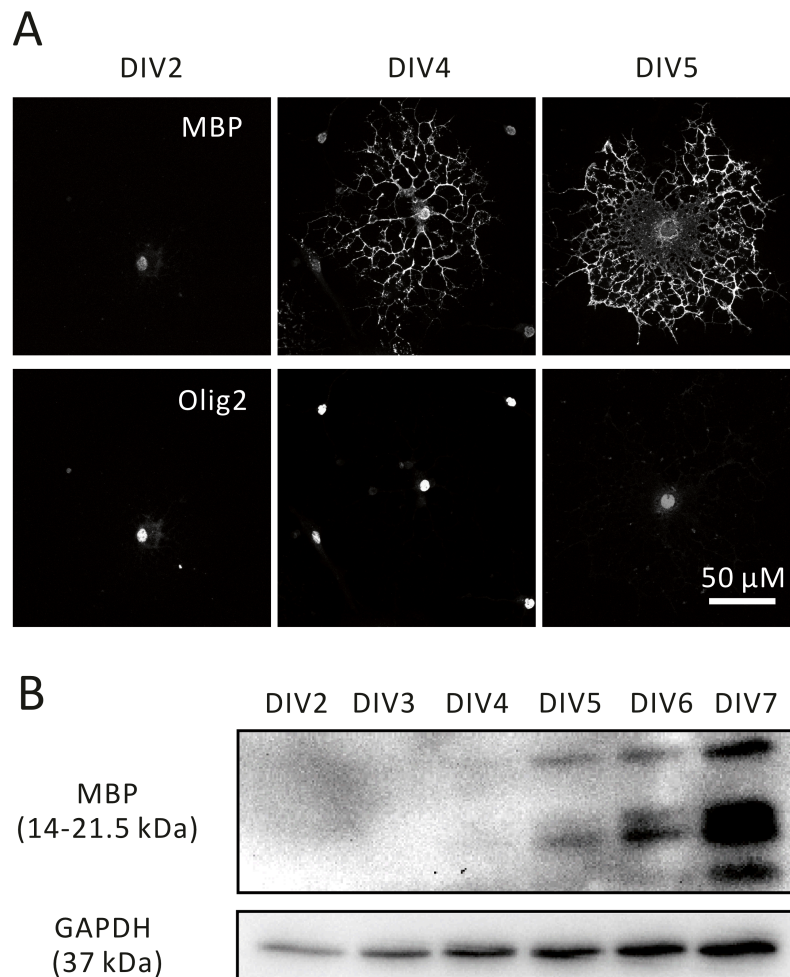

Figure 3-1: Time course of MBP synthesis in cultured OPCs

A) Representative MBP stainings performed at DIV2, 4 and 5. B) Representative Western blots demonstrate MBP levels in OPC cultures lysed at different DIVs. Detectable MBP synthesis commences between DIV4 and 5.

Immunocytochemistry and western blot analysis were applied at different time points in OL development. It was revealed that MBP synthesis starts at around DIV4 (Figure 3-1), which is in line with previously published findings (Dubois-Dalcq et al. 1986) and provesproper cell culture conditions for further experiments.

To check whether ionic changes coinside with MBP expression, intracellular resting calcium levels during the first week *in vitro* were measured using the ratiometric Ca^{2+} sensitive dye Fura-2. It could be shown that there is an increase of resting calcium levels around DIV4 with a peak in DIV5 (Figure 3-2, B). Corresponding values were 37±3 nM at DIV4 (n=49, three cultures) and 66±5 nM at DIV5 (n=43, three cultures). At DIV6 the Ca^{2+} levels significantly decreased again to 47±5 nM (n=31, three cultures, $p < 0.05$ as compared to DIV5).

The sodium calcium exchanger (NCX) has been shown to influence MBP synthesis (Boscia et al. 2012). As NCX is an electrogenic transporter, its operation modes depend on $[Ca^{2+}]_i$ as well as on $[Na^+]_i$. Therefore the ratiometric Na^+ sensitive dye SBFI was used to measure $[Na^+]_i$ in OPCs during the first week *in vitro*. In Figure 3-2 C it is shown that $[Na^+]_i$ were indeed significantly increased at DIV5 and dropped down to their normal levels at DIV6. Corresponding values were 15±1 mM (n=57), 17±1 mM (n=64, $p < 0.05$ as compared to DIV4) and 13±1 mM (n=36, $p < 0.05$ as compared to DIV5) at DIV4, DIV5 and DIV6.
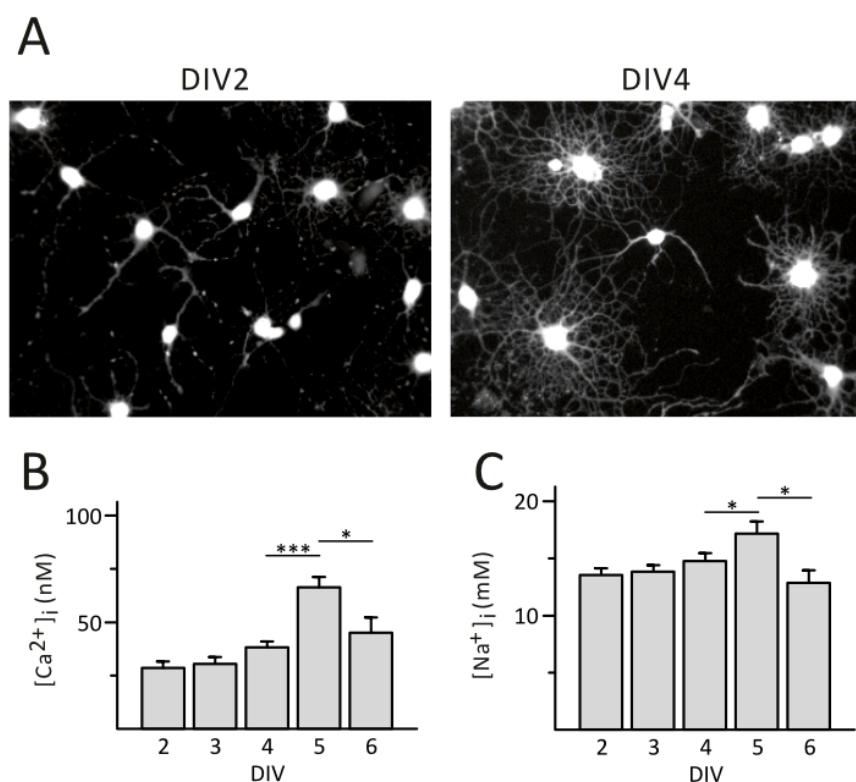
Figure 3-2: [Na$^+$]$_i$ and [Ca^{2+}]$_i$ levels during development in OPC monoculture

A) Representative images of OPC cultures at DIV2 and DIV4 stained with the Ca^{2+}-sensitive probe Fura-2. B) [Ca^{2+}]$_i$ in OPCs at different levels. Data obtained from three cultures at each DIV. C) [Na$^+$]$_i$ in cultured OPCs. Data obtained from three cultures at each DIV.

As developmental changes of [Ca^{2+}]$_i$ and [Na$^+$]$_i$ occur OPCs in culture, the next step was to test if these changes also occur in *in situ* situations. In rodents myelination of the corpus callosum starts around P10-15 and goes on until about P35 (Hamano et al. 1996). There-fore acute callosal slices from 3 different age groups (P10-15, P20-25 and P30-35) were used. The tissue was loaded with Fura-2 for [Ca^{2+}]$_i$ or with SBFI for [Na$^+$]$_i$ measurements (Figure 3-3). Also in slices a significant increase of [Ca^{2+}]$_i$ at P30-35 (34±3 nM, n=66, three mice) compared to P20-25 (26±2 nM, n=97, three mice, p < 0.05) could be shown. [Na$^+$]$_i$ even showed a significant increase already at P20-25 (15±1 mM, n=92, three mice) com-pared to the P10-15 group (9±1 mM, n=60, three mice, p < 0.001).
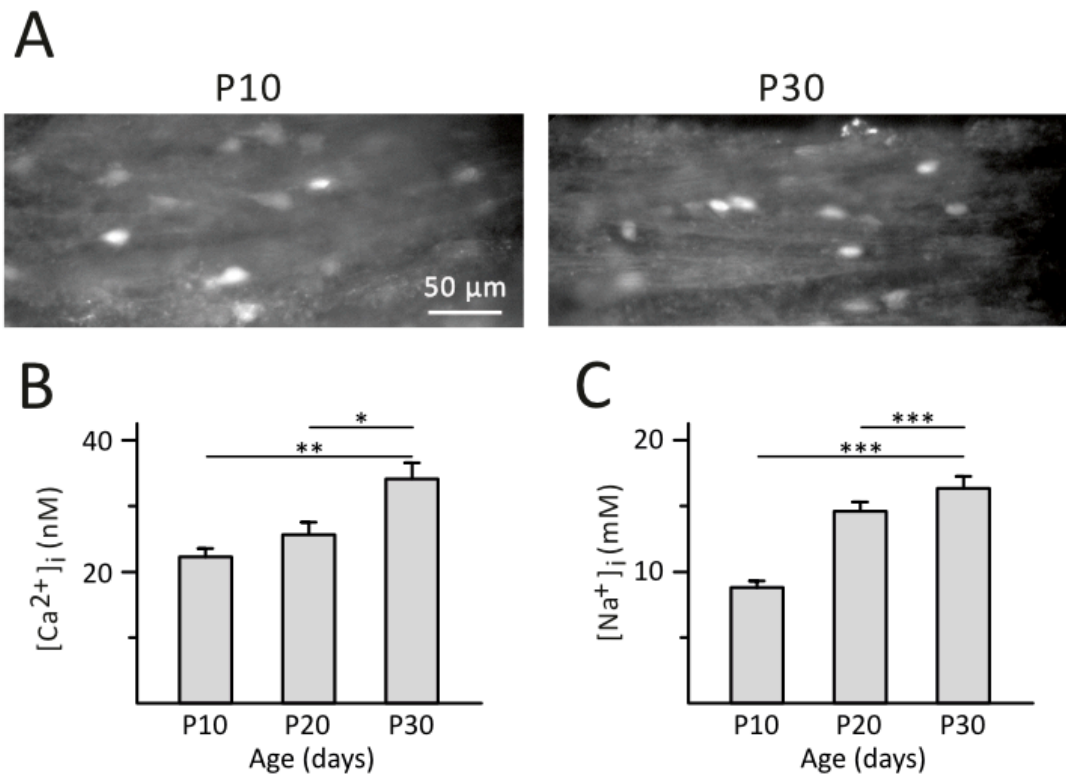
Figure 3-3: [Na$^+$]$_i$ and [Ca^{2+}]$_i$ levels during development in acute callosal slices

A) Acute slice of the corpus callosum from P10 and P30 mice stained with Fura-2, B) [Ca^{2+}]$_i$ in OPCs at different postnatal days (P). Data obtained from three mice at each age. C) [Na$^+$]$_i$ in OPCs at different postnatal days. Data obtained from three mice at each age.

3.2 Influence of the sodium-calcium exchanger in developmental ion changes

Because the onset of MBP synthesis and changes in the [Na$^+$]$_i$ and [Ca^{2+}]$_i$ in oligodendrocytes occur at the same time, it was assumed that both could be coupled. As it is already proven that NCX affects MBP synthesis (Boscia et al. 2012) and MBP synthesis is CaM-kinase dependent (Waggener et al. 2013), it was necessary to find out, if NCX works in this critical period in reverse mode, meaning that it brings Ca^{2+} into the cell. This could influence MBP expression.

To verify this hypothesis, OPCs of different developmental stages were loaded with SBFI. After a short period of baseline recordings KB-R7943, a blocker of the NCX reverse mode was applied.
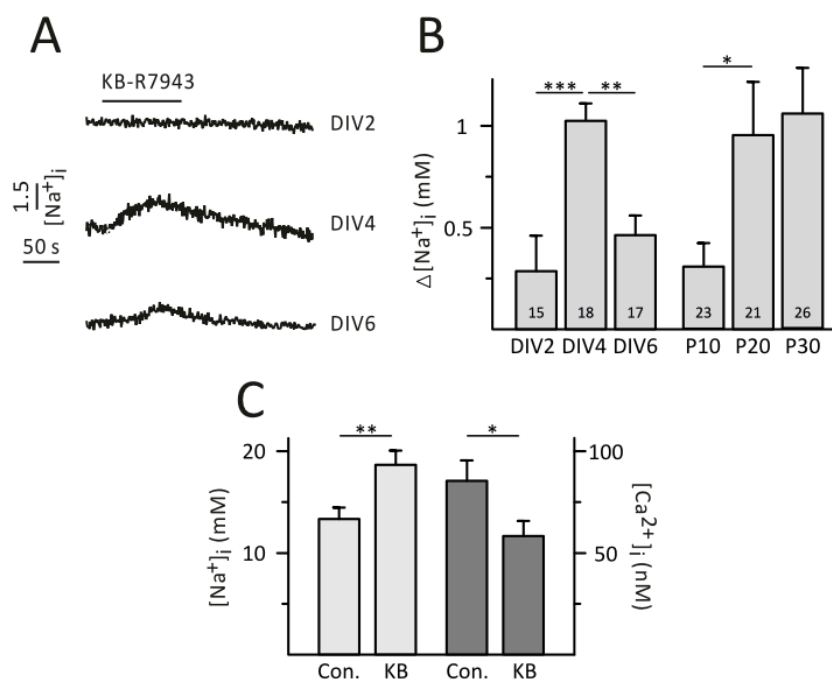
Figure 3-4: NCX in OPCs operates in reverse mode

A) Representative traces demonstrate that partial NCX blockade with KB-R7943 (1µM) results in $[Na^+]_i$ elevation in OPCs at DIV4 but not at DIV2. B) Statistical graph shows that KB-R7943 elicited larger $[Na^+]_i$ responses at DIV4 as compared to DIV2 and DIV6. In brain slices the KB-R7943-induced $[Na^+]_i$ elevation was larger at P20 and P30 as compared to P10. Numbers represent the number of cells tested. C) Incubation of DIV4 OPCs for 12 h with KB-R7943 (1µM) resulted in $[Na^+]_i$ increase and $[Ca^{2+}]_i$ decrease at DIV5 (2 cultures).

Figure 3-4 shows that OPCs in early developmental stage showed almost no response. In contrast, KB-R7943 triggered an increase of $[Na^+]_i$ in DIV4 OPCs. The $[Na^+]_i$ amplitude in OPC somata had its peak at 1.1±0.1 mM (18 OPCs, two cultures). Interestingly, the induced responses became smaller in later developmental stages, meaning that NCX in OPCs operated in reverse mode only in a small time window (DIV4-DIV5). These experiments performed in callosal slices revealed that KB-R7943 induced a rise of $[Na^+]_i$ starting at P20. In contrast to cultures, in slices from older mice KB-R7943-induced $[Na^+]_i$ rise did not decrease, allowing to suggest that the critical period lasts longer *in vivo* compared to OPC monoculture.

In the next experiments it was tested if chronic KB-R7943 application also influences $[Na^+]_i$, $[Ca^{2+}]_i$ and MBP synthesis in OPC cultures. DIV4 OPC cultures were treated with KB-R7943 for 12 hours. Figure 3-4 C shows an increase of $[Na^+]_i$ and a decrease of $[Ca^{2+}]_i$ compared to the control condition (two cultures, more than 17 OPCs per condition).
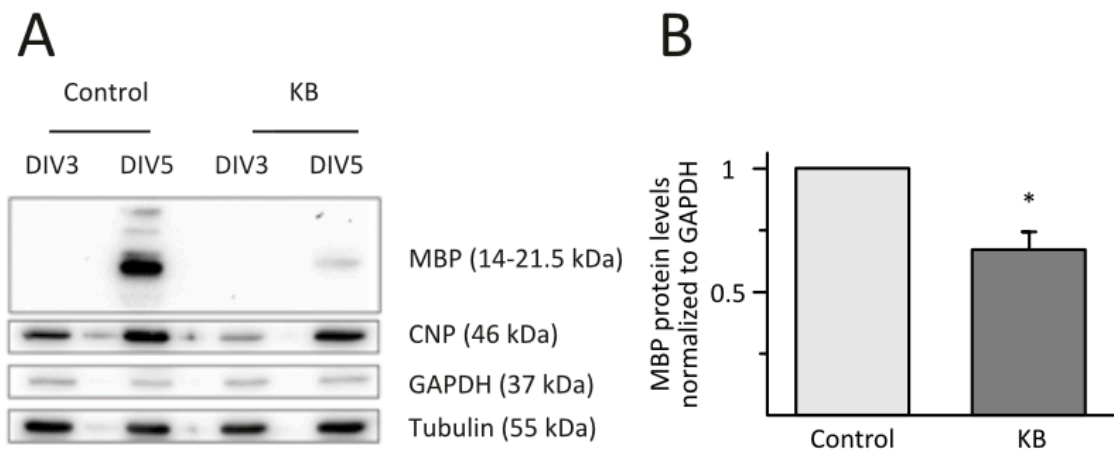
Figure 3-5: NCX influences MBP expression in OPCs

A) A representative Western blot shows that incubation with KB-R7943 (1 µM) suppressed MBP synthesis. The same treatment performed at DIV2 failed to stimulate MBP synthesis. B) Statistical graph illustrating suppression of MBP synthesis by KB-R7943 at DIV4 (5 cultures)

In addition to these findings, in Figure 3-5 it was further shown via densitometric western blot analyses that the chronic treatment of KB-R7943 led to reduced MBP levels (5 cultures, $p < 0.05$, one population Student´s test). These results suggest that NCX operating in reverse mode provides Ca^{2+} influx into the cell what might be needed to start the MBP synthesis.

3.3   Influence of a slight increase of $[K^+]_e$ on $[Na^+]_i$ and $[Ca^{2+}]_i$ levels and the synthesis on MBP

Neuronal activity leads to a mild increase of $[K^+]_e$ levels. Since NCX is an electrogenic transporter, the question arose whether depolarization of the membrane by an increase of $[K^+]_e$ leads to changes in the intracellular sodium and calcium concentration. First it was

tested if an application of potassium (+5mM) shows an effect on $[Ca^{2+}]_i$ levels at single cell levels. The cultures were examined at three different development stages:

(1) DIV2: before changes at the resting levels of $[Na^+]_i$ and $[Ca^{2+}]_i$ were determined

(2) DIV4: when peak of ion changes was determined

(3) DIV6: ion changes almost went back to initial data

In this case to measure intracellular calcium levels, cells were loaded with calcium sensitive probe *Oregon Green Bapta-1 (OGB1)*.
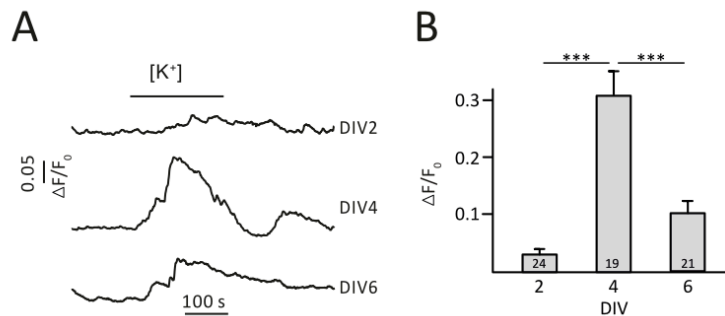
Figure 3-6: $[Ca^{2+}]_i$ transients elicited by elevated $[K^+]_e$ in cultured OPCs at different DIVs

A) $[Ca^{2+}]_i$ transients induced by elevated $[K^+]_e$ (+5 mM) in the OPCs at different DIVs. Bar above the traces depicts the application period. B) Statistical graph shows that elevated $[K^+]_e$ elicited larger $[Ca^{2+}]_i$ responses at DIV4 as compared to DIV2 and DIV6 (3 cultures at each DIV).

Figure 3-6 demonstrates that the application of elevated $[K^+]_e$ at DIV2 cultures did not change $[Ca^{2+}]_i$. However, this treatment led to a reliable $[Ca^{2+}]_i$ transients at DIV4. Further, evoked transients at DIV6 were significantly smaller than those at DIV4.
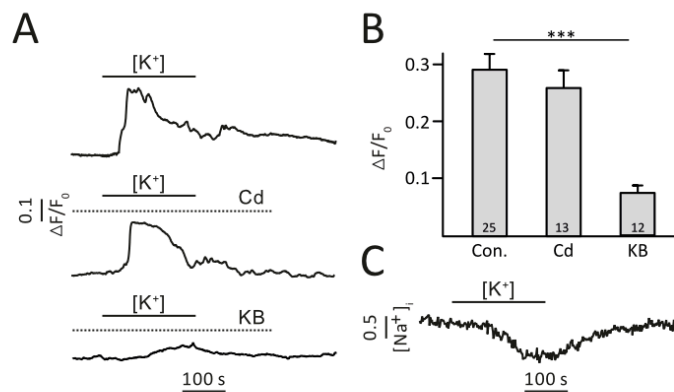
Figure 3-7: $[K^+]_e$ -induced $[Ca^{2+}]_i$ transients are linked with NCX activity

A) Representative $[Ca^{2+}]_i$ responses induced by elevated $[K^+]_e$ in control and in the presence of either Cd^{2+} (100 μM) or KB-R7943 (1 μM). B) Statistical graph shows that elevated $[K^+]_e$-induced $[Ca^{2+}]_i$ were strongly suppressed by KB-R7943 but not by Cd^{2+}. Numbers represent the number of cells tested. C) A representative $[Na^+]_i$ transient induced by elevated $[K^+]_e$ at DIV4.

Next, the source of $[Ca^{2+}]_i$ was identified. As cadmium (100 μM) failed to affect the transients, involvement of voltage-dependent calcium channels (VGCC) appers to be unlikely (Figure 3-7). In contast, KB-R7943 almost completely blocked K^+-induced transients. Moreover, elevation of $[K^+]_e$ led to a decrease of $[Na^+]_i$, favoring the idea that NCX mediates K^+ -induced $[Ca^{2+}]_i$ signals.

Taken together the experiments underlined the hypothesis that K^+-triggered $[Ca^{2+}]_i$ transients are mediated through NCX.

The next step was to find out if a chronic increase of $[K^+]_e$ has any impact on changes of $[Na^+]_i/[Ca^{2+}]_i$ and/or MBP expression. Therefore K^+ was added to DIV2 and DIV4 OPC monocultures for 24 hours. Following this chronic treatment, the cells were analyzed at DIV3 and DIV5 by using ratiometric dyes to see if there might be any changes in the steady state levels of $[Na^+]_i$ (SBFI) and $[Ca^+]_i$ (Fura-2).
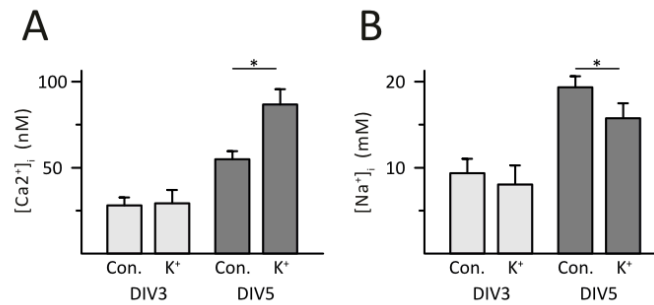
Figure 3-8: Elevated [K$^+$]$_e$ treatment shifts [Ca^{2+}]$_i$ and [Na+]i levels in cultured OPCs

A) [Ca^{2+}]$_i$ levels observed in control and cultures (DIV3 and DIV5) treated for 24 h with elevated [K$^+$]$_e$ (+5 mM). B) [Na$^+$]$_i$ levels observed in control and cultures (DIV3 and DIV5) treated for 24 h with elevated [K$^+$]$_e$ (+5 mM).

The younger cultures (DIV3) did not show any changes in the [Na$^+$]$_i$ and [Ca^{2+}]$_i$ after the chronical treatment with K$^+$. The older cultures (DIV5) however showed an increase in the [Ca^{2+}]$_i$ levels and a decrease of [Na$^+$]$_i$ levels (Figure 3-8). Both values were analyzed compared to untreated control groups and were statistically significant ($p < 0.05$).

In addition to the analysis of [Na$^+$]$_i$ and [Ca^{2+}]$_i$, immunocytochemical experiments were carried out. These experiments also showed that OPCs with an increased [K$^+$]$_e$ seemed to clearly be more developed than those with fewer [K$^+$]$_e$. The K$^+$-treated cells appeared morphologically more differentiated, since they showed more MBP-positive membrane sheets than the untreated control ones (Figure 3-9, A).
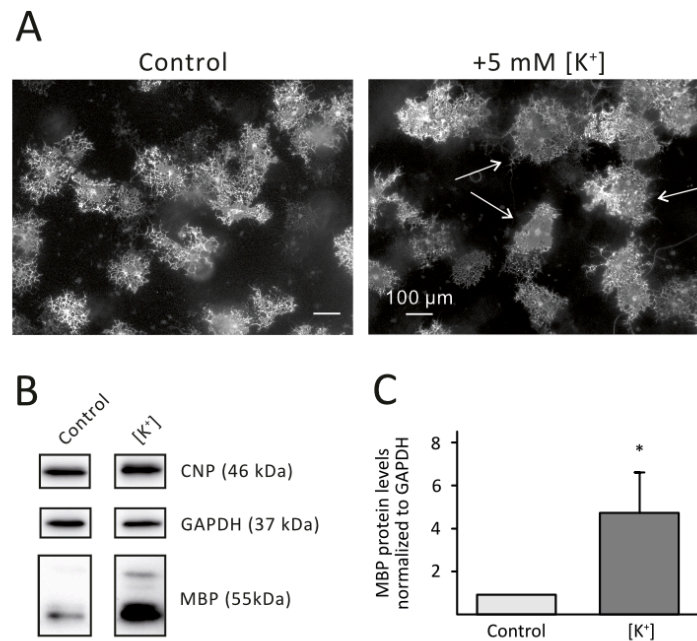
Figure 3-9: Elevated [K$^+$]$_e$ treatment stimulates MBP synthesis in cultured OPCs at DIV5

A) MBP immunostaining shows that elevated [K$^+$]$_e$ for 24 h stimulates myelin-containing sheet formation (arrows) in DIV5 OPC cultures. B) Representative Western blot shows that treatment with elevated [K$^+$]$_e$ stimulates MBP synthesis. C) Statistical graph illustrating potentiation of MBP synthesis by elevated [K$^+$]$_e$ (7 cultures).

As an alternative way to quantify cellular maturation, densitometric Western Blot analyses were implemented and the amounts of MBP determined (Figure 3-9, B/C). OPCs treated with increased [K$^+$]$_e$ showed nearly five times more MBP than the untreated ones.

All these results support the hypothesis that a small increase of [K$^+$]$_e$ within the critical time window (approx. DIV4) leads to a change of [Na$^+$]$_i$ and [Ca^{2+}]$_i$ and an increased MBP expression.

3.4   Manipulation of [Na$^+$]$_i$ by partially blocking Na$^+$/K$^+$-ATPase

The above results allow assuming that the membrane potential of OPCs is close to the reversal potential of NCX. In that case, a small increase of [Na$^+$]$_i$ could switch NCX in reverse mode because [Na+]$_i$ shifts the NCX reversal potential to a negative value.

Na$^+$, K$^+$-ATPase (NKA) is one of the most important cellular regulator of [Na$^+$]$_i$ in every cell. As it was assumed that a small increase of [Na$^+$]$_i$ can induce a shift of the NCX potential to the reversal potential, OPCs were treated with a very low dose of the NKA-blocker ouabain to partially block NKA. A higher dose would have led to a full blockage of NKA and would have been lethal for the cells.
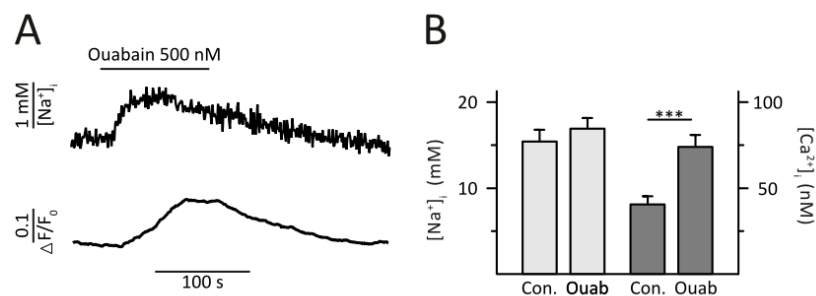
Figure 3-10: Ouabain-induced [Na$^+$]$_i$ and [Ca^{2+}]$_i$ responses in OPCs

A) Representative traces demonstrate ouabain (500 nM)-induced [Na$^+$]$_i$ and [Ca^{2+}]$_i$ transients in OPCs at DIV4. B) Incubation of DIV4 OPCs for 24 h with ouabain (500 nM) resulted in [Ca^{2+}]$_i$ increase at DIV5.

The experiment showed that already 500 nM ouabain lead to an increase of [Na$^+$]$_i$ (43 OPCs, two cultures) on DIV4 on all measured cells (Figure 3-10).

Next it was tested, if ouabain treatment induces [Ca^{2+}]$_i$ responses. If the increase of [Na$^+$] did result in a switch of NCX to reverse mode, there also had to be an increase in [Ca$^+$]$_i$ because of the Ca^{2+} influx. With this test it could in fact be shown that an application of 500 nM ouabain could trigger Ca^{2+} transients in OPC somata. These transients could be prevented through the addition of 1 µM KB-R7349 (n = 5, two cultures, data not shown). This means that an increase of [K$^+$]$_e$ as well as the partial blocking of NKA can lead to [Ca^{2+}]$_i$ responses.

A chronical treatment of OPC monocultures with 500 nM ouabain over the time period of 12 hours (DIV4-5) failed to increase of steady state $[Na^+]_i$ (38 OPCs, three cultures). However it lead to a significant rise of $[Ca^+]_i$ in OPCs (44 OPCs, three cultures).
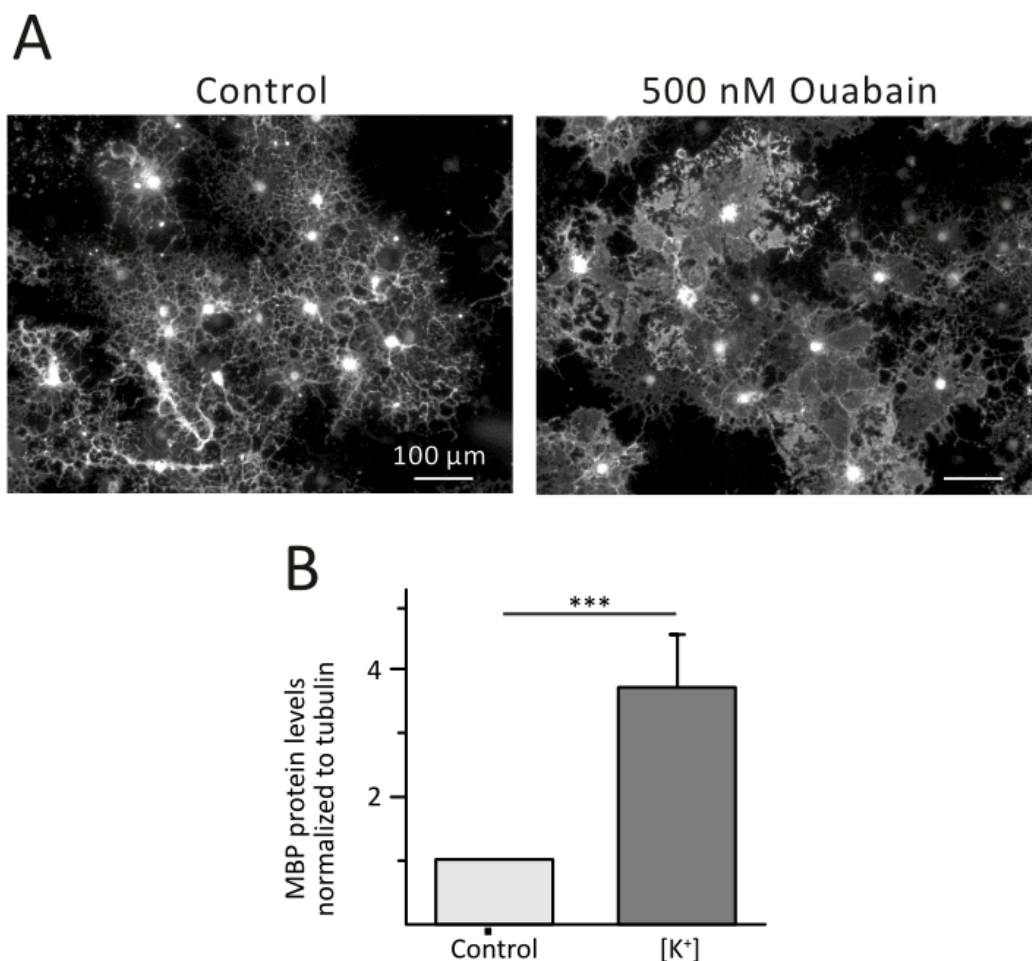
Figure 3-11: Ouabain treatment stimulates MBP synthesis in cultured OPCs

A) Quantitative analyses of Western blot shows that NKA blockade stimulates MBP synthesis (7 cultures). B) Representative examples of DIV5 OPC cultures stained with MBP antibody. Before staining DIV4 OPC cultures were incubated for 12 h with ouabain. Note that ouabain stimulates myelin-comtaining sheets formation in OPCs.

As shown, a partial blockage of NKA lead to an increase of steady state $[Ca^+]_i$ and triggered $[Ca^+]_i$ transients, like the application of K^+. Therefore the question appeared if ouabain treatment would also lead to an increase in MBP expression. Indeed, as shown inFigure 3-11, densitometric Western Blot analyses presented a potentiation of MBP levels of $370 \pm 80\%$ ($p < 0.001$, 7 cultures, one population Student's t-test) after chronical ouabain

application for 12 hours. Similar to the K^+ treatment, the OPCs treated with 500 nM oua-bain also showed MBP positive sheets, which are a typical sign for mature oligodendro-cytes. This means the treated cells were more advanced in their development compared to the non-treated control cells. These findings allow to assume that already small, local changes in $[Na^+]_i$ are sufficient to influence NCX-transmitted MBP expressions.

3.5   Expression of Na$^+$/K$^+$-ATPase α2 subunit in cultured OPCs

A partially blockage of the Na^+, K^+-ATPase (NKA) with only 500 nM ouabain led to a signifi-cant increase of MBP expression. The subunit composition of the NKA however remains elusive. It is known that OPCs express α1 and α2 subunit, though α2 subunit expression has not been shown in cultured OPCs. To find out if the α2 subunit is also expressed by cultured OPCs, different concentrations of ouabain starting from 1000 nM down to 10 nM were tested for an application period of 12h. As previously described in chapter 1.3.5, α1 and α2 subunits have different affinities to this cardiac glycoside. The K_D of α1 is around 2 mM, whereas the K_D of α2 is at 50 nM, meaning that low ouabain concentrations prefer-entially block the α2 subunit.
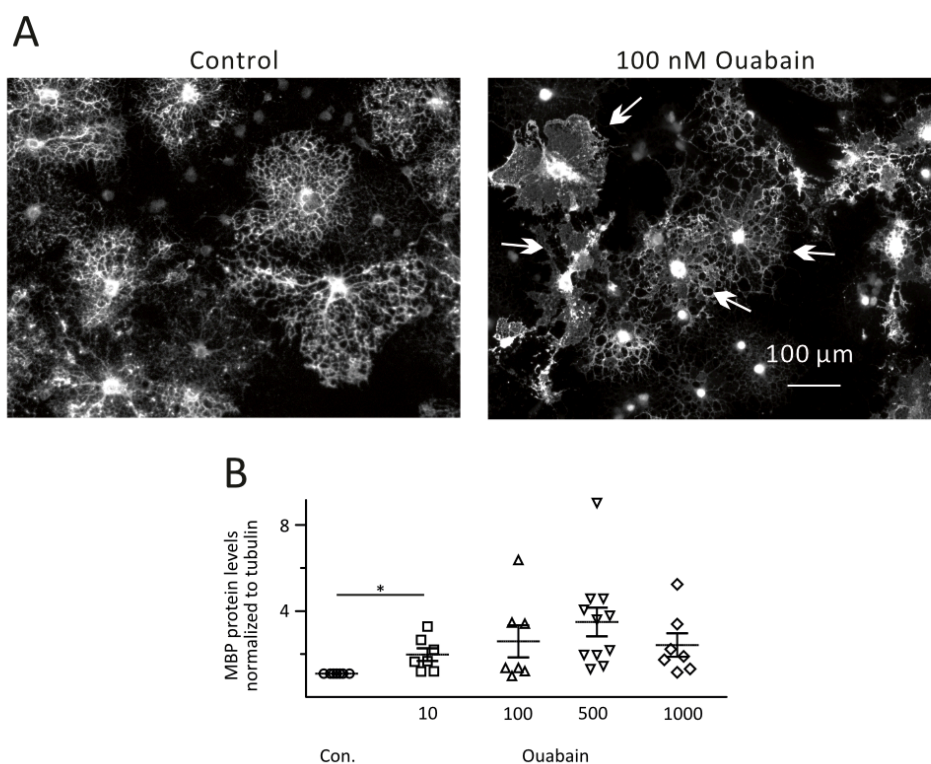
Figure 3-12: Ouabain at low concentrations stimulates MBP synthesis in OPC cultures presumably by blocking α2-NKA

A) Representative examples of control and ouabain-treated (100 nM, 12h) OPC cultures stained with MBP antibody. Note that ouabain stimulates the formation of MBP-positive sheets (arrows). B) Densitometric analyses of Western blots show that NKA blockade at DIV4 withe different ouabain concentrations stimulates MBP synthesis at DIV5. Each symbol represents one OPC culture.

With increasing concentration of ouabain, also the amount of MBP in the cultures augmented to a peak at a concentration of 500 nM (Figure 3-12, B). The expression of MBP at that point rose to nearly a 4-fold compared to the control treated cultures. This drop of the MBP expression at a concentration of 1000 nM might have been caused by the partial blocking of the α1 subunit, which is also expressed by OPCs and crucial for the maintenance of the ion homeostasis. Blocking it might thereby cause cell death. The treatment of the cultures with ouabain not only resulted in an increase of MBP expression but also led to a faster maturation, revealed by the appearance of myelin sheets - an indicator of mature oligodendrocytes (Figure 3-12, A). Therefore the observed potentiation of MBP

synthesis by ouabain at low concentrations is presumably mediated by the $\alpha 2$ subunit of NKA ($\alpha 2$-NKA).

3.6   Is MBP synthesis influenced by the NKA $\alpha 2$ subunit?

Since the increased MBP expression in ouabain treated cultures could occur also due to a partial blockage of the $\alpha 1$ subunit, to verify the hypothesis, we knocked down the expression of $\alpha 2$ by applying $\alpha 2$-siRNA. This application was supposed to target the $\alpha 2$-NKA more precisely. After two days in culture, the cells were treated with $\alpha 2$-siRNA or control siRNA for the control condition. Western blot analysis was performed after DIV4 and DIV5. The aim of these experiments was to find out if the $\alpha 2$ subunit is involved in the MBP synthesis process, how $\alpha 2$ and MBP synthesis are correlated and if it is possible to shift the onset of MBP synthesis.
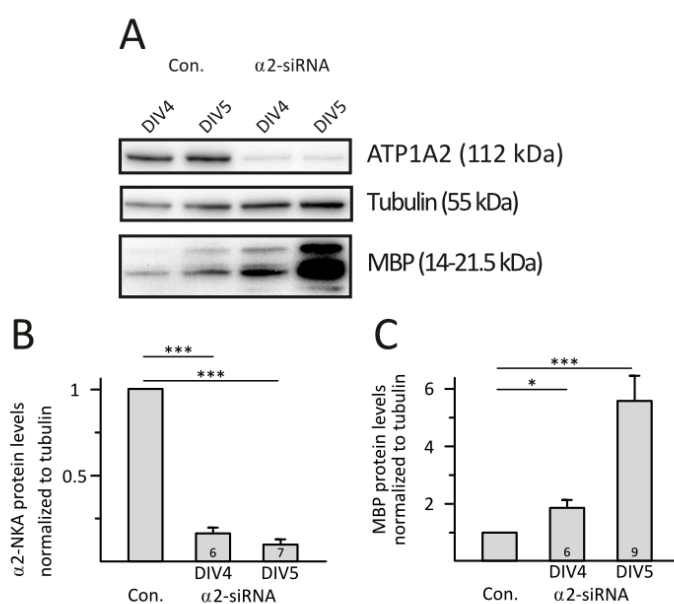
Figure 3-13: $\alpha 2$-knockdown with $\alpha 2$-siRNA potentiates MBP expression

A) Representative Western blots demonstrate $\alpha 2$-siRNA-induced effects on $\alpha 2$-NKA and MBP expression at DIV4 and 5. B) Densitometric analyses of Western blots show that $\alpha 2$-NKA applied at DIV2 strongly reduced the amount of $\alpha 2$-NKA at DIV4 and 5. C) $\alpha 2$-siRNA applied at DIV2 substantially increased the amount of MBP at DIV4 and 5. Numbers represent the number of OPC cultures tested.

Figure 3-13 shows that the application of α2-siRNA indeed led to a significant decrease of α2-NKA levels at DIV4 (to 16 ± 4% of control, n = 6, p < 0.001) and DIV5 (to 10 ± 3% of control, n = 7, p < 0.001). In untreated cultures MBP expression normally occurs around DIV4 to DIV5. Like the previous treatment with ouabain, the performed experiments also showed that knocking down the NKA α2 subunit led to a boost of MBP at DIV5 to almost six times the amount of the control conditions normalized to tubulin. This indicates that α2-NKA expression and MBP expression are linked. Furthermore a significant increase of MBP even at DIV4 compared to the control condition was shown, meaning that treating the cultures with α2-siRNA can shift the onset of MBP expression and potentially mye-lination to an earlier time point in OPC development.
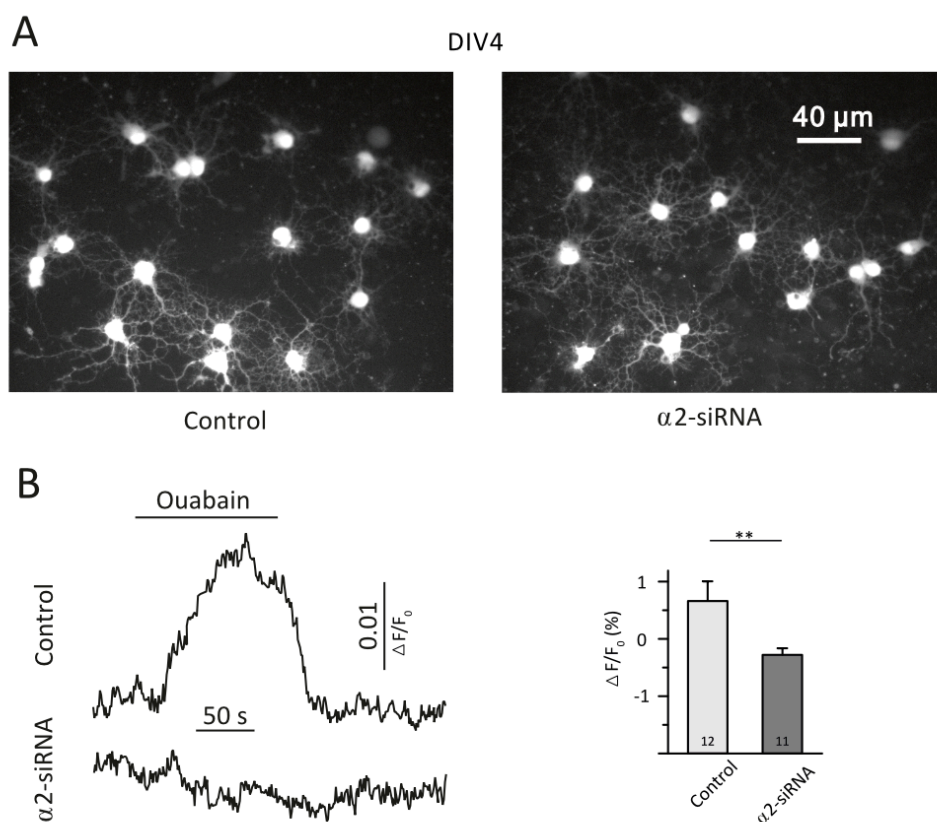
Figure 3-14: α2-NKA knockdown reduces ouabain-induced $[Ca^{2+}]_i$ responses

A) Representative images of DIV4 OPCs loaded with the Ca^{2+} probe OGB1. OPCs were treated either with control-siRNA (left) or with α2-siRNA for 48 h. B+C) Averaged Ca^{2+} responses (traces B) and statistics C)) induced by ouabain (500 nM) in control-siRNA- and α2-siRNA-treated cultures. Numbers represent number of cells tested (2 OPC cultures in each case).

Assumed that α2-NKA is responsible for the $[Ca^{2+}]_i$ responses triggered by ouabain application, it was assumed that knocking down α2-NKA would prevent those responses. Figure 3-14 A shows OPC cultures loaded with the Ca^{2+}-sensitive probe OGB1 and demonstrates that the knockdown had no influence on the culture density. Additionally Figure 3-14 B+C depicts that indeed ouabain failed to elicit $[Ca^{2+}]_i$ responses in α2-siRNA treated OPC cultures.

These results demonstrate that the NKA α2 subunit seems to negatively control the MBP synthesis.

3.7   The link between α2-NKA and MBP

Sensitivity of α2-NKA to neuronal activity has already been hypothesized. However cultured OPCs were shown not to express α2 subunit in monocultures but do express it at DIV6 in OPC-neuron co-cultures (Knapp, Itkis, and Mata 2000). That is why the first experiments concerning the α2-NKA expression were also dedicated to verify this existence of α2 subunit in OPC monocultures. Immunocytochemical stainings showed the expression of the α2-NKA in OPCs already at DIV2. A co-staining with CNP, a marker for early OPCs, could prove that the examined cells indeed were OPCs (Figure 3-15, A). In addition, it could be concluded through this experiment that at least in early development stages expression of α2-NKA is homogeneously spread over the cell surface.
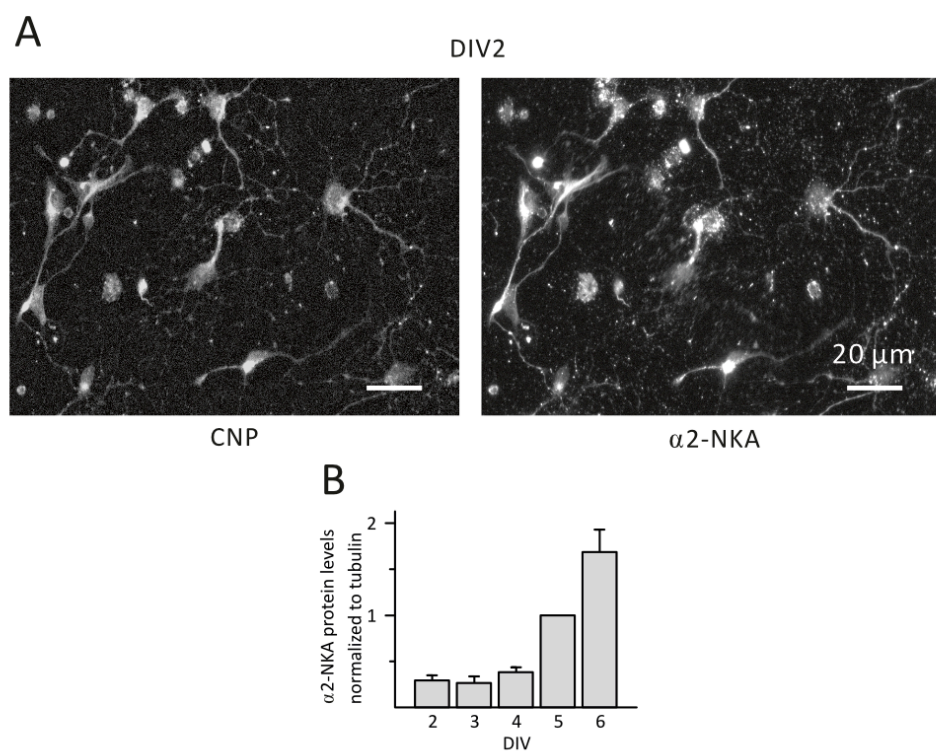
Figure 3-15: α2-NKA expression by cultured OPCs

A) Representative images demonstrate DIV2 OPCs stained with CNP (left) and α2-NKA (right image) antibodies. Note strong overlap of the two immunosignals at DIV2. B) Densitometric analyses of Western blots show the time course of α2-NKA expression by OPCs.

Furthermore, it is important to find out how the pattern of α2-NKA expression changes throughout cell maturation. For this purpose densotimetric Western Blot analyses were implemented. Already on DIV2, an expression of α2-NKA can be detected (30±5% of its level at DIV5) and it demonstrated a strong increase on DIV4 to DIV5 (Figure 3-15, B). Interestingly, the experiment showed that in the same time frame MBP expression also severely increased. Since α2-NKA seems to inhibit MBP expression, it was interesting to find out if MBP provides a negative feedback on α2-NKA expression.
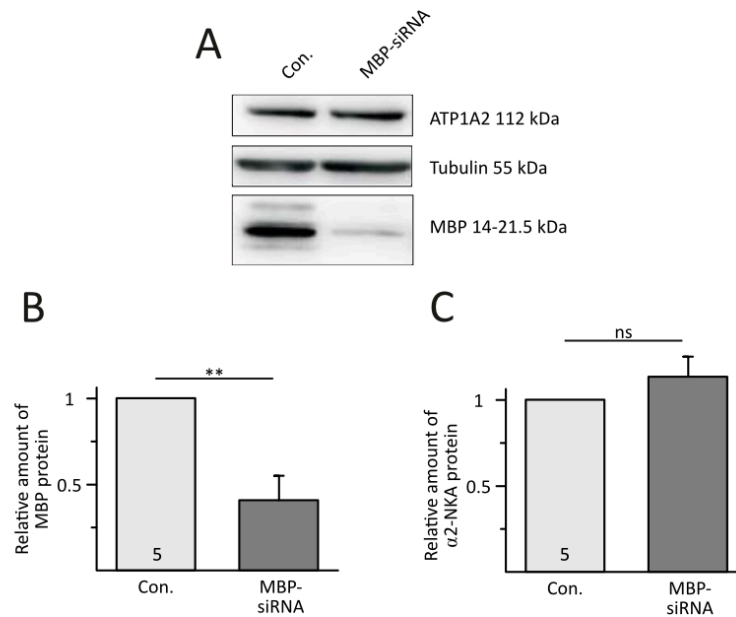
Figure 3-16: MBP knockdown does not affect α2-NKA synthesis

A) Representative Western blot demonstrates reduced levels of MBP in OPC cultures at DIV5 after MBP-siRNA application at DIV2. B+C) Densitometric analyses of Western blots show a reduction of MBP levels (B) but the knockdown failed to affect α2-NKA protein levels (C) in cultured OPCs.

Treatment of OPC monocultures with MBP-siRNA at DIV2 led to reduced MBP levels which was examined by densitometric Western Blot analyses. This reduction of MBP at DIV5 did not alter the global expression behavior of α2-NKA in OPCs, even though knock down of α2-NKA stimulated MBP expression (Figure 3-16).

To find out if potential spatio-temporal changes in the expression pattern of MBP and α2-NKA exist, co-stainings against both proteins were carried out and possible co-localization analyzed through ImageJ and the appropriate Macro Jacop.
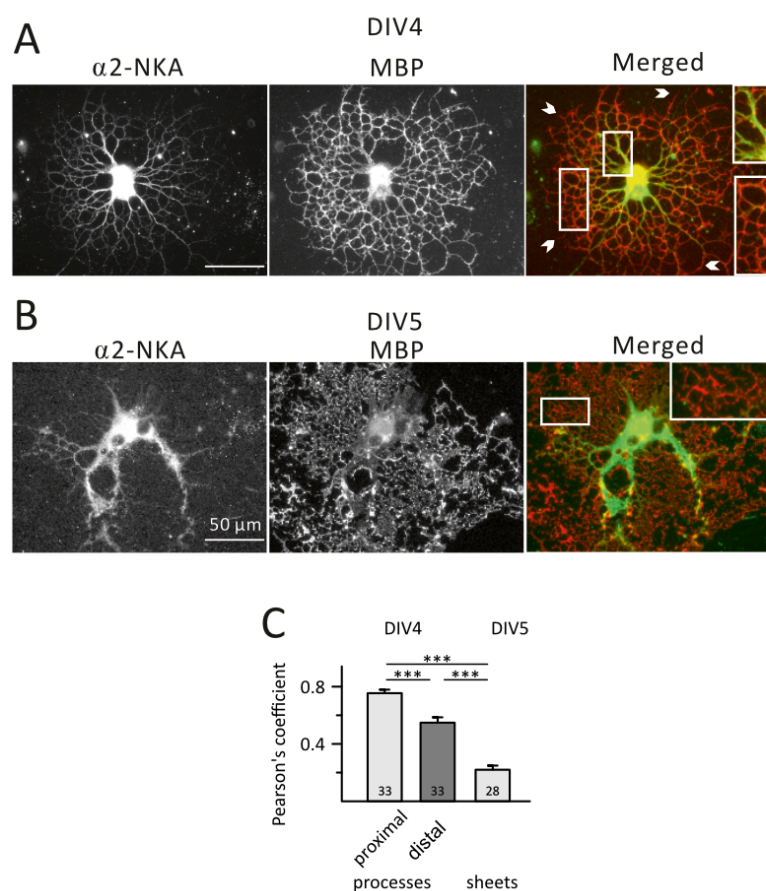
Figure 3-17: α2-NKA and MBP become less co-localized during development

A) Representative images show MBP and α2-NKA staining at DIV4. Note a strong co-localization in proximal (the upper inset) but not in distal processes (the lower inset). B) Representative stainings with MBP and α2-NKA antibodies at DIV5. Note low level of α2-NKA expression in distal MBP-positive sheets (the inset). C) Statistical data shows co-localization (Pearson's coefficient) of MBP and α2-NKA in different cellular compartments at DIV4 and DIV5. Numbers represent number of ROIs analyzed (from 3 different OPC cultures).

Figure 3-17 shows that on DIV4 the immunosignals of α2-NKA and MBP overlap more on the proximal processes (Pearson´s coefficient 0.72±0.03) than on the distal processes (Pearson´s coefficient 0.51±0.04, p<0.001, 2-3 ROIs per cell, 10 cells, 3 cultures). Further, co-localization is lowest on MBP-positive membrane sheets occurring on DIV5 (Pearson´s coefficient 0.20±0.03, 3 ROIs per cell, 7 cells, 3 cultures). These results lead to the assumption that α2-NKA plays an important role in controlling the initiation of MBP synthesis, but does not stay in MBP-positive sections later on in the development of OPCs.

3.8   Influence of α2-NKA and MBP on Ca^{2+} signaling in OPCs

The main task of NKA is to keep transmembrane Na^+ and K^+ gradients. This raises the question of how NKA can have an influence on MBP expression.

It has already been shown that NCX influenses MBP synthesis, respectively myelination (Boscia et al. 2012). The next step therefore was to find out if the increase of MBP synthesis induced through α2-NKA was mediated by NCX. For that purpose OPC monocultures were treated with α2-siRNA on DIV2 as described in chapter 3.6. On DIV3, respectively DIV4, KB-R7943, a blocker for the NCX reverse mode, was added to the culture and incubated for 24 hours.
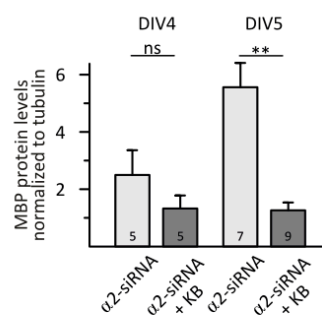
Figure 3-18: α2-NKA-induced effects on MBP expression are mediated by NCX operating in reverse mode

Statistical analysis shows that potentiation of MBP expression by α2-NKA knockdown is alleviated in the presence of KB-R7943 (1µM), a NCX blocker. Numbers represent the number of OPC cultures tested.

Densitometric Western Blot analyses demonstrated that the increase of MBP expression created through α2-siRNA on DIV5, could be significantly decreased by the chronic KB-R7943 application (from 5.6±0.8 to 1.3±0.3 in α2-siRNA- and α2-siRNA+KB-R7943-treated cultures, respectively, p < 0.003, n=7 and 9). This finding however could not be observed in cultures that were treated on DIV3 for 24 hours and analyzed the following day (Figure 3-18). This shows that the changes of MBP expression levels created by α2-NKA are imparted by NCX.

Since NCX is an electrogenic exchanger that could work in default direction (Ca^{2+}

transport out of the cell) as well as in the opposite direction (Ca^+ transport into the cell), it was important to find out what the working direction in the critical time frame of the myelination onsets is. As previously described, siRNA-treated cultures were loaded with OGB-1 to identify the Ca^{2+} changes within OPCs after the addition of KB-R7043 (1 µM). If NCX workes in reverse mode, the blockage of it with KB-R7043 would lead to a decrease of $[Ca^{2+}]_i$ level. Indeed, a reduction of the $[Ca^{2+}]_i$ in the cells could be observed on DIV4. Cultures that were treated with control siRNA showed this effect only on DIV5 whereas cultures treated with α2-siRNA experienced it one day earlier (Figure 3-19, A,B). These results therefore lead to the conclusion that α2-NKA influences the NCX function.

Based on these experiments, where Ca^{2+} transients were evoked by the application of +5mM K^+, the cells treated with siRNA were analyzed and compared the same way. Figure 3-19 C, D demonstrates that OPC cultures that were treated with α2-siRNA produced significantly larger calcium responses on DIV4 after $[K^+]_e$ elevation as compared to the cells treated with control siRNA. On DIV5 however the $[K^+]_e$-induced transients in α2-siRNA-treated OPC cultures are noticeably smaller compared to the control group. Since previous experiments showed that there was a decreased $[K^+]_e$-induced transient in untreated cells on DIV6, it could be explained through different development stages between α2-NKA knock down and control.
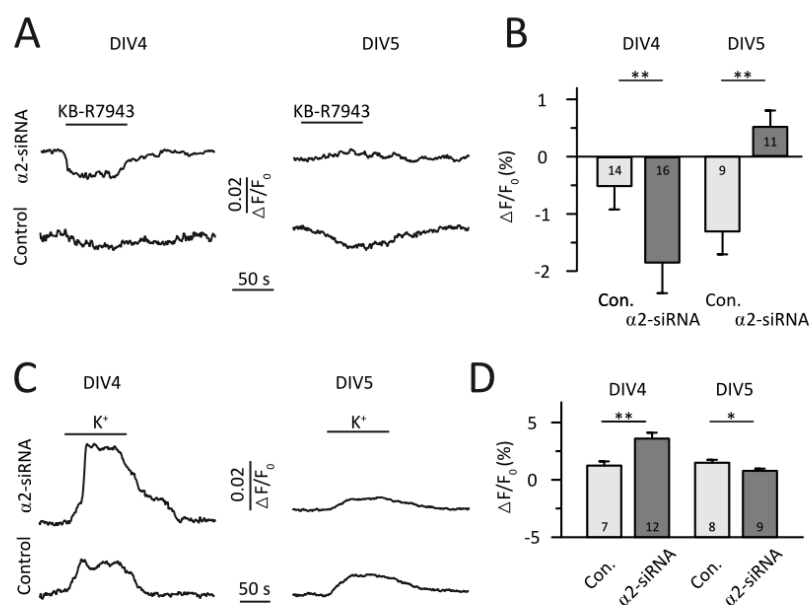
Figure 3-19: α2-NKA-induced effects on [Ca^{2+}]$_i$responses are mediated by NCX reverse mode

A) KB-R7943 (1µM) induced [Ca^{2+}]$_i$ reduction in α2-siRNA-treated OPCs at DIV4 and in control OPCs at DIV5. [Ca^{2+}]$_i$ transients were measured using OGB1, a Ca^{2+}-sensitive probe. B) Averaged amplitude of KB-R7943-induced [Ca^{2+}]$_i$ transients in α2-siRNA-treated and control cultures at DIV4 and 5. Numbers represent number of OPCs tested (3 different cultures). C) Representative traces show Ca^{2+} responses induced by elevation of [K^+]$_e$ (+5mM) at DIV4 and 5. D) Averaged responses induced by elevated [K^+]$_e$ at DIV4 and 5.

In addition to the mentioned experiments, the steady state levels of [Na^+]$_i$ and [Ca^{2+}]$_i$ after treatment with siRNA on DIV4 and 5 were studied with the help of ratiometric stainings SBFI and fura-2. Figure 3-20 shows that those cultures treated with α2-siRNA presented significantly higher levels of [Na^+]$_i$ und [Ca^{2+}]$_i$ compared to the control cultures on DIV4. On DIV5 there were no differences in the [Na^+]$_i$ level between control cultures and knock-down treatment. Solely the [Ca^{2+}]$_i$ values of the α2-siRNA treated cells were strongly reduced on DIV5.
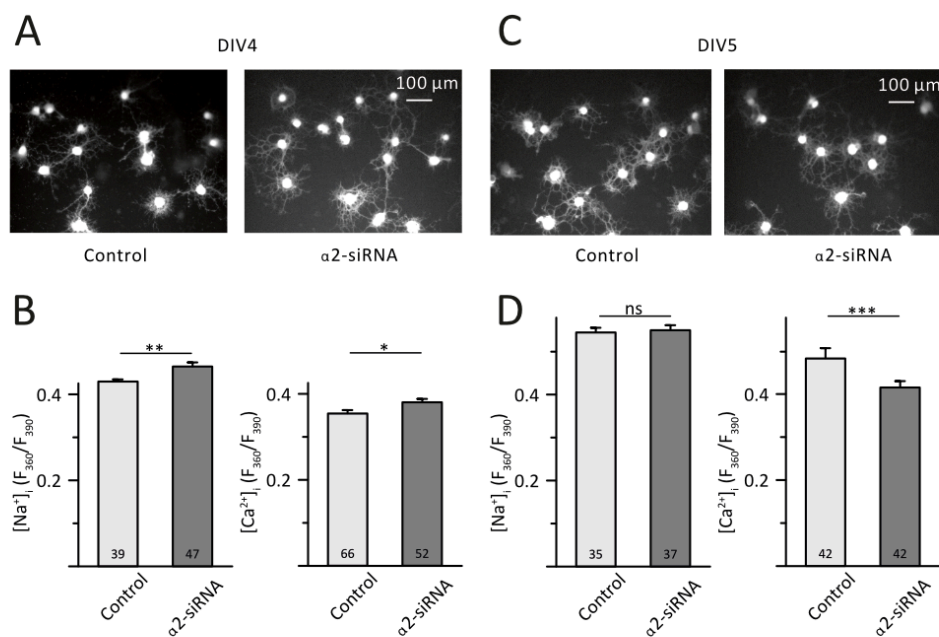
Figure 3-20: aα2-siRNA treatments affects [Na$^+$]$_i$ and [Ca^{2+}]$_i$ levels in cultured OPCs at DIV4 and 5

A) Representative images of DIV4 OPCs stained with Fura-2. B) Statistical analysis shows that knockdown of α2-NKA subunit leads to an increase in [Na$^+$]$_i$ and [Ca^{2+}]$_i$ in OPCs at DIV4. Numbers represent number of OPCs tested (3 different cultures). C) Representative images of DIV5 OPCs stained with Fura-2. D) Statistical analysis shows that knockdown of α2-NKA subunit leads to a decrease in [Ca^{2+}]$_i$ in DIV5 OPCs. Numbers represent number of OPCs tested (3 different cultures).

Thus it is concluded that MBP could negatively affect [Ca^{2+}]$_i$ signaling in cultured OPCs which is in line with the results of Smith and collegues (Smith et al. 2011).

To support this hypothesis, OPCs were treated with MBP-siRNA at DIV2 to decrease their expression and to find out effects of MBP on calcium changes.
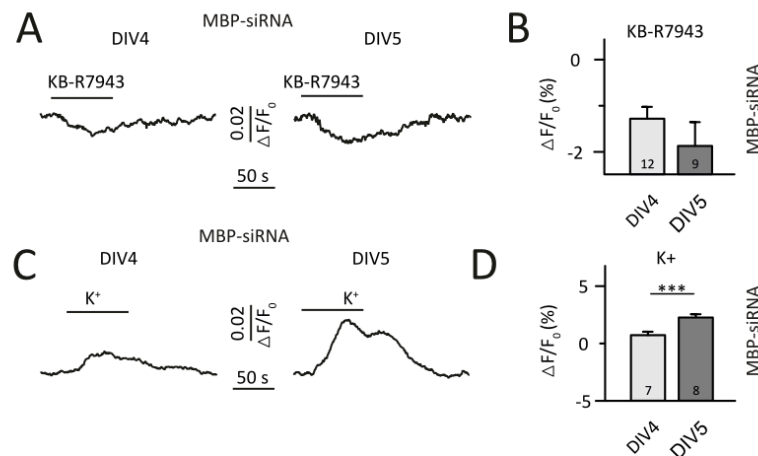
Figure 3-21: Knockdown of MBP with siRNA potentiates Ca^{2+} signaling at DIV5

A+B) Averaged Ca^{2+} responses induced by KB-R7943 (1 μm, A) and elevated [K$^+$]$_e$ (+5mM, B) in DIV4 OPC cultures treated with MBP-siRNA from DIV2 on. C) Statistical summary of experiments shown in A) and B). Note that [K$^+$]$_e$-induced Ca^{2+} responses increased at DIV5.

Application of KB-R7943 to the MBP knock-down OPCs elicited comparable [Ca^{2+}]$_i$ transients at DIV4 and DIV5, which led to the assumption that NCX works in reverse mode even without MBP (Figure 3-21, A, B). [Ca^{2+}]$_i$ transients ([Ca^{2+}]$_t$) could also be elicited by K$^+$ application. These [Ca^{2+}]$_t$ however did not, like shown in the control group previously, decrease on DIV5 but actually increased further (Figure 3-21, C,D). These findings lead to the conclusion that MBP has a negative effect on [Ca^{2+}]$_i$ signaling in OPC cultures and therefore coincides with results from (Smith et al., 2011).

3.9   α2-NKA and MBP have inverse influence on spontaneous [Ca^{2+}]$_i$ activity in immature oligodendrocytes

It has already been shown that spontaneous [Ca^{2+}]$_t$ in immature oligodendrocytes are important for migration and myelination (Jacobs et al. 2009; Paez et al. 2009). Since earlier experiments showed the influence of MBP on released [Ca^{2+}]$_i$ responses, it was interesting to test if MBP, but also α2-NKA, has an effect on these spontaneous [Ca^{2+}]$_i$ activities. Therefore OPC cultures were again treated with either control-, α2- or MBP-siRNA at DIV2 to then analyze spontaneously occuring [Ca^{2+}]$_i$ changes on DIV4, DIV5 und DIV6 via

OGB-1 bulk load (Figure 3-22).
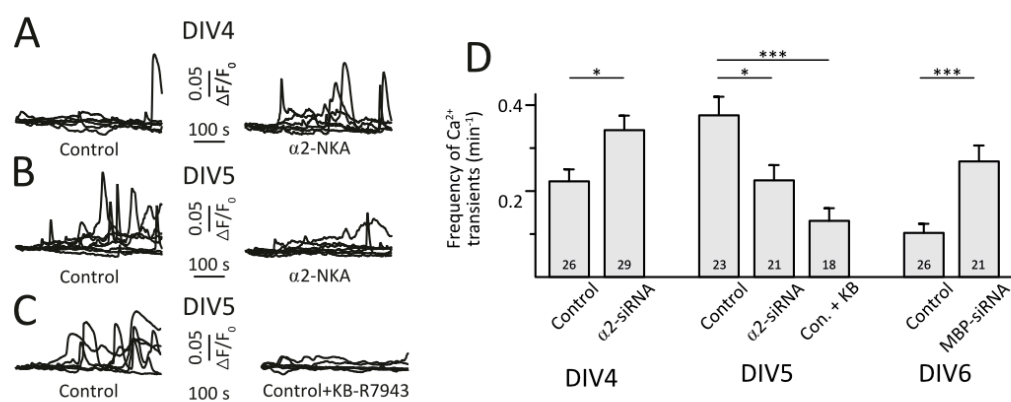
Figure 3-22: Spontaneous Ca^{2+} activity in cultured OPCs depepends on α2-NKA, NCX and MBP

A) Representative traces (8 OPCs from one view field in each case) recorded in DIV4 control (left) and α2-siRNA-treated (right) OPC cultures. B) Representative traces (8 from one view field in each case) recorded in DIV5 (left) and α2-siRNA-treated (right) OPC cultures. Representative traces (6 from one view field in each case) recorded in DIV5 OPC cultures in control and in the presence of KB-R7943 (1 µM). D) Statistical analysis demonstrates dependence of spontaneous Ca^{2+} activity in cultured OPCs on α2-NKA, NCX and MBP. Numbers represent numbers of cells tested (always in 3 different cultures).

None of these approaches induced spontaneous [Ca^{2+}]$_i$ activity on DIV2 OPCs (34 OPCs, 3 cultures). On DIV4 spontaneous [Ca^{2+}]$_i$ transients could be observed. Moreover, OPC cultures treated with α2-siRNA showed significantly higher frequencies as those treated with control siRNA. These frequencies of α2-siRNA-treated OPCs clearly decreased on DIV5 so that the control groups now showed a higher frequency of the spontaneous [Ca^{2+}]$_i$ activity. Cells treated either with control siRNA or α2-siRNA, showed nearly no spontaneous [Ca^{2+}]$_i$ activities on DIV6. Interestingly, solely those cultures treated with MBP-siRNA showed unaltered spontaneous [Ca^{2+}]$_i$ activities at DIV6.

Earlier experiments presented that an increase of MBP expression, released by a knock down of α2-NKA, could be reduced through the application of KB-R7943. The next step therefore was to study if KB-R7943 could also prevent spontaneous [Ca^{2+}]$_i$ transients in immature oligodendrocytes. It was indeed possible to strongly decrease the frequency of those activities through the addition of 1 µM KB-R7943 on DIV5 – the day which presents

the peak of spontaneous $[Ca^{2+}]_i$ activity on untreated OPCs

These results allow suggesting that α2-NKA blockade shifts the onset of spontaneous $[Ca^{2+}]_t$ to an earlier time point in OPC development. Moreover, it could be proven that MBP expression has an inhibiting effect on $[Ca^{2+}]_i$ activities.

3.10 α2-NKA has no effect on MBP expression, but decreases myelination in cortical organotypical slice cultures

Under the assumption that MBP expression correlates with the initiation of myelination, it was found that MBP expression starts at around DIV7 in cortical organotypic slice cultures (Cosc).

Like the OPC monocultures before, the slice cultures were treated with α2-siRNA on DIV2 and then fixed at DIV7. To see if the slice cultures showed a change in MBP expression, immunostainings were conducted. For the analysis of the slices the entire surface of axons (neurofilament-stainings) and myelin (MBP-stainings) was measured and calculated, as well as the relation between them (Figure 3-23, A/B).
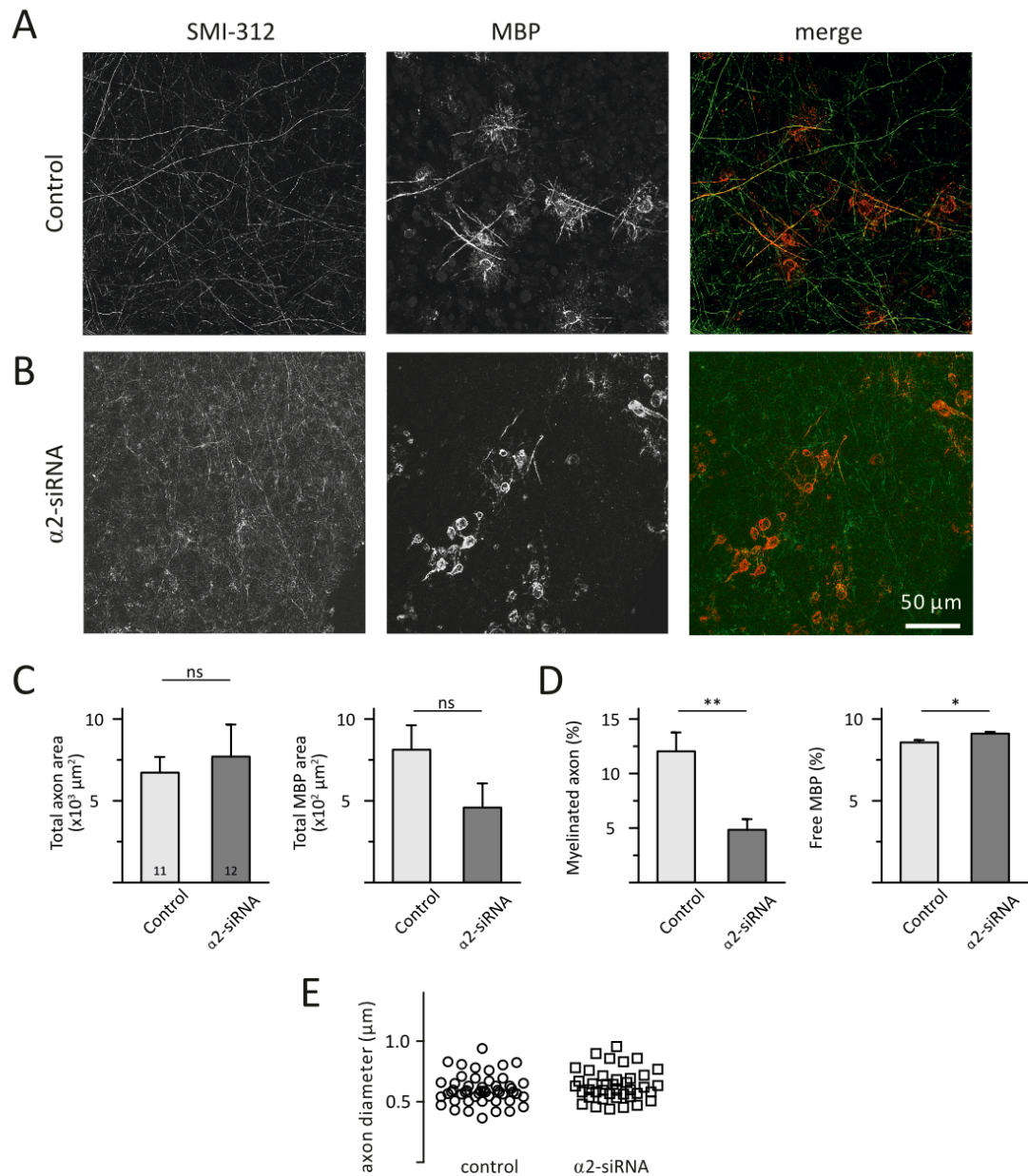
Figure 3-23: α2-siRNA fails to influence MBP synthesis but decreases axon wrapping *in situ*

A+B) Representative images show neurofilament (left), MBP (center) and merged immunostainings of control (A) and α2-siRNA-treated (B) cortial slice cultures at DIV7. C) Statistical analysis shows that α2-siRNA treatment does not result in any significant change in the amount of either neurofilaments (left) or MBP (right). D) Statistical analysis demonstrating that α2-siRNA treatment decreses co-localization of MBP and neurofilaments (left) and increases the amount of free, i.e.not co-localized with neurofilament, MBP. E) α2-siRNA treatment did not change the diameter of the axons.

It was shown that, compared to the control siRNA slices, there are no significant changes in the density of the axons or the MBP signal after the treatment with α2-siRNA (Figure 3-

23, C). In addition, the diameter of the axons was measured, which did not show a difference between the treatments (Figure 3-23, E). However, by means of the stainings, it could be determined that those slices treated with α2-siRNA showed a weaker co-localization of MBP and axons than those treated with control siRNA (Figure 3-23, D).

By implication, this means that the amount of MBP-positive sections, which did not co-localize with axons, is increased in slices treated with α2-siRNA. Hence, different to OPC monocultures, a treatment with α2-siRNA in slice cultures did not lead to an increase of MBP expression.

4   Discussion

This study presents the role of α2-NKA and NCX in changes of $[Na^+]_i$ and $[Ca^{2+}]_i$ in immature oligodendrocytes *in vitro* and their effect on MBP synthesis. It was shown that oligodendrocytes manifest a significant change of $[Na^+]_i$ and $[Ca^{2+}]_i$ around DIV4-5 even without neurons. Intriguingly, at the same time point also the onset of MBP expression in OPC monocultures starts. At that time NCX works in reverse mode and its activity is shown to be linked to MBP expression. Application of $[K^+]_e$ at DIV4 leads to an elevation of $[Ca^{2+}]_i$ levels in immature OLs and stimulates MBP expression. Already very small concentrations of ouabain block NKA partially, which enhances the maturation of the cultured OPCs and subsequently leads to an increase of MBP synthesis. The $[Ca^{2+}]_i$ transients induced by $[K^+]_e$ as well as ouabain application are eliminated by blocking the NCX reverse mode. These findings demonstrate that local $[Na^+]_i$ and/or changes in the membrane potential can induce NCX-mediated $[Ca^{2+}]_i$ transients and affect MBP synthesis.

The response of OPCs to a very low concentration of ouabain gave a hint to analyze if α2-NKA contributes to this effect. Indeed similar to ouabain, Knocking down the α2-NKA leads to a faster maturation of the OPCs and a stronger MBP expression. This effect is mediated by the NCX as well. NCX provides Ca^{2+} ions which are required for at least the initiation of local MBP synthesis, while MBP itself reduces spontaneous activity. In cortical organotypic slice cultures α2-NKA deletion does not cause an increase of MBP synthesis like in OPC monocultures but surprisingly leads to a reduced co-localization of MBP with axons. We suggest that α2-NKA hampers the onset of MBP synthesis by shifting local NCX reversal potential to more negative values. Neuronal activity, presumably through $[K^+]_e$ elevations, depolarizes the OPC membrane and stimulates α2-NKA, resulting in NCX reversal. NCX-mediated Ca^{2+} influx triggers selective myelination of most active axons. α2-NKA deletion results in facilitation of MBP synthesis but the latter takes place in spatially stochastic, i.e. axon dependent manner.

4.1   Developmental changes of $[Na^+]_i$ and $[Ca^{2+}]_i$ in OPC monocultures

It is known that $[Ca^{2+}]_i$ transients are important for OPC migration, differentiation and myelination. With the expression of numerous neurotransmitter receptors like AMPA (Ziskin et al. 2007), NMDA (Káradóttir et al. 2005) and metabotropic (Luyt, Varadi and Molnar 2003) glutamate receptors, ionotropic (Matute et al. 2007) and metabotropic (Kirischuk et al. 1995) purinoreceptors, there are a lot of possible pathways to induce $[Ca^{2+}]_i$ transients in OPCs. Furthermore, OPCs express voltage-gated calcium channels (Kirischuk et al. 1995; Blankenfeld, Verkhratsky and Kettenmann 1992) and all three isoforms of NCX (NCX1-3) (Chen et al. 2007; Boscia et al. 2012; Quednau, Nicoll and Philipson 1997). NCX is an electrogenic antiporter that imports three Na^+ ions for the cost of one Ca^{2+} ion by default. Unlike the previously mentioned receptors, which need a neurotransmitter for their activation, the fate of the NCX operation mode is dependent on the membrane potential and the transmembrane Na^+ and Ca^{2+} gradients. To date, only a few publications are available on absolute $[Na^+]_i$ and $[Ca^{2+}]_i$ levels in OPCs. In enriched rat oligodendrocyte cultures values of 40 nM of $[Ca^{2+}]_i$ and 18 nM of $[Na^+]_i$ were measured in young cultures (DIV1-3) (Chen et al. 2007). The same values for $[Ca^{2+}]_i$ (40 nM) were obtained in the human oligodendroglial cell line MO3.13 (Boscia et al. 2012). The detected data of this thesis match with these results. In addition, developmental changes of resting $[Na^+]_i$ and $[Ca^{2+}]_i$ in cultured OPCs could be shown even without stimulation as well as in oligodendrocytes in cortical slice cultures. In those slice cultures the values of $[Na^+]_i$ were about 8 mM at P10-15 but increased to 15 mM at P20-30.

4.2   Relation of NCX and intracellular signaling in OPCs

The shown intracellular changes of $[Na^+]_i$ und $[Ca^{2+}]_i$ during the development of OPCs might have an influence on the transport direction of NCX. An increase of $[Na^+]_i$ leads to a more negative reversal potential, which would then again benefit the reversal mode of NCX. Through the application of KB-R7943, a blocker for reversal mode of NCX, an increase of $[Na^+]_i$ could in fact be shown. However, this increase only occurs in the short critical time frame on DIV4 in OPC monocultures or in acute brain slices of mice with the age of approx. P20. This is in the myelination onset phase of mice - at least in the barrel

cortex (Barrera et al. 2013). Furthermore, it was determined that a blockage of the reversal mode for 12 hours in this critical time frame leads to a decrease of MBP synthesis. These results thus underline the previously reported important role of NCX in myelination (Boscia et al. 2012).

This study shows the changes in transport direction of NCX on DIV4 in OPC monocultures. Since monocultures are free from neurons it leads to the assumption that these changes follow a given internal signal. It can further be assumed that neuronal activity changes the transport direction of NCX and thus have a local influence on $[Na^+]_i$ and $[Ca^{2+}]_i$ in OPCs. It is possible that the inhibiting contribution of α2-NKA in respect to the Ca^{2+} signaling and MBP synthesis might be regulated by this internal signal and the disappearance of it during development allows external signals like the elevation of $[K^+]_e$ to switch NCX into reverse mode.

4.3   Changes of K^+ sensitivity of OPCs during development

Neuronal activity inevitably leads to a local increase of $[K^+]_e$. OPCs seem to detect this increase regardless of axonal neurotransmitter release. That is why it was suggested that in OPCs voltage gated calcium channels (Paez et al. 2009; Kirischuk et al. 1995; Haberlandt et al. 2011) as well as the reverse mode of NCX (Boscia et al. 2012; Tong et al. 2009) mediate K^+-induced $[Ca^{2+}]_i$ transients. The experiments in this thesis show that the ability of NCX to evoke responses of $[Ca^{2+}]_i$ depends on the developmental stage. Moreover it is shown that the highest spontaneous Ca^{2+}activity of OPC cultures was observed between DIV4 and DIV5, which could be mediated by voltage-gated potassium channels. It was already shown that an activation of AMPA/kainate receptors inhibits the differentiation of OPCs through a blockage of delayed rectifier K^+ channels (Gallo et al. 1996). Mature oligodendrocytes detect $[K^+]_e$ changes through the upregulation of Kir4.1 channels (Maldonado et al. 2013). Kir4.1 channels could have several roles. Firstly they contribute to the resting membrane potential by hyperpolarizing it more intensely. Secondly, Kir4.1 channels allow a better K^+ detection. On basis of these two factors, it can be assumed that $[K^+]_e$ changes may be converted into intracellular signaling at the plasma membrane via voltage-dependent mechanisms.

An increase of $[K^+]_e$ does not only shift the resting membrane potential but also activates NKA. An increase of NKA activity leads to hyperpolarization which in turn counteracts the depolarization through increase of $[K^+]_e$. According to this, an activation of NKA leads to a decrease of $[K^+]_e$ which then results in a change of NCX from reverse to default mode. Assuming that NKA and NCX would form a complex in a very small compartment, e.g. in the distal tips of the oligendrocyte processes, they would not only transform an increase of $[K^+]_e$ into a $[Ca^{2+}]_i$ transient, but even release complex local $[Ca^{2+}]_i$ signals which are individually tailored to the adjacent axons and their activity. This means that this hypothesis describes a mechanism for axon-directed oligodendroglial response in respect to the myelination process.

4.4 K^+-induced stimulation of MBP in immature oligodendrocytes

Increasing $[K^+]_e$ as well as partially blocking of NKA leads to a $[Ca^{2+}]_i$ responses in immature oligodendrocytes. Since those responses could not be prevented through the application of cadmium, mediation through voltage-gated calcium channels can be excluded. The application of KB-R7943 however leads to an almost complete suppression of $[K^+]$-induced answers and therefore draws the focus on NCX. If NKA is partially blocked though, there is also an onset of $[Ca^{2+}]_i$ transients parallel to the expected increase of $[Na^+]_i$, as well as an increased MBP synthesis. These are the same effects that occur after the treatment of immature oligodendrocytes with $[K^+]_e$.

Due to those reasons, it is assumed that the resting membrane potential of immature oligodendrocytes on DIV4 lies close to the reversal potential of NCX. This means that already a small depolarization caused by the increase of $[K^+]_e$ or $[Na^+]_i$ shifts NCX in reverse mode. Consequently Ca^{2+} ions are transported into the cells and releases $[Ca^{2+}]_i$ transients (Maldonado et al. 2013).

4.5   Can $[Na^+]_i$ be considered as second messenger?

It has been repeatedly shown that $[Na^+]_i$ and the related transmembrane Na^+-gradient are not only important as an energy supplier for many transmembrane transport processes but also influence intracellular signaling pathways (Kirischuk, Parpura and Verkhratsky

2012; Rose and Karus 2013). Activation of ionotropic glutamate receptors leads to an elevation of $[Na^+]_i$ in OPCs and suppresses the expression of K^+ channels and OPC proliferation (Knutson et al. 1997). These K^+ channels lead to a change of the membrane potential and make the OPCs sensitive for $[K^+]_e$. Interestingly, $[Ca^{2+}]_i$ transients can also be evoked by activation of NMDA receptors (Wake, Lee and Fields 2011) leading to a stimulation of NCX3 isoform expression in OPCs (Boscia et al. 2012). Additionally, it was shown that in OPCs either Na^+, H^+ exchanger or Na^+, HCO_3-co-transporter can be co-localized with carbonic anhydrase II, resulting in spatially changes of pH (Ro and Carson 2004). If NKA and NCX are also co-localized in small compartments like the distal OPC processes as shown in astrocytes (Blaustein et al. 2002), they could together set the local K^+ sensitivity of individual processes. A precise local membrane potential respectively local ion concentration changes could set a standby mode of a single process waiting for extracellular activity to be converted into intracellular signals. If this standby mode is set correctly inan OPC process, changes in $[Na^+]_i$ – independent from their origin - can be converted by NCX into $[Ca^{2+}]_i$ signals. Those $[Ca^{2+}]_i$ signals could initiate and/or modulate a local MBP synthesis and myelination, for each process independently. Since the results of the main part of this thesis were obtained in cultured OPCs, further experiments performed *in vivo* are required to examine the hypothesis.

4.6 α2-NKA expression in cultured OPCs

The main task of NKA is the maintenance of the transmembrane Na^+ and K^+ gradients which are crucial for secondary transport processes and adjusting the membrane potential. The smallest functional unit of the NKA is composed of a catalytic (α) subunit and glycoprotein (β) subunit (Blanco 2005; Crambert et al. 2000). Tissue-dependent isoforms of those subunits were discovered: four α subunits, three β subunits and seven different γ subunits (Blanco 2005; Clausen, Hilbers and Poulsen 2017). While neurons are α1- and α3-NKA-positive, astrocytes and oligodendrocytes express α1- and α2-NKA (Cameron et al. 1994; Watts et al. 1991). α4-NKA was only demonstrated in spermatozoa (Shamraj, Lingrelt and Hoffman 1994; Blanco et al. 1999). The main difference between the α subunits lies in their ion affinity. α1 subunit of NKA shows K^+ affinity in a range of 1-2 mM,

while the α2 subunit especially in combination with β2 subunit demonstrates a reduced K$^+$ affinity in the 3-5 mM range (Blanco et al. 1995; Crambert et al. 2000; Sweadner 1985). Interestingly, this affinity constant lies close to physiological [K$^+$]$_e$ levels. Together with the high voltage sensitivity of α2-NKA (Blanco 2005) this makes it an efficient sensor of [K$^+$]$_e$ fluctuations. Intriguingly, it was demonstrated that in astrocytic processes, surrounding dendrites, α2-NKA is expressed (Cholet 2002). In astrocytic (Peng, Arystarkhova and Sweadner 1998) as well as in OPC (Knapp, Itkis and Mata 2000) monocultures without neuronal input, lack or low expression levels of α2 subunit were reported. However, in contrast to studies from 2000, where almost no α2-NKA was expressed by mature OPCs (Knapp, Itkis and Mata 2000) in this thesis α2-NKA in OPCs monocultures was already detected at DIV2 and its expression level increased during development even in the absence of neurons (Figure 3-15). More modern detection methods and antibodies could explain this discrepancy.

4.7   Distribution of α2-NKA in plasma membrane of OPCs

It was reported that the astrocytic α2-NKA distribution in the plasma membrane was heterogeneous (Juhaszova and Blaustein 1997). Localization of α2-NKA in OPCs co-cultured with neurons (their Fig. 4) was only shown in perisomatic areas (Knapp, Itkis and Mata 2000). Thespatial distribution of α2-NKA in OPC processes was not analyzed. In this thesis it is demonstrated that α2-NKA cannot only be detcted at the perisomatic areas, but also at the thick proximal processes. OPCs at DIV2, which are not yet expressing MBP, show an almost homogeneous distribution over the whole cell. The co-localization with CNP signals confirms the α2-NKA location on immature OPCs. This homogeneous distribution changes during development. At DIV4 and DIV5, the critical period of the onset of MBP expression, α2-NKA is mainly localized at the thick proximal OPC processes in relatively immature OPCs. However, compared to the thick proximal processes the fine distal ones and the MBP-positive sheets show reduced levels of α2-NKA at DIV4 and DIV5, indicating a decrease of MBP-α2-NKA co-localisation during OPC development (Figure 3-17). Therefore it is suggested that the onset of MBP synthesis is controlled by α2-NKA and is not required for later MBP production in distal processes.

4.8   α2-NKA interacts with NCX

Boscia et al. (Boscia et al. 2012) showed that NCX3 isoform and the myelin associated glycoprotein (MAG) are co-localized in the thick proximal OPC processes. Additionally, they demonstrated the NCX3 expression pattern which is quite similar to the α2-NKA immunostaining obtained in this thesis. Intriguingly, it was reported that α2-NKA and NCX cooperate in astrocytes. In astrocytic plasma membranes α2-NKA was shown to be organized in a reticular pattern co-localized with NCX, suggesting that α2-NKA via NCX may regulate local levels of $[Ca^{2+}]_i$ in the cytosol (Juhaszova et al. 1996; Juhaszova and Blaustein 1997). Since the increase of MBP expression created through α2-siRNA on DIV5 could be significantly decreased by the chronic KB-R7943 application, it seems that NCX mediates the observed α2-NKA-dependent suppression of MBP synthesis. Tong et al. (Tong et al. 2009) reported that NCX-mediated Ca^{2+} signaling is required for migration of NG2 positive cells. This Ca^{2+} signaling, however, was mediated by NCX1. Nevertheless, MBP synthesis in turn was shown to be linked to the NCX3 isoform (Boscia et al. 2012). Unfortunately, no selective NCX3 blocker is available, but the obtained data allow suggesting that α2-NKA interaction with NCX3 is important for initiation of MBP synthesis. Further experiments need to be performed to verify this hypothesis.

4.9   Mechanisms linking α2-NKA and MBP synthesis

What is the mechanism of NCX-mediated initiation of MBP synthesis? Blocking α2-NKA results in $[Na^+]_i$ elevation. This $[Na^+]_i$ elevation shifts NCX reversal potential to a more negative value and might subsequently initiate NCX-mediated Ca^{2+} influx. The latter occurs in control cultures under resting conditions at DIV5, whereas cultures treated with α2-siRNA show this Ca^{2+} influx already at DIV4 (Figure 3-22). Furthermore, NCX-mediated Ca^{2+} influx initiates spontaneous Ca^{2+} transients in OPCs. Various effects of Ca^{2+} activity like modulation of process extension/retraction (Paez et al. 2007) or migration (Paez et al. 2009) of OPCs has already been shown. In parallel, Haberlandt et al. (Haberlandt et al. 2011) reported that Ca^{2+} influx via voltage-gated Ca^{2+} channels facilitated by Ca^{2+}-induced Ca^{2+} release from endoplasmic reticulum controls the process motility of NG2 cells.

After application of NCX reverse mode blocker KB-R7943 a cease of spontaneous Ca^{2+} activity was shown in this thesis, indicating that Ca^{2+} influx mediated by NCX facilitates spontaneous Ca^{2+} activity. Furthermore, it was demonstrated that silencing of $\alpha2$-KNA shifts NCX reversal from DIV5 to DIV4 and subsequently the onset of spontaneous Ca^{2+} activity.

It is hypothesized that this form of Ca^{2+} signaling is required for the onset of MBP synthesis, since the chronical blocking of the NCX reverse mode reduces MBP levels in control OPC cultures (Boscia et al. 2012; this thesis) and suppresses the $\alpha2$-NKA-induced facilitation of MPB production in this thesis (Figure 3-18). Interestingly, Krasnow and collegues also demonstrated that neuronal activity leads to an increase in $[Ca^{2+}]_i$ levels followed by high frequencies of $[Ca^{2+}]_i$ oscillations which subsequently leads to sheath elongation in zebrafish OPCs (Krasnow et al. 2018).

Nevertheless, the role of Ca^{2+} oscillations in MBP synthesis requires further investigation (Boscia et al. 2012; Haberlandt et al. 2011; Martinez-Lozada et al. 2014; Santiago González et al. 2017).

4.10   Mechanism of termination of spontaneous Ca^{2+} activity

Furthermore it is demonstrated that spontaneous NCX-mediated Ca^{2+} transients occur only in a limited time frame in OPC cultures. Basically, this Ca^{2+} activity is relatively strong in DIV4-5 cultured OPCs but it starts disappearing at DIV6. Also, $[K^+]_e$-induced Ca^{2+} transients are significantly reduced at DIV6 as compared to DIV4. Interestingly, it was demonstrated by Smith et al. (Smith et al. 2011) that over-expression of the classical MBP isoforms leads to a reduction of Ca^{2+} influx after elevation of $[K^+]_e$ to 20 mM in cultured OPCs. In contrast to the MBP over-expression, in this thesis the levels of MBP were reduced by siRNA application. The MBP knock downleads to a facilitation of $[K^+]_e$-induced responses and additionally relatively high responses are still observed at DIV6. This supports the hypothesis that Ca^{2+} activity is negatively controlled by MBP expression.

Primary oligodendrocyte precursor cells are able to develop and produce MBP positive sheets – the equivalent of the *in vivo* myelin sheath – even without the presence of neurons. This leads to the conclusion that there seems to be an intrinsic genetic program,

which can start myelination even without axonal activity. It is hypothesized that an initial Ca^{2+} influx, mediated by the reversal mode of the NCX, can lead to a calcium release from internal stores of the endoplasmatic reticulum. The resulting Ca^{2+} oscillations were blocked by application of thapsigargin, a blocker of sarco/endoplasmatic reticulum Ca^{2+} ATPase (SERCA) (unpublished data). It is suggested that NCX and NKA are clustered at the fine tips of the processes in special microdomains and are closely located to endoplasmatic reticulum (ER) below the plasma membrane. Since the volume in these small compartments is low, already a small change of $[Na^+]_i$ could lead to a switch of the NCX into reverse mode, modulate the local Ca^{2+} storage of the ER, initiating Ca^{2+} signaling and start MBP expression. This mechanism has already been shown in other cell types such as neurons, astrocytes and cardiac myocytes (M P Blaustein et al. 2002; Despa, Lingrel, and Bers 2012) and supports the hypothesis mentioned. Figure 3-17 shows that the α2-NKAs become more located towards the thick proximal processes during maturation of the OPCs. This can influence the communication between NKA/NCX domains with the ER since the volume of the cytosol is increased. It would also explain the depletion of the spontaneous Ca^{2+} activity after DIV5 in control condition and DIV4 after down regulation of α2-NKA. Together with the fact that there is almost no α2-NKA left in the distal processes, it seems that proximal α2-NKA is not sufficient to generate calcium transients.

Definitely, MBP-Ca^{2+}-signaling interaction characterization needs further investigations, but it can be speculated that MBP itself may serve as a terminating signal of spontaneous Ca^{2+} activity.

4.11   Is α2-NKA together with NCX a sensor of neuronal activity?

Since the formation of compact myelin is impaired in the absence of MBP, it has been declared to be the 'executive molecule of myelin' (Boggs 2006). It is the second most abundant myelin protein and mutant mice lacking MBP like Shiverer or rats like Long-Evans shaker show a severe hypomyelination of the CNS (Kwiecien et al. 1998; Readhead and Hood 1990). The transport of MBP mRNA from the nucleus to the axon-glial contact site is achieved in a translationally silenced state (Müller et al. 2013). Many publications show that axon-glial contact triggers localized MBP translation and subsequently mye-

lination (Lisbeth S Laursen, Chan, and FfrenchConstant 2011; Wake, Lee, and Fields 2011; White et al. 2008). Even though MBP is necessary for myelination (Snaidero and Simons 2017), it is still unclear if a facilitation of MBP synthesis subsequently leads to a stronger myelination *in vivo*.

The experiments within this thesis demonstrate that a knock down of α2-NKA stimulates MBP synthesis in cultured OPCs. It can be proposed that the α2-NKA sets the membrane potential close to the reversal potential of the NCX and thereby prevents the initiation of spontaneous NCX-mediated Ca^{2+} influx, which in turn postpones the onset of MBP synthesis in OPC monocultures. The absence of neurons does not prevent the initiation of spontaneous Ca^{2+} signals or the onset of MBP synthesis, giving hint that there might be a genetically encoded program, which can be modulated by α2-NKA.

However, the α2-NKA-mediated negative role on MBP synthesis seems to be not transferable to the cortical organotypic slice culture model, since here the α2-NKA knock down does not influence the MBP levels. Intriguingly, even though the MBP levels in Cosc do not differ between knock down and control conditions, a decrease of co-localisation of MBP-positive (myelin) and neurofilament-positive (axons) is shown after α2-NKA reduction. It rather seems that this treatment has an influence on the myelination of the axons: α2-NKA appears to serve as a sensor of neuronal activity which at first locally prevents expression of MBP. However, as soon as α2-NKA is activated through an increase of extracellular K^+ concentration, it does allow myelination of the axon's trongly active areas. This leads to the assumption that the spatial location of myelin is modified. Even though the treatment of Cosc with α2-siRNA showed changes compared to the control conditions, it has not been proven that the knock down was really successful. Future densitometric western blot analyses should be performed to verify this. As described in chapter 1.3.5, not only oligodendrocytes, but also astrocytes express the α2 subunit of the NKA. And since siRNA is not cell type specific, it cannot be excluded that the observed effects in Cosc are contributed by astrocytes. Silencing of α2-NKA only limited to OPCs – for example via adeno-associated viruses – is required to verify the demonstrated results. In any case it is tempting to speculate that NKA and NCX act together as a local sensor of neuronal activity, in particular for $[K^+]_e$ fluctuations. The inhibiting action of α2-NKA observed

in OPC cultures could then be repealed by the depolarizing effect of local $[K^+]_e$ changes. It should also be mentioned that not only NKA, but all Na^+-dependent transporters like neurotransmitter transporters (Fattorini et al. 2017; Martinez-Lozada et al. 2014) or NKCC1 (Chen et al. 2007; Zonouzi et al. 2015) could be considered as potential sidekick of NCX, provided that they are located close to distal OPC processes and neuronal active fibers.

4.12   Conclusion and Outlook

Myelination of neuronal axons in the CNS is a complex multi-step procedure and the pathway of an oligodendrocyte recognizing an axon to its myelination has not yet been fully deciphered. With the results of the present thesis it was possible to shed some light into the darkness of this pathway. At least in OPC monocultures it could be shown that $[Ca^{2+}]_i$ and $[Na^+]_i$ in OPCs vary during development. It is likely that those developmental ion transients are induced by the activity of NKA and this in turn influences the transport direction of NCX. Reversal mode of NCX leads to a Ca^{2+} influx into the oligodendrogial processes and subsequently initiates $[Ca^{2+}]_i$ signaling which is followed by MBP mRNA translation. Since $[Ca^{2+}]_i$ signaling and myelination even occur without neuronal activity, it seems that oligodendrocyte development is pre-programmed but elevation of extracellular K^+ postpones $[Ca^{2+}]_i$ and $[Na^+]_i$ transients and MBP expression.

Knockdown of α2-NKA in Cosc results in another way than in OPC monocultures: here not the amount of MBP expression is altered, but spatial location of myelin seems to be disturbed. As mentioned before not only OPCs but also astrocytes express α2-NKA. To investigate the effect of only oligodendroglial α2-NKA in complex tissues like Cosc and to exclude the contribution of astrocytes, it is necessary to direct the silencing only to oligodendrocytes. Electron-microscopy analyses need to be done to verify the change of myelination after α2-NKA silencing.

The role of Ca^{2+} oscillations in MBP synthesis requires further investigation. It would be interesting to see if the oscillations lead to an activation of Fyn. Additionally, co-localization experiments could prove that NCX and NKA are clustered in microdomains

and if they share a microdomain with F3/contactin and thereby create a pro myelination unit within the plasmamembrane of the oligodendroglial processes.

Since NCX operation mode depends on $[Na^+]_i$, all Na^+-dependent transporters, including neurotransmitter transporters or NKCC1, may be considered as potential detectors of neuronal activity. The link between those transporters and NCX-mediated Ca^{2+} oscillations and subsequently MBP synthesis would also be interesting verify with future experiments.

5 References

Abràmoff, Michael D., Paulo J Magalhães, and Sunanda J Ram. 2004. "Image Processing with ImageJ." *Biophotonics International*. doi:10.1117/1.3589100.

Aggarwal, Shweta, Nicolas Snaidero, Gesa Pähler, Steffen Frey, Paula Sánchez, Markus Zweckstetter, Andreas Janshoff, et al. 2013. "Myelin Membrane Assembly Is Driven by a Phase Transition of Myelin Basic Proteins Into a Cohesive Protein Meshwork." Edited by Ben A. Barres. *PLoS Biology* 11 (6). Public Library of Science: e1001577. doi:10.1371/journal.pbio.1001577.

Ainger, Kevin, Daniela Avossa, Amy S Diana, Christopher Barry, Elisa Barbarese, and John H Carson. 1997. "Transport and Localization Elements in Myelin Basic Protein MRNA." *Journal of Cell Biology* 138 (5). The Rockefeller University Press: 1077–87. doi:10.1083/jcb.138.5.1077.

Alberts, B., A. Johnson, J. Lewis, M. Raff, K. Roberts, and P. Walter. 2004. *Molekularbiologie Der Zelle*. 4th ed. Weinheim: WILEY-VCH.

Ballanyi, K., and H. Kettenmann. 1990. "Intracellular Na+ Activity in Cultured Mouse Oligodendrocytes." *Journal of Neuroscience Research* 26 (4): 455–60. doi:10.1002/jnr.490260408.

Baron, Wia, Holly Colognato, and Charles Ffrench-Constant. 2005. "Integrin-Growth Factor Interactions as Regulators of Oligodendroglial Development and Function." *GLIA* 49 (4). Wiley-Blackwell: 467–79. doi:10.1002/glia.20132.

Barrera, Kyrstle, Philip Chu, Jason Abramowitz, Robert Steger, Raddy L Ramos, and Joshua C Brumberg. 2013. "Organization of Myelin in the Mouse Somatosensory Barrel Cortex and the Effects of Sensory Deprivation." *Developmental Neurobiology* 73 (4). NIH Public Access: 297–314. doi:10.1002/dneu.22060.

Barres, B.A., M.A. Lazar, and M.C. Raff. 1994. "A Novel Role for Thyroid Hormone, Glucocorticoids and Retinoic Acid in Timing Oligodendrocyte Development." *Development*. http://dev.biologists.org/content/develop/120/5/1097.full.pdf.

Bauer, Nina M, Christina Moos, Jack van Horssen, Maarten Witte, Paul van der Valk, Benjamin Altenhein, Heiko J Luhmann, and Robin White. 2012. "Myelin Basic Protein Synthesis Is Regulated by Small Non-Coding RNA 715." *EMBO Reports* 13 (9). Nature Publishing Group: 827–34. doi:10.1038/embor.2012.97.

Belachew, Shibeshih, Brigitte Malgrange, Jean Michel Rigo, Bernard Register, Pierre Leprince, Gregory Hans, Laurent Nguyen, and Gustave Moonen. 2000. "Glycine Triggers an Intracellular Calcium Influx in Oligodendrocyte Progenitor Cells Which Is Mediated by the Activation of Both the Ionotropic Glycine Receptor and Na+-Dependent Transporters." *European Journal of Neuroscience* 12 (6). Blackwell Science Ltd: 1924–30. doi:10.1046/j.1460-9568.2000.00085.x.

Besse, Florence, and Anne Ephrussi. 2008. "Translational Control of Localized MRNAs: Restricting Protein Synthesis in Space and Time." *Nature Reviews Molecular Cell Biology*. Nature Publishing Group. doi:10.1038/nrm2548.

Blanco, Gustavo. 2005. "Na,K-ATPase Subunit Heterogeneity as a Mechanism for Tissue-Specific Ion Regulation." *Seminars in Nephrology*. doi:10.1016/j.semnephrol.2005.03.004.

Blanco, Gustavo, Joseph C Koster, Gladis Sanchez, and Robert W Mercer. 1995. "Kinetic Properties of the A2/?L and A2/32 Isozymes of the Na,K-ATPase'." *Biochemistry* 34: 319–25. http://pubs.acs.org/doi/pdf/10.1021/bi00001a039.

Blanco, Gustavo, Roger J Melton, Gladis Sánchez, and Robert W Mercer. 1999. "Functional Characterization of a Testes-Specific α-Subunit Isoform of the Sodium/Potassium Adenosinetriphosphatase." *Biochemistry* 38 (41): 13661–69. doi:10.1021/bi991207b.

Blanco, Gustavo, and Robert W Mercer. 1998. "Isozymes of the Na-K-ATPase: Heterogeneity in Structure, Diversity in Function." *The American Journal of Physiology, Renal Physiology* 275 (5 Pt 2): F633–50. doi:10.1152/ajprenal.00721.2010.

Blankenfeld, Gabriela v., Alexej N. Verkhratsky, and Helmut Kettenmann. 1992. "Ca 2+ Channel Expression in the Oligodendrocyte Lineage." *European Journal of Neuroscience* 4 (11). Blackwell Publishing Ltd: 1035–48. doi:10.1111/j.1460-9568.1992.tb00130.x.

Blaustein, M P, M. JUHASZOVA, V. A. GOLOVINA, P. J. CHURCH, and E. F. STANLEY. 2002. "Na/Ca Exchanger and PMCA Localization in Neurons and Astrocytes." *Annals of the New York Academy of Sciences*, no. 976: 356–66. doi:10.1111/j.1462-2920.2007.01501.x.

Blaustein, Mordecai P, and W Jonathan Lederer. 1999. "Sodium/Calcium Exchange: Its Physiological Implications" 79 (3): 763–854. http://www.physiology.org/doi/pdf/10.1152/physrev.1999.79.3.763.

Boggs, J. M. 2006. "Myelin Basic Protein: A Multifunctional Protein." *Cellular and Molecular Life Sciences* 63 (17): 1945–61. doi:10.1007/s00018-006-6094-7.

Bolte, S., and F. P. Cordelières. 2006. "A Guided Tour into Subcellular Colocalization Analysis in Light Microscopy." *Journal of Microscopy*. Wiley/Blackwell (10.1111). doi:10.1111/j.1365-2818.2006.01706.x.

Boscia, F, C D'Avanzo, A Pannaccione, A Secondo, A Casamassa, L Formisano, N Guida, Sophie Sokolow, André Herchuelz, and L Annunziato. 2012. "Silencing or Knocking out the Na(+)/Ca(2+) Exchanger-3 (NCX3) Impairs Oligodendrocyte Differentiation." *Cell Death and Differentiation* 19 (4): 562–72. doi:10.1038/cdd.2011.125.

Brophy, Peter J., Graciela L. Boccaccio, and David R. Colman. 1993. "The Distribution of Myelin Basic Protein MRNAs within Myelinating Oligodendrocytes." *Trends in Neurosciences*. Elsevier Current Trends. doi:10.1016/0166-2236(93)90196-S.

Cai, Jun, Yingchuan Qi, Xuemei Hu, Min Tan, Zijing Liu, Jianshe Zhang, Qun Li, Maike Sander, and Mengsheng Qiu. 2005. "Generation of Oligodendrocyte Precursor Cells from Mouse Dorsal Spinal Cord Independent of Nkx6 Regulation and Shh Signaling." *Neuron* 45 (1). Cell Press: 41–53. doi:10.1016/j.neuron.2004.12.028.

Calver, Andrew R, Anita C Hall, Wei Ping Yu, Frank S Walsh, John K Heath, Christer Betsholtz, and William D Richardson. 1998. "Oligodendrocyte Population Dynamics and the Role of PDGF in Vivo." *Neuron* 20 (5). Cell Press: 869–82. doi:10.1016/S0896-6273(00)80469-9.

Cameron, Richard, Laura Klein, Andrew W Shyjan, Pasko Rakic, and Robert Levenson. 1994. "Neurons and Astroglia Express Distinct Subsets of Na,K-ATPase α and β Subunits." *Molecular Brain Research* 21 (3–4): 333–43. doi:10.1016/0169-328X(94)90264-X.

Chandran, Siddharthan, Hidemasa Kato, Dianne Gerreli, Alastair Compston, Clive N. Svendsen, and Nicholas D. Allen. 2003. "FGF-Dependent Generation of Oligodendrocytes by a Hedgehog-Independent Pathway." *Development* 130 (26). The Company of Biologists Ltd: 6599–6609. doi:10.1242/dev.00871.

Chen, Hai, Douglas B. Kintner, Mathew Jones, Toshio Matsuda, Akemichi Baba, Lech Kiedrowski, and Dandan Sun. 2007. "AMPA-Mediated Excitotoxicity in Oligodendrocytes: Role for Na +-K+-Cl- Co-Transport and Reversal of Na +/Ca2+ Exchanger." *Journal of Neurochemistry* 102 (6): 1783–95. doi:10.1111/j.1471-4159.2007.04638.x.

Cholet, N. 2002. "Similar Perisynaptic Glial Localization for the Na+,K+-ATPase Alpha2 Subunit and the Glutamate Transporters GLAST and GLT-1 in the Rat Somatosensory Cortex." *Cerebral Cortex* 12 (5). Oxford University Press: 515–25. doi:10.1093/cercor/12.5.515.

Clapham, David E. 2007. "Calcium Signaling." *Cell* 131 (6). Cell Press: 1047–58. doi:10.1016/j.cell.2007.11.028.

Clapham, David E. 1995. "Calcium Signaling." *Cell*. doi:10.1016/0092-8674(95)90408-5.

Clarke, Laura E, Kaylene M Young, Nicola B Hamilton, Huiliang Li, William D Richardson, and David Attwell. 2012. "Properties and Fate of Oligodendrocyte Progenitor Cells in the Corpus Callosum, Motor Cortex,

and Piriform Cortex of the Mouse." *Journal of Neuroscience* 32 (24). Society for Neuroscience: 8173–85. doi:10.1523/JNEUROSCI.0928-12.2012.

Clausen, Michael V., Florian Hilbers, and Hanne Poulsen. 2017. "The Structure and Function of the Na,K-ATPase Isoforms in Health and Disease." *Frontiers in Physiology*. Frontiers. doi:10.3389/fphys.2017.00371.

Colello, R J, L R Devey, E Imperato, and U Pott. 1995. "The Chronology of Oligodendrocyte Differentiation in the Rat Optic Nerve: Evidence for a Signaling Step Initiating Myelination in the CNS." *The Journal of Neuroscience : The Official Journal of the Society for Neuroscience* 15 (November): 7665–72. doi:10.1523/jneurosci.0727-08.2008.

Crambert, Gilles, Udo Hasler, Ahmed T Beggah, Chuliang Yu, Nikolai N Modyanov, Jean-Daniel Horisberger, Lionel Lelièvre, and Käthi Geering. 2000. "Transport and Pharmacological Properties of Nine Different Human Na,K-ATPase Isozymes." *Journal of Biological Chemistry* 275 (3). American Society for Biochemistry and Molecular Biology: 1976–86. doi:10.1074/jbc.275.3.1976.

Crawford, Abbe H, Richa B Tripathi, William D Richardson, and Robin J M Franklin. 2016. "Developmental Origin of Oligodendrocyte Lineage Cells Determines Response to Demyelination and Susceptibility to Age-Associated Functional Decline." *Cell Reports* 15: 761–73. doi:10.1016/j.celrep.2016.03.069.

Czopka, Tim, Charles ffrench-Constant, and DavidA Lyons. 2013. "Individual Oligodendrocytes Have Only a Few Hours in Which to Generate New Myelin Sheaths Invivo." *Developmental Cell* 25 (6): 599–609. doi:10.1016/j.devcel.2013.05.013.

Denter, D G, N Heck, T Riedemann, R White, W Kilb, and H J Luhmann. 2010. "GABACreceptors Are Functionally Expressed in the Intermediate Zone and Regulate Radial Migration in the Embryonic Mouse Neocortex." *Neuroscience* 167 (1): 124–34. doi:10.1016/j.neuroscience.2010.01.049.

Denzer, Kristin, Monique J. Kleijmeer, Harry F.G. Heijnen, Willem Stoorvogel, Hans J. Geuze, R. J. Advani, B. Yang, et al. 2000. "Exosome: From Internal Vesicle of the Multivesicular Body to Intercellular Signaling Device." *Journal of Cell Science* 113 Pt 19 (19): 3365–74. doi:10.1083/jcb.146.4.765.

Despa, Sanda, Jerry B Lingrel, and Donald M Bers. 2012. "Na+/K+-ATPase ??2-Isoform Preferentially Modulates Ca2+ Transients and Sarcoplasmic Reticulum Ca2+ Release in Cardiac Myocytes." *Cardiovascular Research* 95 (4). Oxford University Press: 480–86. doi:10.1093/cvr/cvs213.

Dubois-Dalcq, M, T Behar, L Hudson, and R A Lazzarini. 1986. "Emergence of Three Myelin Proteins in Oligodendrocytes Cultured without Neurons." *Journal of Cell Biology* 102 (2): 384–92. doi:10.1083/jcb.102.2.384.

Edgar, Julia M, Mark McLaughlin, Donald Yool, Su-Chun Zhang, Jill H Fowler, Paul Montague, Jennifer A Barrie, et al. 2004. "Oligodendroglial Modulation of Fast Axonal Transport in a Mouse Model of Hereditary Spastic Paraplegia." *The Journal of Cell Biology* 166 (1). The Rockefeller University Press: 121–31. doi:10.1083/jcb.200312012.

Fahlke, Ch., W. Linke, B. Raßler, and R. Wiesner. 2015. *Taschenatlas Physiologie*. 2nd ed. Elsevier.

Fambrough, Douglas M, M V Lemas, Maura Hamrick, Mark Emerick, Karen J Renaud, Elizabeth M Inman, Ben Hwang, and Kunio Takeyasu. 1994. "Analysis of Subunit Assembly of the Na-K-ATPase." *The American Journal of Physiology* 266 (3 Pt 1): C579-89. http://www.physiology.org/doi/pdf/10.1152/ajpcell.1994.266.3.C579.

Fattorini, Giorgia, Marcello Melone, Marï¿½a Victoria Sï¿½nchez-Gï¿½mez, Rogelio O. Arellano, Silvia Bassi, Carlos Matute, and Fiorenzo Conti. 2017. "GAT-1 Mediated GABA Uptake in Rat Oligodendrocytes." *GLIA* 65 (3): 514–22. doi:10.1002/glia.23108.

Fogarty, Matthew, William D. Richardson, and Nicoletta Kessaris. 2005. "A Subset of Oligodendrocytes Generated from Radial Glia in the Dorsal Spinal Cord." *Development* 132 (8): 1951–59. doi:10.1242/dev.01777.

Friedrich, V. 1993. "The Oligodendrocyte and Its Many Cellular Processes." *Trends in Cell Biology* 3: 191–97. https://ac.els-cdn.com/096289249390213K/1-s2.0-096289249390213K-main.pdf?_tid=a09f63c8-

126a-4750-b0fa-bbf36de088be&acdnat=1524392446_4e05f7eace704196c51a066e3191b9e7.

Frohlich, D., Wen Ping Kuo, C. Fruhbeis, J.-J. Sun, Christoph M Zehendner, Heiko J Luhmann, Sheena Pinto, Joern Toedling, Jacqueline Trotter, and E.-M. Kramer-Albers. 2014. "Multifaceted Effects of Oligodendroglial Exosomes on Neurons: Impact on Neuronal Firing Rate, Signal Transduction and Gene Regulation." *Philosophical Transactions of the Royal Society B: Biological Sciences* 369 (1652). The Royal Society: 20130510–20130510. doi:10.1098/rstb.2013.0510.

Frühbeis, Carsten, Dominik Fröhlich, Wen Ping Kuo, Jesa Amphornrat, Sebastian Thilemann, Aiman S Saab, Frank Kirchhoff, et al. 2013. "Neurotransmitter-Triggered Transfer of Exosomes Mediates Oligodendrocyte-Neuron Communication." *PLoS Biology* 11 (7). Public Library of Science: e1001604. doi:10.1371/journal.pbio.1001604.

Fulton, Daniel, Pablo M Paez, and Anthony T Campagnoni. 2010. "The Multiple Roles of Myelin Protein Genes During the Development of the Oligodendrocyte." *ASN Neuro* 2 (1). SAGE Publications: AN20090051. doi:10.1042/AN20090051.

Gallo, Vittorio, J.M. Zhou, C.J. McBain, Paul Wright, P.L. Knutson, and R.C. Armstrong. 1996. "68 Oligodendrocyte Progenitor Cell Proliferation and Lineage Progression Are Regulated by Glutamate Receptor-Mediated K+ Channel Block." *International Journal of Developmental Neuroscience* 14 (8): 67. doi:10.1016/0736-5748(96)80263-2.

Giladi, Moshe, Reut Shor, Michal Lisnyansky, and Daniel Khananshvili. 2016. "Structure-Functional Basis of Ion Transport in Sodium–Calcium Exchanger (NCX) Proteins." *International Journal of Molecular Sciences*. Multidisciplinary Digital Publishing Institute. doi:10.3390/ijms17111949.

Giladi, Moshe, Inbal Tal, and Daniel Khananshvili. 2016. "Structural Features of Ion Transport and Allosteric Regulation in Sodium-Calcium Exchanger (NCX) Proteins." *Frontiers in Physiology*. Frontiers. doi:10.3389/fphys.2016.00030.

Glynn, I M, and S J D Karlish. 1990. "OCCLIJDED CATIONS IN ACTIVE TRANSPORT." *Annu. Rev. Biochem* 59: 171–205. https://www.annualreviews.org/doi/pdf/10.1146/annurev.bi.59.070190.001131.

Griffiths, Ian, Matthias Klugmann, Thomas Anderson, Donald Yool, Christine Thomson, Markus H Schwab, Armin Schneider, et al. 1998. "Axonal Swellings and Degeneration in Mice Lacking the Major Proteolipid of Myelin." *Science* 280 (5369). American Association for the Advancement of Science: 1610–13. doi:10.1126/science.280.5369.1610.

Haberlandt, Christian, Amin Derouiche, Alexandra Wyczynski, Julia Haseleu, Jörg Pohle, Khalad Karram, Jacqueline Trotter, et al. 2011. "Gray Matter Ng2 Cells Display Multiple Ca2+-Signaling Pathways and Highly Motile Processes." *PLoS ONE* 6 (3). Public Library of Science: e17575. doi:10.1371/journal.pone.0017575.

Hamano, Kenzo, Nobuaki Iwasaki, Toshiki Takeya, and Hitoshi Takita. 1996. "A Quantitative Analysis of Rat Central Nervous System Myelination Using the Immunohistochemical Method for MBP." *Developmental Brain Research* 93 (1): 18–22. doi:10.1016/0165-3806(96)00025-9.

Harauz, George, and Joan M Boggs. 2013. "Myelin Management by the 18.5-KDa and 21.5-KDa Classic Myelin Basic Protein Isoforms." *Journal of Neurochemistry*. PMC Canada manuscript submission. doi:10.1111/jnc.12195.

Hartline, D. K., and D. R. Colman. 2007. "Rapid Conduction and the Evolution of Giant Axons and Myelinated Fibers." *Current Biology* 17 (1): 29–35. doi:10.1016/j.cub.2006.11.042.

Jacobs, Erin C, Samuel D Reyes, Celia W Campagnoni, M Irene Givogri, Kathy Kampf, Vance Handley, Vilma Spreuer, Robin Fisher, Wendy Macklin, and Anthony T Campagnoni. 2009. "Targeted Overexpression of a Golli-Myelin Basic Protein Isoform to Oligodendrocytes Results in Aberrant Oligodendrocyte Maturation and Myelination." *ASN Neuro* 1 (4). SAGE Publications: AN20090029. doi:10.1042/AN20090029.

Jahn, Olaf, Stefan Tenzer, and Hauke B Werner. 2009. "Myelin Proteomics: Molecular Anatomy of an Insulating Sheath." *Molecular Neurobiology*. doi:10.1007/s12035-009-8071-2.

Jo, Euijung, and Joan M. Boggs. 1995. "Aggregation of Acidic Lipid Vesicles by Myelin Basic Protein: Dependence on Potassium Concentration." *Biochemistry* 34 (41). American Chemical Society: 13705–16. doi:10.1021/bi00041a053.

Juhaszova, Magdalena, and Mordecai P Blaustein. 1997. "Na+ Pump Low and High Ouabain Affinity Alpha Subunit Isoforms Are Differently Distributed in Cells." *Proceedings of the National Academy of Sciences of the United States of America* 94 (5): 1800–1805. doi:10.1073/pnas.94.5.1800.

Juhaszova, Magdalena, Hiroshi Shimizu, Mikhail L Borin, Rick K Yip, Eligio M Santiago, George E Lindenmayer, and Mordecai P Blaustein. 1996. "Localization of the Na+-Ca2+ Exchanger in Vascular Smooth Muscle, and in Neurons and Astrocytesa." *Annals of the New York Academy of Sciences* 779 (1). Wiley/Blackwell (10.1111): 318–35. doi:10.1111/j.1749-6632.1996.tb44804.x.

Kamholz, J, J Toffenetti, and R A Lazzarini. 1988. "Organization and Expression of the Human Myelin Basic Protein Gene." *J. Neurosci. Res.* 21 (1): 62–70. doi:10.1002/jnr.490210110.

Kaplan, Jack H. 2002. "Biochemistry of Na,K-ATPase." *Annual Review of Biochemistry* 71 (1): 511–35. doi:10.1146/annurev.biochem.71.102201.141218.

Kaplan, M. R., A. Meyer-Franke, S. Lambert, Vann Bennett, I D Duncan, S Rock Levinson, and Ben A Barres. 1997. "Induction of Sodium Channel Clustering by Oligodendrocytes." *Nature* 386 (6626): 724–28. doi:10.1038/386724a0.

Kaplan, Miriam R., Min Hee Cho, Erik M Ullian, Lori L Isom, S. Rock Levinson, and Ben A Barres. 2001. "Differential Control of Clustering of the Sodium Channels Nav1.2 and Nav1.6 at Developing CNS Nodes of Ranvier." *Neuron* 30 (1). Cell Press: 105–19. doi:10.1016/S0896-6273(01)00266-5.

Kaplan, Miriam R, Min Hee Cho, Erik M Ullian, Lori L Isom, S Rock Levinson, and Ben A Barres. 2001. "Differential Control of Clustering of the Sodium Channels Nav1.2 and Nav1.6 at Developing CNS Nodes of Ranvier." *Neuron* 30 (1). Elsevier: 105–19. doi:10.1016/S0896-6273(01)00266-5.

Káradóttir, Ragnhildur, Pauline Cavelier, Linda H. Bergersen, and David Attwell. 2005. "NMDA Receptors Are Expressed in Oligodendrocytes and Activated in Ischaemia." *Nature* 438 (7071). Nature Publishing Group: 1162–66. doi:10.1038/nature04302.

Kessaris, Nicoletta, Matthew Fogarty, Palma Iannarelli, Matthew Grist, Michael Wegner, and William D Richardson. 2006. "Competing Waves of Oligodendrocytes in the Forebrain and Postnatal Elimination of an Embryonic Lineage." *Nature Neuroscience* 9 (2). Nature Publishing Group: 173–79. doi:10.1038/nn1620.

Kessaris, Nicoletta, Francoise Jamen, Lee L. Rubin, and William D. Richardson. 2004. "Cooperation between Sonic Hedgehog and Fibroblast Growth Factor/MAPK Signalling Pathways in Neocortical Precursors." *Development* 131 (6). The Company of Biologists Ltd: 1289–98. doi:10.1242/dev.01027.

Khananshvili, Daniel. 2013. "The SLC8 Gene Family of Sodium-Calcium Exchangers (NCX)-Structure, Function, and Regulation in Health and Disease." *Molecular Aspects of Medicine*. Pergamon. doi:10.1016/j.mam.2012.07.003.

Khananshvili, Daniel. 2014. "Sodium-Calcium Exchangers (NCX): Molecular Hallmarks Underlying the Tissue-Specific and Systemic Functions." *Pflugers Archiv European Journal of Physiology*. Springer Berlin Heidelberg. doi:10.1007/s00424-013-1405-y.

Kirischuk, S, T Möller, N Voitenko, H Kettenmann, and a Verkhratsky. 1995. "ATP-Induced Cytoplasmic Calcium Mobilization in Bergmann Glial Cells." *The Journal of Neuroscience : The Official Journal of the Society for Neuroscience* 15 (12): 7861–71.

Kirischuk, S, J Scherer, H Kettenmann, and A Verkhratsky. 1995. "Activation of P2-purinoreceptors Triggered Ca2+ Release from InsP3-sensitive Internal Stores in Mammalian Oligodendrocytes." *The Journal of Physiology* 483 (1). Wiley-Blackwell: 41–57. doi:10.1113/jphysiol.1995.sp020566.

Kirischuk, Sergei, Vladimir Parpura, and Alexei Verkhratsky. 2012. "Sodium Dynamics: Another Key to Astroglial Excitability?" *Trends in Neurosciences* 35 (8). Elsevier Ltd: 497–506. doi:10.1016/j.tins.2012.04.003.

Kirischuk, Sergei, Jürgen Scherer, Thomas Möller, Alexei Verkhratsky, and Helmut Kettenmann. 1995. "Subcellular Heterogeneity of Voltage-Gated Ca2+ Channels in Cells of the Oligodendrocyte Lineage." *Glia* 13 (1): 1–12. doi:10.1002/glia.440130102.

Kirkpatrick, L L, A S Witt, H R Payne, H D Shine, and S T Brady. 2001. "Changes in Microtubule Stability and Density in Myelin-Deficient Shiverer Mouse CNS Axons." *The Journal of Neuroscience* 21 (7). Society for Neuroscience: 2288–97. http://www.ncbi.nlm.nih.gov/pubmed/11264304.

Knapp, P. E., O. S. Itkis, and M. Mata. 2000. "Neuronal Interaction Determines the Expression of the ??-2 Isoform of Na, K-ATPase in Oligodendrocytes." *Developmental Brain Research* 125 (1–2): 89–97. doi:10.1016/S0165-3806(00)00125-5.

Knutson, P, C A Ghiani, J M Zhou, V Gallo, and C J McBain. 1997. "K+ Channel Expression and Cell Proliferation Are Regulated by Intracellular Sodium and Membrane Depolarization in Oligodendrocyte Progenitor Cells." *The Journal of Neuroscience : The Official Journal of the Society for Neuroscience* 17 (8). Society for Neuroscience: 2669–82. doi:10.1523/JNEUROSCI.17-08-02669.1997.

Kondo, T, and M Raff. 2000. "Oligodendrocyte Precursor Cells Reprogrammed to Become Multipotential CNS Stem Cells." *Science* 289 (5485). American Association for the Advancement of Science: 1754–57. doi:10.1126/science.289.5485.1754.

Kosturko, Linda D. 2005. "The Microtubule-Associated Protein Tumor Overexpressed Gene Binds to the RNA Trafficking Protein Heterogeneous Nuclear Ribonucleoprotein A2." *Molecular Biology of the Cell* 16 (4). American Society for Cell Biology: 1938–47. doi:10.1091/mbc.E04-08-0709.

Kosturko, Linda D, Michael J Maggipinto, George Korza, Joo Won Lee, John H Carson, and Elisa Barbarese. 2006. "Heterogeneous Nuclear Ribonucleoprotein (HnRNP) E1 Binds to HnRNP A2 and Inhibits Translation of A2 Response Element MRNAs." *Molecular Biology of the Cell* 17 (8). American Society for Cell Biology: 3521–33. doi:10.1091/mbc.E05-10-0946.

Krämer-Albers, Eva Maria, and Robin White. 2011. "From Axon-Glial Signalling to Myelination: The Integrating Role of Oligodendroglial Fyn Kinase." *Cellular and Molecular Life Sciences* 68 (12): 2003–12. doi:10.1007/s00018-010-0616-z.

Krasnow, Anna M., Marc C. Ford, Leonardo E. Valdivia, Stephen W. Wilson, and David Attwell. 2018. "Regulation of Developing Myelin Sheath Elongation by Oligodendrocyte Calcium Transients in Vivo." *Nature Neuroscience* 21 (1). Nature Publishing Group: 24–30. doi:10.1038/s41593-017-0031-y.

Kukley, Maria, Estibaliz Capetillo-Zarate, and Dirk Dietrich. 2007. "Vesicular Glutamate Release from Axons in White Matter." *Nature Neuroscience* 10 (3). Nature Publishing Group: 311–20. doi:10.1038/nn1850.

Kuster, B, A Shainskaya, H X Pu, R Goldshleger, R Blostein, M Mann, and S J Karlish. 2000. "A New Variant of the Gamma Subunit of Renal Na,K-ATPase. Identification by Mass Spectrometry, Antibody Binding, and Expression in Cultured Cells." *The Journal of Biological Chemistry* 275 (24). American Society for Biochemistry and Molecular Biology: 18441–46. doi:10.1074/jbc.M001411200.

Kwiecien, J.M., L.T. O'Connor, B. D. Goetz, K. H. Delaney, A.L. Fletch, and I.D. Duncan. 1998. "Morphological and Morphometric Studies of the Dysmyelinating Mutant, the Long Evans Shaker Rat." *Journal of Neurocytology* 27: 581–591.

Lappe-Siefke, Corinna, Sandra Goebbels, Michel Gravel, Eva Nicksch, John Lee, Peter E. Braun, Ian R. Griffiths, and Klaus Armin Navel. 2003. "Disruption of Cnp1 Uncouples Oligodendroglial Functions in Axonal Support and Myelination." *Nature Genetics* 33 (3). Nature Publishing Group: 366–74. doi:10.1038/ng1095.

Laursen, Lisbeth S, Colin W Chan, and Charles FfrenchConstant. 2011. "Translation of Myelin Basic Protein MRNA in Oligodendrocytes Is Regulated by Integrin Activation and HnRNP-K." *Journal of Cell Biology* 192 (5). The Rockefeller University Press: 797–811. doi:10.1083/jcb.201007014.

Laursen, Lisbeth Schmidt, Colin W Chan, and C. Ffrench-Constant. 2009. "An Integrin-Contactin Complex Regulates CNS Myelination by Differential Fyn Phosphorylation." *Journal of Neuroscience* 29 (29). Society for Neuroscience: 9174–85. doi:10.1523/JNEUROSCI.5942-08.2009.

Liang, Man, Ting Cai, Jiang Tian, Weikai Qu, and Zi Jian Xie. 2006. "Functional Characterization of Src-Interacting Na/K-ATPase Using RNA Interference Assay." *Journal of Biological Chemistry* 281 (28). American Society for Biochemistry and Molecular Biology: 19709–19. doi:10.1074/jbc.M512240200.

Liu, Tongyu, Xingjian Jin, Rahul M. Prasad, Youssef Sari, and Surya M. Nauli. 2014. "Three Types of Ependymal Cells with Intracellular Calcium Oscillation Are Characterized by Distinct Cilia Beating Properties." *Journal of Neuroscience Research* 92 (9): 1199–1204. doi:10.1002/jnr.23405.

Lutsenko, Svetlana, and Jack H. Kaplan. 1994. "Molecular Events in Close Proximity to the Membrane Associated with the Binding of Ligands to the Na,K-ATPase." *Journal of Biological Chemistry* 269 (6): 4555–64. http://www.jbc.org/content/269/6/4555.full.pdf.

Luyt, Karen, Aniko Varadi, and Elek Molnar. 2003. "Functional Metabotropic Glutamate Receptors Are Expressed in Oligodendrocyte Progenitor Cells." *Journal of Neurochemistry* 84 (6): 1452–64. doi:10.1046/j.1471-4159.2003.01661.x.

Maldonado, Paloma P, M. Velez-Fort, Françoise Levavasseur, and María Cecilia Angulo. 2013. "Oligodendrocyte Precursor Cells Are Accurate Sensors of Local K+ in Mature Gray Matter." *Journal of Neuroscience* 33 (6): 2432–42. doi:10.1523/JNEUROSCI.1961-12.2013.

Martinez-Lozada, Zila, Christopher T Waggener, Karam Kim, Shiping Zou, Pamela E Knapp, Yasunori Hayashi, Arturo Ortega, and Babette Fuss. 2014. "Activation of Sodium-Dependent Glutamate Transporters Regulates the Morphological Aspects of Oligodendrocyte Maturation via Signaling through Calcium/Calmodulin-Dependent Kinase IIβ's Actin-Binding/-Stabilizing Domain." *GLIA* 62 (9). NIH Public Access: 1543–58. doi:10.1002/glia.22699.

Matute, Carlos, Iratxe Torre, F Perez-Cerda, A Perez-Samartin, Elena Alberdi, Estibaliz Etxebarria, Amaia M Arranz, et al. 2007. "P2X(7) Receptor Blockade Prevents ATP Excitotoxicity in Oligodendrocytes and Ameliorates Experimental Autoimmune Encephalomyelitis." *J Neurosci* 27 (35). Society for Neuroscience: 9525–33. doi:10.1523/JNEUROSCI.0579-07.2007.

Michalski, John-Paul, and Rashmi Kothary. 2015. "Oligodendrocytes in a Nutshell." *Frontiers in Cellular Neuroscience* 9. Frontiers Media SA: 340. doi:10.3389/fncel.2015.00340.

Miller, Robert H. 2002. "Regulation of Oligodendrocyte Development in the Vertebrate CNS." *Progress in Neurobiology*. Pergamon. doi:10.1016/S0301-0082(02)00058-8.

Miron, Veronique E., Tanja Kuhlmann, and J. P. Antel Jack P. 2011. "Cells of the Oligodendroglial Lineage, Myelination, and Remyelination." *Biochimica et Biophysica Acta - Molecular Basis of Disease* 1812 (2). Elsevier B.V.: 184–93. doi:10.1016/j.bbadis.2010.09.010.

Müller, Christina, Nina M Bauer, Isabelle Schäfer, and Robin White. 2013. "Making Myelin Basic Protein - from MRNA Transport to Localized Translation." *Frontiers in Cellular Neuroscience* 7 (September): 169. doi:10.3389/fncel.2013.00169.

Müller, Christina, Isabelle Schäfer, Heiko J Luhmann, and Robin White. 2015. "Oligodendroglial Argonaute Protein Ago2 Associates with Molecules of the Mbp MRNA Localization Machinery and Is a Downstream Target of Fyn Kinase." *Frontiers in Cellular Neuroscience* 9. Frontiers Media SA: 328. doi:10.3389/fncel.2015.00328.

Munro, Trent P, Rebecca J Magee, Grahame J Kidd, John H Carson, Elisa Barbarese, Lisa M. Smith, and Ross Smith. 1999. "Mutational Analysis of a Heterogeneous Nuclear Ribonucleoprotein A2 Response Element for RNA Trafficking." *Journal of Biological Chemistry* 274 (48). American Society for Biochemistry and Molecular Biology: 34389–95. doi:10.1074/jbc.274.48.34389.

Nave, Klaus-Armin, and Hauke B. Werner. 2014. "Myelination of the Nervous System: Mechanisms and Functions." *Annual Review of Cell and Developmental Biology* 30 (August): 503–33. doi:10.1146/annurev-cellbio-100913-013101.

Newville, Jessie, LaurenL Jantzie, and LeeAnna Cunningham. 2017. "Embracing Oligodendrocyte Diversity in the Context of Perinatal Injury." *Neural Regeneration Research* 12 (10): 1575. doi:10.4103/1673-5374.217320.

Nicoll, Debora A, Michela Ottolia, Joshua I Goldhaber, and Kenneth D Philipson. 2013. "20 Years from NCX Purification and Cloning: Milestones." In *Advances in Experimental Medicine and Biology*, 961:17–23. NIH Public Access. doi:10.1007/978-1-4614-4756-6-2.

Nielsen, Morten Schak, Lene Nygaard Axelsen, Paul L Sorgen, Vandana Verma, Mario Delmar, and Niels-Henrik Holstein-Rathlou. 2012. "Gap Junctions." *Comprehensive Physiology* 2 (3). NIH Public Access: 1981–2035. doi:10.1002/cphy.c110051.Gap.

Nishiyama, Akiko, Mila Komitova, Ryusuke Suzuki, and Xiaoqin Zhu. 2009. "Polydendrocytes (NG2 Cells): Multifunctional Cells with Lineage Plasticity." *Nature Reviews Neuroscience*. Nature Publishing Group. doi:10.1038/nrn2495.

Norton, William T. 1984. "Recent Advances in Myelin Biochemistry." *Annals of the New York Academy of Sciences* 436 (1). Blackwell Publishing Ltd: 5–10. doi:10.1111/j.1749-6632.1984.tb14772.x.

Nowak, Mark W., and Harvey Alan Berman. 1991. "Fluorescence Studies on the Interactions of Myelin Basic Protein in Electrolyte Solutions." *Biochemistry* 30 (30). American Chemical Society: 7642–51. doi:10.1021/bi00244a037.

Orentas, D M, Jeanette E. Hayes, Kimberly L. Dyer, and Robert H. Miller. 1999. "Requirement for Shh during Oligodendrocyte Appearance." *Development* 126: 2419–29. http://dev.biologists.org/content/develop/126/11/2419.full.pdf.

Paez, Pablo M, Daniel J Fulton, Vilma Spreuer, Vance Handley, Celia W Campagnoni, Wendy B Macklin, Christopher Colwell, and Anthony T Campagnoni. 2009. "Golli Myelin Basic Proteins Regulate Oligodendroglial Progenitor Cell Migration through Voltage-Gated Ca++ Influx." *J. Neurosci* 29 (20). NIH Public Access: 6663–76. doi:10.1523/JNEUROSCI.5806-08.2009.Golli.

Paez, Pablo M, Vilma Spreuer, Vance Handley, J.-M. Feng, C. Campagnoni, and Anthony T Campagnoni. 2007. "Increased Expression of Golli Myelin Basic Proteins Enhances Calcium Influx into Oligodendroglial Cells." *Journal of Neuroscience* 27 (46). Society for Neuroscience: 12690–99. doi:10.1523/JNEUROSCI.2381-07.2007.

Panatier, Aude, Misa Arizono, and U. V. Nagerl. 2014. "Dissecting Tripartite Synapses with STED Microscopy." *Philosophical Transactions of the Royal Society B: Biological Sciences* 369 (1654). The Royal Society: 20130597–20130597. doi:10.1098/rstb.2013.0597.

Parras, Carlos M, Charles Hunt, Michiya Sugimori, Masato Nakafuku, David Rowitch, and François Guillemot. 2007. "The Proneural Gene Mash1 Specifies an Early Population of Telencephalic Oligodendrocytes." *Journal of Neuroscience* 27 (16). Society for Neuroscience: 4233–42. doi:10.1523/JNEUROSCI.0126-07.2007.

Peng, Liang, Elena Arystarkhova, and Kathleen J Sweadner. 1998. "Plasticity of Na , K-ATPase Isoform Expression in Cultures of Flat Astrocytes : Species Differences in Gene Expression." *Glia* 271 (February): 257–71. https://onlinelibrary.wiley.com/doi/pdf/10.1002/%28SICI%291098-1136%28199811%2924%3A3%3C257%3A%3AAID-GLIA1%3E3.0.CO%3B2-%23.

Pringle, Nigel P, Wei Ping Yu, Sarah Guthrie, Henk Roelink, Andrew Lumsden, Alan C Peterson, and William D Richardson. 1996. "Determination of Neuroepithelial Cell Fate: Induction of the Oligodendrocyte Lineage by Ventral Midline Cells and Sonic Hedgehog." *Developmental Biology* 177 (1): 30–42. doi:10.1006/dbio.1996.0142.

Qazzaz, Hassan M.A.M., Zhimin Cao, Duane D Bolanowski, Barbara J Clark, and Roland Valdes. 2004. "De Novo Biosynthesis and Radiolabeling of Mammalian Digitalis-Like Factors." *Clinical Chemistry* 50 (3). Clinical Chemistry: 612–20. doi:10.1373/clinchem.2003.022715.

Qiu, Li Yan, Elmar Krieger, Gijs Schaftenaar, Herman G.P. Swarts, Peter H.G.M. Willems, Jan Joep H.H.M. De Pont, and Jan B Koenderink. 2005. "Reconstruction of the Complete Ouabain-Binding Pocket of Na,K-ATPase in Gastric H,K-ATPase by Substitution of Only Seven Amino Acids." *Journal of Biological Chemistry* 280 (37). American Society for Biochemistry and Molecular Biology: 32349–55. doi:10.1074/jbc.M505168200.

Quednau, Beate D, Debora A Nicoll, and Kenneth D Philipson. 1997. "Tissue Specificity and Alternative

Splicing of the Na+/Ca2+ Exchanger Isoforms NCX1, NCX2, and NCX3 in Rat." *The American Journal of Physiology* 272 (4 Pt 1): C1250–61. https://www.physiology.org/doi/pdf/10.1152/ajpcell.1997.272.4.C1250.

Raju, Chandrasekhar S, C. Goritz, Ylva Nord, Ola Hermanson, C. Lopez-Iglesias, Neus Visa, Goncalo Castelo-Branco, and Piergiorgio Percipalle. 2008. "In Cultured Oligodendrocytes the A/B-Type HnRNP CBF-A Accompanies MBP MRNA Bound to MRNA Trafficking Sequences." *Molecular Biology of the Cell* 19 (7). American Society for Cell Biology: 3008–19. doi:10.1091/mbc.E07-10-1083.

Readhead, Carol, and Leroy Hood. 1990. "The Dysmyelinating Mouse Mutations Shiverer (Shi) and Myelin Deficient (Shimld)." *Behavior Genetics* 20 (2): 213–34. doi:10.1007/BF01067791.

Richardson, William D., Nicoletta Kessaris, and Nigel Pringle. 2006. "Oligodendrocyte Wars." *Nature Reviews Neuroscience*. doi:10.1038/nrn1826.

Richardson, William D, Kaylene M Young, Richa B Tripathi, and Ian McKenzie. 2011. "NG2-Glia as Multipotent Neural Stem Cells: Fact or Fantasy?" *Neuron*. NIH Public Access. doi:10.1016/j.neuron.2011.05.013.

Ro, Hyun Ah, and John H Carson. 2004. "PH Microdomains in Oligodendrocytes." *Journal of Biological Chemistry* 279 (35). American Society for Biochemistry and Molecular Biology: 37115–23. doi:10.1074/jbc.M403099200.

Rose, Christine R., and Claudia Karus. 2013. "Two Sides of the Same Coin: Sodium Homeostasis and Signaling in Astrocytes under Physiological and Pathophysiological Conditions." *GLIA*. doi:10.1002/glia.22492.

Ruffini, Francesca, Nathalie Arbour, Manon Blain, André Olivier, and Jack P Antel. 2004. "Distinctive Properties of Human Adult Brain-Derived Myelin Progenitor Cells." *American Journal of Pathology* 165 (6). American Society for Investigative Pathology: 2167–75. doi:10.1016/S0002-9440(10)63266-X.

Rushton, W A H. 1951. "A Theory of the Effects of Fibre Size in Medullated Nerve." *The Journal of Physiology* 115 (1): 101–22. doi:10.1113/jphysiol.1951.sp004655.

Sakry, Dominik, Khalad Karram, and Jacqueline Trotter. 2011. "Synapses between NG2 Glia and Neurons." *Journal of Anatomy*. Wiley/Blackwell (10.1111). doi:10.1111/j.1469-7580.2011.01359.x.

Santiago González, Diara A, Veronica T Cheli, Norma N Zamora, Tenzing N Lama, Vilma Spreuer, Geoffrey G Murphy, and Pablo M Paez. 2017. "Conditional Deletion of the L-Type Calcium Channel Cav1.2 in NG2 Positive Cells Impairs Remyelination in Mice." *The Journal of Neuroscience* 37 (42). Society for Neuroscience: 1787–17. doi:10.1523/JNEUROSCI.1787-17.2017.

Schoner, Wilhelm. 2002. "Endogenous Cardiac Glycosides, a New Class of Steroid Hormones." *European Journal of Biochemistry*. Blackwell Science, Ltd. doi:10.1046/j.1432-1033.2002.02911.x.

Segall, Laura, Zahid Z Javaid, Stephanie L Carl, Lois K Lane, and Rhoda Blostein. 2003. "Structural Basis for ??1 versus ??2 Isoform-Distinct Behavior of the Na,K-ATPase." *Journal of Biological Chemistry* 278 (11). American Society for Biochemistry and Molecular Biology: 9027–34. doi:10.1074/jbc.M211636200.

Shamraj, Olga I, Jerry B Lingrelt, and Joseph F Hoffman. 1994. "A Putative Fourth Na+,K+-ATPase a-Subunit Gene Is Expressed in Testis (ATPIAL2/Sodium Pump/A4 Isoform/Tissue-Speciflc Gene Expression)." *Physiology* 91: 12952–56. doi:10.1073/pnas.91.26.12952.

Shull, Gary E, Jeannette Greeb, and Jerry B Lingrel. 1986. "Molecular Cloning of Three Distinct Forms of the Na+,K+-ATPase a-Subunit from Rat Brain." *Biochemistry* 25 (25): 8125–32. doi:10.1021/bi00373a001.

Silbernagl, S., and A. Despopoulos. 2012. *Taschenatlas Physiologie*. 8th ed. Thieme.

Simons, Mikael, and Katarina Trajkovic. 2006. "Neuron-Glia Communication in the Control of Oligodendrocyte Function and Myelin Biogenesis." *Journal of Cell Science* 119 (21): 4381–89. doi:10.1242/jcs.03242.

Simpson, Peter B., and Regina C. Armstrong. 1999. "Intracellular Signals and Cytoskeletal Elements Involved

in Oligodendrocyte Progenitor Migration." *GLIA* 26 (1). John Wiley & Sons, Inc.: 22–35. doi:10.1002/(SICI)1098-1136(199903)26:1<22::AID-GLIA3>3.0.CO;2-M.

Smith, Graham S.T., Pablo M Paez, Vilma Spreuer, Celia W. Campagnoni, Joan M Boggs, Anthony T Campagnoni, and George Harauz. 2011. "Classical 18.5-and 21.5-KDa Isoforms of Myelin Basic Protein Inhibit Calcium Influx into Oligodendroglial Cells, in Contrast to Golli Isoforms." *Journal of Neuroscience Research* 89 (4). PMC Canada manuscript submission: 467–80. doi:10.1002/jnr.22570.

Snaidero, Nicolas, Wiebke Möbius, Tim Czopka, Liesbeth H.P. Hekking, Cliff Mathisen, Dick Verkleij, Sandra Goebbels, et al. 2014. "Myelin Membrane Wrapping of CNS Axons by PI(3,4,5)P3-Dependent Polarized Growth at the Inner Tongue." *Cell* 156 (1–2). Europe PMC Funders: 277–90. doi:10.1016/j.cell.2013.11.044.

Snaidero, Nicolas, and Mikael Simons. 2017. "The Logistics of Myelin Biogenesis in the Central Nervous System." *GLIA*. Wiley-Blackwell. doi:10.1002/glia.23116.

Speckmann, Erwin-Josef, Jürgen Hescheler, and Rüdiger Köhling. 2013. *Physiologie*. 6th ed. München: Elsevier.

Staugaitis, Susan M, P R Smith, and David R Colman. 1990. "Expression of Myelin Basic Protein Isoforms in Nonglial Cells." *Journal of Cell Biology* 110 (5): 1719–27. doi:10.1083/jcb.110.5.1719.

Stevens, Beth, Stefania Porta, Laurel L Haak, Vittorio Gallo, and R Douglas Fields. 2002. "Adenosine: A Neuron-Glial Transmitter Promoting Myelination in the CNS in Response to Action Potentials." *Neuron* 36 (5). NIH Public Access: 855–68. doi:10.1016/S0896-6273(02)01067-X.

Stoppini, L, P.-A Buchs, and D Muller. 1991. "A Simple Method for Organotypic Cultures of Nervous Tissue." *Journal of Neuroscience Methods* 37 (2): 173–82. doi:10.1016/0165-0270(91)90128-M.

Sweadner, K. J. 1985. "Enzymatic Properties of Separated Isozymes of the Na,K-ATPase." *Journal of Biological Chemistry* 260. American Society for Biochemistry and Molecular Biology: 11508–13. http://www.jbc.org/content/260/21/11508.abstract.

Sweadner, Kathleen J. 1989. "Isozymes of the Na+/K+-ATPase." *BBA - Reviews on Biomembranes*. doi:10.1016/0304-4157(89)90019-1.

Tang, Dean G, Yasuhito M Tokumoto, and Martin C Raff. 2000. "Long-Term Culture of Purified Postnatal Oligodendrocyte Precursor Cells: Evidence for an Intrinsic Maturation Program That Plays out over Months." *Journal of Cell Biology* 148 (5). The Rockefeller University Press: 971–84. doi:10.1083/jcb.148.5.971.

Tong, Xiao-ping, Xiang-yao Li, Bing Zhou, Wanhua Shen, Zhi-jun Zhang, Tian-le Xu, and Shumin Duan. 2009. "Ca 2+ Signaling Evoked by Activation of Na + Channels and Na + /Ca 2+ Exchangers Is Required for GABA-Induced NG2 Cell Migration." *The Journal of Cell Biology* 186 (1). Rockefeller University Press: 113–28. doi:10.1083/jcb.200811071.

Toyoshima, Chikashi, Masayoshi Nakasako, Hiromi Nomura, and Haruo Ogawa. 2000. "Crystal Structure of the Calcium Pump of Sarcoplasmic Reticulum at 2.6 A Resolution." *Nature* 405 (6787). Nature Publishing Group: 647–55. doi:10.1038/35015017.

Trepel, M. 2017. *Neuroanatomie - Struktur Und Funktion*. 7th ed. Elsevier.

Tripathi, Richa B, Laura E Clarke, Valeria Burzomato, Nicoletta Kessaris, Patrick N Anderson, David Attwell, and William D Richardson. 2011. "Dorsally and Ventrally Derived Oligodendrocytes Have Similar Electrical Properties but Myelinate Preferred Tracts." *Journal of Neuroscience* 31 (18). Society for Neuroscience: 6809–19. doi:10.1523/JNEUROSCI.6474-10.2011.

Vallstedt, Anna, Joanna M. Klos, and Johan Ericson. 2005. "Multiple Dorsoventral Origins of Oligodendrocyte Generation in the Spinal Cord and Hindbrain." *Neuron* 45 (1). Cell Press: 55–67. doi:10.1016/j.neuron.2004.12.026.

Waggener, Christopher T, Jeffrey L Dupree, Ype Elgersma, and Babette Fuss. 2013. "CaMKII Regulates Oligodendrocyte Maturation and CNS Myelination." *Journal of Neuroscience* 33 (25). Society for Neuroscience: 10453–58. doi:10.1523/JNEUROSCI.5875-12.2013.

Wake, Hiroaki, Philip R Lee, and R Douglas Fields. 2011. "Control of Local Protein Synthesis and Initial Events in Myelination by Action Potentials." *Science (New York, N.Y.)* 333 (6049): 1647–51. doi:10.1126/science.1206998.

Wang, Pei Shan, Jing Wang, Zhi Cheng Xiao, and Catherine J Pallen. 2009. "Protein-Tyrosine Phosphatase α Acts as an Upstream Regulator of Fyn Signaling to Promote Oligodendrocyte Differentiation and Myelination." *Journal of Biological Chemistry* 284 (48). American Society for Biochemistry and Molecular Biology: 33692–702. doi:10.1074/jbc.M109.061770.

Watts, Alan G, G Sanchez-Watts, J R Emanuel, and R Levenson. 1991. "Cell-Specific Expression of MRNAs Encoding Na+,K(+)-ATPase Alpha- and Beta-Subunit Isoforms within the Rat Central Nervous System." *Proceedings of the National Academy of Sciences of the United States of America* 88 (16): 7425–29. doi:10.1073/pnas.88.16.7425.

Waxman, Stephen G. 1997. "Axon-Glia Interactions: Building a Smart Nerve Fiber." *Current Biology* 7 (7): R406–10. doi:10.1016/S0960-9822(06)00203-X.

White, Robin, Constantin Gonsior, Nina M. Bauer, Eva Maria Kr??mer-Albers, Heiko J. Luhmann, and Jacqueline Trotter. 2012. "Heterogeneous Nuclear Ribonucleoprotein (HnRNP) F Is a Novel Component of Oligodendroglial RNA Transport Granules Contributing to Regulation of Myelin Basic Protein (MBP) Synthesis." *Journal of Biological Chemistry* 287 (3): 1742–54. doi:10.1074/jbc.M111.235010.

White, Robin, Constantin Gonsior, Eva Maria Kr??mer-Albers, Nadine St??hr, Stefan H??ttelmaier, and Jacqueline Trotter. 2008. "Activation of Oligodendroglial Fyn Kinase Enhances Translation of MRNAs Transported in HnRNP A2-Dependent RNA Granules." *Journal of Cell Biology* 181 (4): 579–86. doi:10.1083/jcb.200706164.

White, Robin, and Eva-Maria Krämer-Albers. 2014. "Axon-Glia Interaction and Membrane Traffic in Myelin Formation." *Frontiers in Cellular Neuroscience* 7 (JAN): 284. doi:10.3389/fncel.2013.00284.

Woo, Alison L, Paul F James, and Jerry B Lingrel. 2000. "Sperm Motility Is Dependent on a Unique Isoform of the Na,K-ATPase." *Journal of Biological Chemistry* 275 (27). American Society for Biochemistry and Molecular Biology: 20693–99. doi:10.1074/jbc.M002323200.

Wood, D D, G J Vella, and M A Moscarello. 1984. "Interaction between Human Myelin Basic Protein and Lipophilin." *Neurochemical Research* 9 (10): 1523–31. doi:10.1007/BF00964678.

Yu, Yang, Ying Chen, Bongwoo Kim, Haibo Wang, Chuntao Zhao, Xuelian He, Lei Liu, et al. 2013. "Olig2 Targets Chromatin Remodelers to Enhancers to Initiate Oligodendrocyte Differentiation." *Cell* 152 (1–2). Cell Press: 248–61. doi:10.1016/j.cell.2012.12.006.

Zhang, Songbai, Seth Malmersjö, Juan Li, Hideaki Ando, Oleg Aizman, Per Uhlén, Katsuhiko Mikoshiba, and Anita Aperia. 2006. "Distinct Role of the N-Terminal Tail of the Na,K-ATPase Catalytic Subunit as a Signal Transducer." *Journal of Biological Chemistry* 281 (31). American Society for Biochemistry and Molecular Biology: 21954–62. doi:10.1074/jbc.M601578200.

Zhu, Qiang, Scott R. Whittemore, William H. Devries, Xiaofeng Zhao, Nicholas J. Kuypers, and Mengsheng Qiu. 2011. "Dorsally-Derived Oligodendrocytes in the Spinal Cord Contribute to Axonal Myelination during Development and Remyelination Following Focal Demyelination." *GLIA* 59 (11). Wiley Subscription Services, Inc., A Wiley Company: 1612–21. doi:10.1002/glia.21203.

Ziskin, Jennifer L, Akiko Nishiyama, Maria Rubio, Masahiro Fukaya, and Dwight E Bergles. 2007. "Vesicular Release of Glutamate from Unmyelinated Axons in White Matter." *Nature Neuroscience* 10 (3). NIH Public Access: 321–30. doi:10.1038/nn1854.

Zonouzi, Marzieh, Joseph Scafidi, Peijun Li, Brian McEllin, Jorge Edwards, Jeffrey L Dupree, Lloyd Harvey, et al. 2015. "GABAergic Regulation of Cerebellar NG2 Cell Development Is Altered in Perinatal White Matter Injury." *Nature Neuroscience* 18 (5): 674–82. doi:10.1038/nn.3990.

Appendix

A. Danksagung/Acknowledgement

B. Publications and posters

Publications:

Maike Friess, <u>Jens Hammann</u>, Petr Unichenko, Heiko J. Luhmann, Robin White, Sergei Kirischuk (2016). „Intracellular ion signaling influences myelin basic protein synthesis in oligodendrocyte precursor cells" – Cell Calcium. 2016 Nov;60(5):322-330. doi: 10.1016/j.ceca.2016.06.009.

<u>Jens Hammann</u>, Davide Bassetti, Robin White, Heiko J. Luhmann, Sergei Kirischuk (2018). „$\alpha 2$ isoform of Na^+,K^+-ATPase via Na^+,Ca^{2+} exchanger modulates myelin basic protein synthesis in oligodendrocyte lineage cells in vitro" – Cell Calcium. 2018 July; 73:1-10. https://doi.org/10.1016/j.ceca.2018.03.003

Poster:

„Intracellular ion sinaling influences MBP synthesis in OPCs"
<u>Jens Hammann</u>, Maike Friess, Petr Unichenko, Heiko J. Luhmann, Robin White and Sergei Kirischuk
12th Göttingen Meeting of the German Neuroscience Society – Göttingen, 2017

C. Eidesstattliche Erklärung

Ich erkläre hiermit, dass die vorgelegte Dissertation von mir selbstständig, ohne unzulässige Hilfe Dritter und ohne Benutzung anderer als der angegebenen Hilfsmittel, angefertigt wurde. Alle von mir benutzten Veröffentlichungen, ungedruckten Materialien, sonstige Hilfsmittel sowie Textstellen, die ich wörtlich oder inhaltlich aus gedruckten oder ungedruckten Arbeiten übernommen habe, habe ich als solche gekennzeichnet und mit den erforderlichen bibliographischen Angaben nachgewiesen. Unterstützungsleistungen, die ich von anderen Personen erhalten habe, wurden in der Dissertationsschrift als solche benannt. Die Dissertation wurde bei keiner anderen Fakultät oder einem anderen Fachbereich vorgelegt, weder im In- noch im Ausland. Überdies bin ich nicht im Besitz eines anderen Doktorgrades. Ein bisher erworbener Doktorgrad wurde mir nicht aberkannt. Ich habe bisher kein Promotionsverfahren erfolglos beendet. Mir ist bekannt, dass die Zulassung zur Promotion zu versagen ist, wenn die Unterlagen unvollständig oder die Angaben unrichtig sind. Ich bin darüber informiert, dass ich zur Führung des Doktortitels erst mit Aushändigung der Promotionsurkunde berechtigt bin.

_____   _____

Ort, Datum   Unterschrift

D. Curriculum vitae

Jens Hammann

Geboren am 06. November 1982 in Bernkastel-Kues

Anschrift:	Lessingstraße 25, 55118 Mainz
Email:	jens_hammann@web.de
Staatsangehörigkeit :	deutsch
Familienstand:	ledig

Bildungsgang

Dissertation zur Erlangung des Grades Doktor der Naturwissenschaften

Voraussichtlich 06/2018

Fachbereich Biologie, Johannes Gutenberg-Universität Mainz

Seit 03/2014   **Wissenschaftlicher Mitarbeiter, Doktorand**

Universitätsmedizin der Johannes Gutenberg-Universität Mainz

Institut für Physiologie unter der Leitung von Prof. Dr. H. Luhmann

12/2012 – 09/2013   **Diplomarbeit am Institut für Molekulargenetik**

Johannes Gutenberg-Universität Mainz

Titel: „Struktur und Expression des *dsx*-Gens bei Chironomus"

2003 – 2013   **Studium der Biologie**

Johannes Gutenberg-Universität Mainz

Abschluss: Diplom (Gesamtnote: sehr gut)

Schwerpunkte: Molekulargenetik, Biochemie

06/2002 – 03/2003   Zivildienst beim DRK-Sozialwerk, Bernkastel-Kues

08/1993-03/2002   **Nikolaus-von-Kues-Gymnasium Bernkastel-Kues**

Abschluss: Abitur